

CHALMERS



Crack Control of Extended Concrete Walls

Master of Science Thesis in the Master's Programme Structural Engineering and Building Technology

MARCUS ERIKSSON
ELIAS FRITZSON

Department of Civil and Environmental Engineering
Division of Structural Engineering
Concrete Structures
CHALMERS UNIVERSITY OF TECHNOLOGY
Göteborg, Sweden 2014
Master's Thesis 2014:143

MASTER'S THESIS 2014:143

Crack Control of Extended Concrete Walls

*Master of Science Thesis in the Master's Programme Structural Engineering and
Building Technology*

MARCUS ERIKSSON

ELIAS FRITZSON

Department of Civil and Environmental Engineering
*Division of Structural Engineering
Concrete Structures*

CHALMERS UNIVERSITY OF TECHNOLOGY

Göteborg, Sweden 2014

Crack control of extended concrete walls

Master of Science Thesis in the Master's Programme Structural Engineering and Building Technology

MARCUS ERIKSSON

ELIAS FRITZSON

© MARCUS ERIKSSON, ELIAS FRITZSON, 2014

Examensarbete / Institutionen för bygg- och miljöteknik,
Chalmers tekniska högskola 2014:143

Department of Civil and Environmental Engineering

Division of Structural Engineering

Concrete Structures

Chalmers University of Technology

SE-412 96 Göteborg

Sweden

Telephone: + 46 (0)31-772 1000

Cover:

Picture of a crack in a wall

Chalmers Reproservice

Göteborg, Sweden 2014

Crack control of extended concrete walls

Master of Science Thesis in the Master's Programme Structural Engineering and Building Technology

MARCUS ERIKSSON

ELIAS FRITZSON

Department of Civil and Environmental Engineering

Division of Structural Engineering

Concrete Structures

Chalmers University of Technology

ABSTRACT

When a concrete wall is in any way prevented from free movement, the wall is restrained and restraint forces appear. Restraints could be either external, e.g. due to a connecting slab, or internal, e.g. due to reinforcement. A need for movement is generated, besides from external loading, from intrinsic deformations such as shrinkage. This thesis treats the cracking of a concrete wall mainly subjected to shrinkage where both external and internal restraints are accounted for.

Restraint forces introduce tensile stresses in a concrete wall. Since concrete is a material strongly characterised by its low tensile strength and, consequently, tendency to crack, tensile stresses from restraints could result in the formation of cracks. If these cracks are allowed to develop without control, the tightness, durability and performance of a concrete wall could decrease considerably.

In order to control such restraint related cracking a certain minimum amount of reinforcement is required, for which Eurocode 2 provides an expression. However, this expression is of questionable applicability in restraint situations, since it has been derived inconsiderate of restraints. The derivation is based on a beam section subjected to combined moment and axial force assuming an uncracked section.

A Matlab calculation program, inserting and accounting for cracks, was developed to model a restrained concrete wall subjected to shrinkage as a 1D-strip. The model was used in a parametric, study where the applicability of the Eurocode 2 expression and the respective influences of various parameters on the cracking situation were investigated. To further strengthen the investigation and to provide a connection with reality, cellar walls of two existing buildings were investigated. Crack widths and crack distribution in selected walls of the visited buildings were measured and documented.

The thesis concludes that the Eurocode 2 equation is likely to overestimate the needed amount of minimum reinforcement and, due to the questionable applicability and results from the parametric study, that an expression accounting for restraints would be favourable as a replacement of the current expression.

Key words: crack control, shrinkage, minimum reinforcement, restraint, extended walls, one-dimensional strip, Eurocode, crack widths

Sprickbegränsning för långsträckta betongväggar

Examensarbete inom masterprogrammet Structural Engineering and Building Technology

MARCUS ERIKSSON

ELIAS FRITZSON

Institutionen för bygg- och miljöteknik

Avdelningen för Konstruktionsteknik

Betongbyggnad

Chalmers tekniska högskola

SAMMANFATTNING

När en betongvägg av någon anledning hindras från att röra sig fritt är den utsatt för tvång och tvångskrafter uppkommer. Tvång kan vara både externa, t.ex. på grund av en avslutande betongplatta, eller interna, t.ex. på grund av armering. Ett rörelsebehov uppstår, vid sidan av den från belastning, på grund av inre deformationer såsom krympning. Detta examensarbete behandlar sprickor i betongväggar utsatta för krympning och hänsyn tas till både externa och interna tvång.

I betongväggar som utsätts för tvångskrafter uppkommer dragspänningar. Eftersom betong är ett material som starkt karakteriseras av sin låga draghållfasthet och tendens att spricka, kan dragspänningar uppkomma av tvång resultera i sprickor. Om dessa sprickor inte kontrolleras kan betongväggars täthet, hållbarhet och funktionsduglighet minska avsevärt.

För att kontrollera den sprickbildning som uppkommer på grund av tvångsinverkan behövs en viss mängd minimiarmering för sprickbegränsning. Eurokod 2 tillhandahåller ett uttryck för denna minimiarmering. Dock är tillämpbarheten diskutabel i tvångssituationer eftersom ekvationen har härletts utan hänsyn till tvång. Härledningen baseras på ett osprucket balktvärsnitt belastat med moment och normalkraft.

Ett Matlab-program, som sätter in och tar hänsyn till sprickor, har utvecklats för att genom en endimensionell strimla modellera en tvångsutsatt betongvägg under inverkan av krympning. Modellen har använts i en parameterstudie där tillämpbarheten av Eurokod 2 ekvationen undersöktes tillsammans med diverse parameters inverkan på spricksituationen i en betongvägg. Två byggnader besöktes där sprickvidder och sprickfördelningar i utvalda väggar mättes och dokumenterades för att ytterligare stärka slutsatserna från beräkningsprogrammet och för att utgöra en koppling mot verkligheten.

Slutsatsen dras att ekvationen för minimiarmering i Eurokod 2 troligtvis överskattar den mängd armering som behövs för sprickbegränsning. Vidare dras slutsatsen, baserat på den tveksamma tillämpbarheten och resultaten från parameterstudien, att ett uttryck som tar hänsyn till tvång är önskvärt som ersättning till det nuvarande uttrycket för minimiarmering.

Nyckelord: sprickfördelning, krympning, minimiarmering, tvång, långsträckta väggar, endimensionell strimla, Eurokod, sprickvidder

Contents

1	INTRODUCTION	1
1.1	Background	1
1.2	Objective	1
1.3	Limitations	2
1.4	Method	2
1.5	Outline of the thesis	2
2	CONCRETE CELLAR WALLS	4
2.1	Introduction	4
2.2	Importance of restraint and intrinsic deformations	5
2.3	Common problems	5
3	CRACKING BEHAVIOUR OF RESTRAINED CONCRETE WALLS	8
3.1	Material behaviour	8
3.1.1	Concrete	8
3.1.2	Conventional steel reinforcement	8
3.1.3	Typical behaviour of reinforced concrete	10
3.1.4	Interaction between reinforcement and concrete	11
3.1.5	Interaction between concrete and concrete	15
3.1.6	Fibre reinforced concrete	19
3.2	Restraint	22
3.2.1	Stress-dependent strain and stress-independent strain	22
3.2.2	Restraint degree	22
3.2.3	External restraints	23
3.2.4	Internal restraints	26
3.3	Shrinkage	27
3.3.1	Drying shrinkage	27
3.3.2	Autogenous shrinkage	29
3.4	Creep	30
3.5	Cracking process	34
3.5.1	Cracking of plain concrete	34
3.5.2	Cracking of reinforced concrete	35
3.5.3	Effective area in thick reinforced members	37
3.5.4	Cracking of fibre reinforced concrete	39
3.5.5	Crack widths	44
3.6	Crack control	44
3.6.1	According to Eurocode 2	45
3.6.2	According to BBK 04	47
3.6.3	Other	47

4	ANALYSIS OF EXISTING OBJECTS	50
4.1	Introduction	50
4.2	Investigation method	51
4.3	Object A	53
4.3.1	Object description	53
4.3.2	General observations	54
4.3.3	Wall 1	54
4.3.4	Wall 2	58
4.3.5	Evaluation	62
4.4	Object B	62
4.4.1	Object description	62
4.4.2	General observations	64
4.4.3	Wall 1	64
4.4.4	Evaluation	69
5	CALCULATION MODEL FOR NUMERICAL ANALYSIS	70
5.1	Introduction	70
5.2	Program structure	71
5.2.1	Main program	71
5.2.2	Function files	75
5.2.3	Boundary conditions	85
5.2.4	Deformation conditions	85
5.3	Verification of the model	86
5.3.1	Shrinkage strain	86
5.3.2	Creep coefficient	87
5.3.3	Concrete stress	89
5.3.4	Verification of the deformation condition	90
6	PARAMETRIC STUDY	92
6.1	Introduction	92
6.2	Standard wall segment in the parametric study	93
6.3	Common case	95
6.4	Influence of restraint at wall/slab interface	96
6.4.1	Importance of restraint at wall/slab interface	96
6.4.2	Reinforcement area required for crack control	98
6.4.3	Design code comparison	101
6.5	Influence of end support stiffness	103
6.5.1	Importance of considering end support stiffness	103
6.5.2	Reinforcement area needed for crack control	105
6.5.3	Design code comparison	110
6.6	Influence of wall thickness	111
6.6.1	Reinforcement area needed for crack control	111
6.6.2	Design code comparison	116
6.7	Influence of relative humidity	117

6.7.1	Importance of considering relative humidity	117
6.7.2	Reinforcement area required for control	118
6.7.3	Design code comparison	121
6.8	Influence of concrete strength class	123
6.8.1	Reinforcement area required for crack control	123
6.8.2	Design code comparison	125
6.9	Influence of bar diameter	127
6.9.1	Reinforcement area required for crack control	127
6.9.2	Design code comparison	129
6.10	Influence of wall length	130
6.10.1	Importance of considering wall length	130
6.10.2	Reinforcement area needed for crack control	131
6.10.3	Design code comparison	133
7	EVALUATION	135
7.1	Introduction	135
7.2	Fibre reinforced concrete	135
7.3	Visited objects	135
7.4	Parametric study	136
7.5	Minimum reinforcement amount	137
7.6	Suggested alterations of Eurocode 2 equation for minimum reinforcement	138
8	FINAL REMARKS	140
8.1	Conclusions	140
8.2	Further investigations	141
9	REFERENCES	142
APPENDIX A PROTOCOL		A-1
A.1	Protocol from inspections	A-1
A.2	Measured crack widths from object A, wall 1	A-4
A.3	Measured crack widths from object A, wall 2	A-5
A.4	Measured crack widths from object B, wall 1	A-7
APPENDIX B MATLAB CODE		B-1
B.1	Main program	B-1
B.2	Function file for concrete properties	B-11
B.3	Function file for slab interface properties	B-14
B.4	Function file for crack stiffness	B-18

B.5	Function file for shrinkage strain	B-20
B.6	Function file for creep, first approach	B-24
B.7	Function file for creep, second approach	B-27
B.8	Function file for global force vector	B-31
B.9	Function file for global stiffness matrix	B-33
B.10	Function file for calculation of stresses and crack widths	B-40
B.11	Function file for crack insertion	B-45
APPENDIX C VERIFICATION OF MATLAB PROGRAM		C-1
C.1	Verification of shrinkage strain calculation	C-1
C.2	Verification of creep, first approach	C-4
C.3	Verification of creep, several approach	C-8
C.4	Verification of concrete stress calculation	C-11
APPENDIX D SUPPORTING CALCULATION FOR STANDARD WALL		D-1
D.1	Calculations of end support stiffness	D-1
D.2	Calculations of normal compressive stress (σ_n)	D-3
APPENDIX E SIMULATIONS IN PARAMETRIC STUDY		E-2
E.1	Initials simulations	E-2
E.2	Variations of width	E-6
E.3	Variations of slab stiffness	E-10
E.4	Variation of reinforcement diameter	E-14
E.5	Variation of relative humidity	E-18
E.6	Variation of end support stiffenss	E-22
E.7	Variation of concrete strength class	E-26
E.8	Variation of wall length	E-30

Preface

In this master thesis project the cracking behaviour of restrained concrete walls exposed to shrinkage have been studied. The project has been carried out between January and June during 2014 within the master's program of Structural Engineering and Building Technology at Chalmers University of Technology.

The work has been carried out at VBK Konsulternade ingenjörer AB in cooperation with Chalmers University of Technology, Department of Civil and Environmental Engineering, Division of Structural Engineering, Concrete Structures.

A special thank you to our supervisors Rasmus Sylvén, structural engineer at VBK, and Björn Engström, professor in concrete structures at Chalmers, who also was the examiner, for their support and patience during the entire work process, and our opponents Nawar Merza and Ashna Zangana for insightful discussions and joyful moments.

Also, we would like to thank Per Zetterlund, site manager at NCC Construction Sverige AB, Claes Premmert, project manager at Älvstranden Utveckling AB, and Ingemar Löfgren, adjunct professor at Chalmers and R&D manager at Thomas Concrete group AB, for their support. Finally, thank you to all the people at VBK for a pleasant working atmosphere.

Göteborg, June 2014

Marcus Eriksson & Elias Fritzon

Notations

Roman upper case letters

A_c	Concrete cross section area
A_{ct}	Concrete area subjected to tension
A_{ef}	Effective concrete area
$A_{I,ef}$	Effective cross sectional area of state I
A_s	Cross sectional area of reinforcement steel
$A_{s,min}$	Minimum reinforcement area
E	Modulus of elasticity
E_c	Young's modulus for concrete
$E_{c,ef}$	Effective Young's modulus of concrete
E_{cm}	Mean value of Young's modulus of concrete
E_s	Young's modulus for reinforcement steel
F	Global force vector
F_{cs}	Shrinkage force
$F_{element}$	Local element force vector
G_f	Fracture energy
K	Global stiffness matrix
$K_{element}$	Local element stiffness matrix
L_{total}	Total length of segment
N	Normal force
R	Restraint degree
S	Support stiffness

Roman lower case letters

a	Global displacement vector
d	Effective depth of the centroid of the outer layer of reinforcement
f_c	Compressive strength
f_{cc}	Concrete compression strength
f_{ck}	Characteristic concrete compression strength
f_{cm}	Mean concrete compression strength
$f_{ct,h}$	High concrete tensile strength
$f_{ct,eff}$	Mean tensile strength of concrete
$f_{element}$	Element force
f_t	Tensile strength
f_y	Yield stress for reinforcement steel
f_{yk}	Characteristic yield stress for reinforcement steel

h_0	Notional size
h_{cr}	Depth of tensile zone just before cracking
k	Factor considering the effect of non-uniform self-equilibration stresses
$k_{element}$	Element stiffness
k_c	Coefficient depending on the stress distribution
k_h	Coefficient depending on the size of the section
l_{ch}	Characteristic length
l_t	Transmission length
n	Displacement of each support
s	Slip
s_u	Ultimate slip
t	Time at the considered moment
t_0	Age of the concrete when it is loaded
t_s	Age of concrete at the beginning of drying shrinkage
u	Perimeter of the part of the cross section that is exposed to the atmosphere
v	Effectiveness factor for the concrete
w_{crack}	Mean crack width
w_k	Characteristic crack width
w_m	Mean crack width

Greek lower case letters

$\beta(f_{cm})$	Factor that consider the concrete strength
$\beta(t_0)$	Factor that consider the age of concrete when it is loaded
$\beta_{as}(t)$	Time function for autogenous shrinkage
β_c	Coefficient for the strength of the compression strut
$\beta_c(t, t_0)$	Coefficient that describe the development of creep during a time
$\beta_{ds}(t, t_s)$	Time function for drying shrinkage
β_H	Factor considering both relative humidity and notional size
ϵ_{ca}	Autogenous shrinkage strain
ϵ_{cc}	Creep strain
ϵ_{cd}	Drying shrinkage strain
$\epsilon_{cd,0}$	Expected mean value of the shrinkage strain
ϵ_{cs}	Total shrinkage strain
ϵ_{ct}	Concrete tensile strain
$\epsilon_{c,tot}$	Total concrete strain
κ_1	Interaction factor
κ_2	Interaction coefficient

μ	Friction coefficient
ρ	Reinforcement ratio
σ_c	Concrete stress
σ_n	Normal compression stress
σ_s	Steel stress
τ_a	Shear resistant from adhesion/interlocking
τ_b	Bond stress
τ_{fd}	Shear stress at the interface
$\tau_{fu,d}$	Ultimate shear stress, design value
τ_u	Ultimate shear stress
φ	Creep coefficient
φ_0	Notional creep coefficient
φ_{ef}	Effective creep coefficient
φ_{RH}	Factor consider the relative humidity in creep
ϕ	Reinforcement bar diameter
ϕ^*	Maximum bar diameter
ϕ_s	Adjusted maximum bar diameter

1 Introduction

1.1 Background

During hardening of concrete there is a need for deformations within the concrete. If this deformation is in any way restrained, restraint forces appear. Such restraint can for instance occur from reinforcement, which is an internal restraint, or from more or less fixed edges (such as ground slabs or connecting walls), which is an external restraint. Most often in real structures there is a combination of internal and external restraints. If one or several restraints exist, restraint forces can for instance occur due to shrinkage or thermal expansion and contraction. Restraint forces might introduce tensile stresses which, due to the relatively low tensile strength of concrete, could result in cracking. If cracks appear and the crack widths are too large, the tightness of the structure may be compromised. Cracks could also decrease both durability and performance.

Due to the relatively low tensile strength of concrete, cracks are common even in the service state. However, depending on the type of environment the structure is in, the severity of cracks differs between different structures. One type of structure where cracks could essentially decrease durability and performance is cellar walls. These could be exposed to ground water pressure from the neighbouring soil. Hence, too large cracks could result in leakage, which affects the wall itself as well as the indoor environment negatively. In order to avoid such problems, cracks must be either controlled or prevented.

The current Eurocode for design of concrete structures, CEN (2004), provides an expression for calculation of a minimum reinforcement area required for adequate crack control. However, this expression has been derived using a beam section with no consideration of restraints. Furthermore, the resulting minimum reinforcement area is larger than in the corresponding requirement in the Swedish handbook for concrete structures BBK 04, Boverket (2004). The magnitude of the difference is large enough for designers in Sweden to start questioning the requirement given in Eurocode. Previous studies, such as Alfredsson and Spåls (2008), Björnberg and Johansson (2013) and Dahlgren and Svensson (2013), have also indicated that the required minimum reinforcement area in Eurocode might not be fully applicable in restraint situations. There is a need to improve the design procedure for crack controlling reinforcement in restraint situations, especially in cellar walls and similar types of structures.

1.2 Objective

The purpose of this project was to increase the knowledge about restraint related cracking in concrete walls and how to control such cracking in design.

To fulfil this purpose more specific objectives were defined as listed below.

- Examination of concrete walls in existing buildings subjected to restraint forces with regards to cracks and crack patterns, in order to provide a connection with reality and compare with modelling results.
- Investigate the possibility of using fibre reinforcement to reduce the amount of conventional reinforcement needed for crack control.

- Investigate, by means of a parametric study, the amount and distribution of longitudinal reinforcement required for an adequate crack control in concrete walls with regard to restraints and flexibility.
- Investigate, by means of a parametric study, whether or not the requirements of minimum reinforcement areas for crack control given in some structural design codes are appropriate.
- Finding, based on results generated within the project, recommendations on crack control and the design of minimum reinforcement.

1.3 Limitations

This project should focus on the minimum reinforcement needed for crack control in walls. Thus the results should not, without further investigations, be applied to other types of structures such as beams or slabs. Furthermore, the conclusions and recommendations given from this project should to a large extent depend on parametric studies. Such modelling includes simplifications and requires simplified assumptions which will impose some limitations with regard to reality. No full scale tests were to be performed for verification of the modelling results. However, a comparison with existing structures should be carried out.

1.4 Method

The project should be initiated with a literature study, which had two main reasons. Reason one was to increase understanding and knowledge within the subject of restrained concrete. Facts were to be collected from different sources, such as research publications and literature from both Sweden and other countries. While reason two was to build a foundation of previous studies and literature from which new approaches and areas to study could be found. Information about this was assumed to mainly come from previous master's theses.

The next part of the project was to visit some different buildings and examine cracks due to restraint forces in their concrete walls. This part was intended to provide a connection with reality and to look for common crack patterns in order to compare with modelling results.

In the last part of the project a parametric study should be carried out. This part was intended to, in combination with the examination of existing buildings, provide a bases for conclusions and recommendations regarding the amounts and distribution of the minimum reinforcement needed for adequate crack control.

1.5 Outline of the thesis

Background information and an introduction to concrete cellar walls is presented in Chapter 2. Besides the background the importance of considering restraints and intrinsic deformations as well as common problems found in cellar walls are treated.

A theoretical background to the thesis is presented in Chapter 3. The presented theory explains the cracking behaviour of restrained concrete walls by treating material

behaviour, restraints, the effects of shrinkage and creep, the cracking process of plain, reinforced and fibre reinforced concrete and, finally, methods for crack control.

Existing cracking of cellar walls in two buildings were investigated as a part of this project. The method of these investigations, intended to provide a connection with reality, are presented in Chapter 44 along with the results.

In order to model cracking of restrained concrete walls and investigate the influence of various parameters on the cracking response, a calculation model using the Matlab software was developed. The calculation procedure is described in Chapter 5 and the parametric study, including its results conducted using the program, is treated in Chapter 5.3.4.

Finally, the thesis is concluded by the evaluation presented in Chapter 7 and the final remarks in Chapter 8.

2 Concrete cellar walls

2.1 Introduction

Cellar walls in residential buildings in Sweden have historically been constructed using a variety of different building materials and construction methods. From the medieval period until the early 20th century cellars were mainly used to store food and fuels for heating and constructed using stones, with or without mortar, Bjerking (1989).

During the first half of the 20th century concrete became the predominant building material for cellar walls. However, the type of concrete used and how (or even if) it was reinforced has changed since. For instance, in the early stages of this concrete time period, concrete often contained quite large sized stones and, if any at all, only limited amounts of reinforcement. Since this time cellars have mainly been used for laundry facilities, heating equipment and general storage, Bjerking (1989).

In the 1960s and 1970s more modern concrete with smaller sized aggregates and horizontal reinforcement distributed along the height of the wall was introduced, which basically remains today as the predominant construction method of cellar walls. Björk (2003)

Concrete cellar walls can be, and have been, built using different construction methods and reinforcement configurations. The perhaps most clear distinguishing feature is the one between using in-situ cast concrete or prefabricated concrete elements. In the early years of constructing concrete cellar walls, all walls were in-situ cast. The use of prefabricated elements in cellar wall construction is a more recent method, just as the use of prefabricated concrete in general. Both methods have their respective advantages and disadvantages and today both are widely used.

Using in-situ cast concrete is time consuming and requires extensive preparations at the construction site, including form work and placing of reinforcement. However, an excellent tightness can be achieved and late minute alterations are possible on site, if the prerequisites change. During design of in-situ cast walls the designer has to consider parameters such as the length of casting segments and if shrinkage zones are needed. There are many choices to be made, which all affect the performance and durability of the finished product.

Prefabricated wall elements are precast in a factory and delivered as a finished, ready to place, product at the construction site, which saves time and work hours during construction. However, the tightness of the connections between different prefabricated wall elements as well as adjacent elements (e.g. ground slab and ceiling) are likely to be decreased compared to in-situ cast walls. An advantage of prefabricated elements is that a larger degree of shrinkage has already developed prior to delivery and mounting.

When deciding between in-situ cast and prefabricated cellar walls, a decisive parameter could be the magnitude of ground water pressure that the walls are exposed to. Due to their tightness (when designed correctly) in-situ cast walls are preferable, when a large ground water pressure is present. However, if the pressure is lower or absent, prefabricated walls might be preferable due to their rapid construction process.

2.2 Importance of restraint and intrinsic deformations

Sufficiently small crack widths are in numerous situations required to ensure durability. Due to the low tensile strength and limited tensile strain capacity of concrete, concrete structures are normally cracked during their service life; cellar walls present no exception and cracks are commonly found. When concrete cellar walls are treated and designed properly, crack widths are small enough to ensure proper tightness of the wall. However, if cracks are present and uncontrolled, the tightness and also the durability of a cellar wall could decrease considerably. In order to avoid such problems, cracking must be either avoided or controlled.

Cracks might occur due to tensile stresses originating from either direct loading or restrained intrinsic deformations. In design of reinforced concrete members most effort is often dedicated to stresses, strains and deformations occurring as a result of direct loading. However, in the same concrete member there can be intrinsic deformations, independent of the external loading. Such effects could be strains due to shrinkage and thermal fluctuations.

If a need for deformation exist due to intrinsic deformations and it is fully or partially prevented, restraint forces are generated. Although a structure theoretically could be completely free from restraints, real structures never are. Thus, in any real structure there will always be some prevented need for deformation and hence stresses due to restraint. If restraint forces introduce tensile stresses reaching the tensile strength, cracks occur. In order to control such cracking a certain minimum amount of crack controlling reinforcement is needed.

Stresses originating from restrained intrinsic deformations can be hard to predict and there are some uncertainties about how they are best treated in design of concrete structures. Consequently, there are some uncertainties about how to treat restraint cracking of concrete members. The equation for crack controlling minimum reinforcement provided in Eurocode 2, CEN (2004), has been derived using a beam section subjected to combined bending and axial force, see European Concrete Platform ASBL (2008), and might be unsuitable for restraint situations. Previous studies, such as Alfredsson and Spåls (2008), Björnberg and Johansson (2013) and Dahlgren and Svensson (2013), have indicated that the required minimum reinforcement area in Eurocode 2 might not be fully applicable in restraint situations.

Concrete cellar walls are in general exposed to several restraints, external as well as internal. For instance, a concrete cellar wall is cast against a concrete slab and adjacent cellar walls are also attached. At such interfaces between concrete cast at different times, concrete cellar walls are restrained by an external restraint. Hence, to prevent possible problems with restraint cracking due to intrinsic deformations, such as shrinkage it is important to correctly consider the actual restraints and flexibility.

2.3 Common problems

Problems and damages in cellar walls often occur due to either mechanical action or moisture penetration. Damages from mechanical actions are often caused by irregular settlements, which could generate cracks throughout the structure. Moisture related problems occur when moisture penetrates the structure, which could be noticed by discolouration or flaking paint on the painted surface. If there are any organic materials connected to or near the moisture penetrated concrete, there is according to

Bjerking (1989) a large risk of rot or mould, Bjerking (1989). Reinforcement corrosion is another type of moisture related problem that can occur in a reinforced concrete wall.

When a ground water pressure or poorly functioning drainage exists on the outside of a cellar wall, moisture could penetrate the wall either through untight concrete or through cracks. If crack widths are too large, which allows moisture to penetrate the wall, a common observation is paint deterioration through flaking paint and discolouration, as illustrated in Figure 2.1.



Figure 2.1 Flaking of paint near a crack due to moisture penetration

In the long term water leakage through a crack can reduce the durability of the wall and can lead to reinforcement corrosion and consequently spalling of the surrounding concrete. Reinforcement corrosion often leads to a discoloration in a rust brown colour near the crack, see Figure 2.2.



Figure 2.2 Discolouration near a crack caused by corroding reinforcement

Figure 2.3 illustrates a case where water leakage has taken place due to insufficient tightness. It should be noted that insufficient tightness could originate from several different causes, where cracking is one. Such leakage could cause, besides possible problems with the wall itself (e.g. as illustrated in Figure 2.1 and Figure 2.2), durability problems for other structural elements (for instance a connecting slab or ceiling), a poor indoor climate due to excess moisture, discomfort due to wet floors and a negative perception of the building.



Figure 2.3 Water leakage in a cellar due to insufficient tightness

3 Cracking behaviour of restrained concrete walls

3.1 Material behaviour

3.1.1 Concrete

Perhaps the most typical property of plain concrete is that its tensile strength is considerably lower than its compressive strength. For instance, the concrete strength class C30/37 has a mean compressive strength of 38 MPa, while its mean tensile strength is 2,9 MPa, CEN (2004). Thus, the compressive strength is about 13 times greater than the tensile strength. This difference is illustrated in Figure 3.1, which displays a typical stress-strain relation for concrete including both tension and compression.

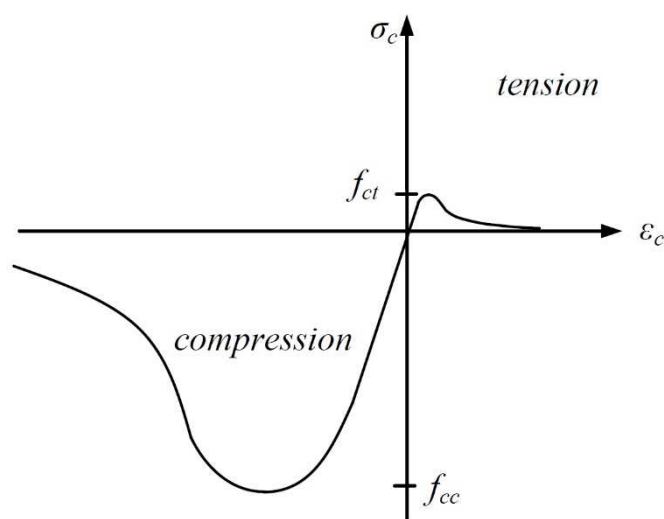


Figure 3.1 Typical stress-strain relation for plain concrete

Due its low tensile strength and low ultimate tensile strain it is natural for concrete structures to crack even when only exposed to low stresses. However, there are some exceptions, such as fully prestressed structures, structures loaded only in compression or structures with only limited tensile stresses. The limited tensile capacity greatly influences the behaviour, usage and design of concrete structures, irrespectively of they are plain, reinforced or prestressed.

3.1.2 Conventional steel reinforcement

To compensate for concrete's limited tensile capacity, it is most often reinforced. In the resulting composite reinforced concrete section, reinforcement is used to carry the tensile forces, which concrete is unable to do after cracking. The conventional and most widely used way to reinforce concrete is by using steel bars, while prestressing and fibre reinforcement represent alternative approaches to reinforce concrete.

There are many parameters influencing the classification of the different standardised reinforcement bars being used today. One of the most common types in Sweden is a ribbed hot worked bar denoted K500C-T, with a characteristic yield strength f_{yk} of 500 MPa, Engström (2011d). The most widely used reinforcement bars are hot-rolled

bars, Figure 3.2 illustrates a typical stress-strain relation for a hot-rolled bar in tension.

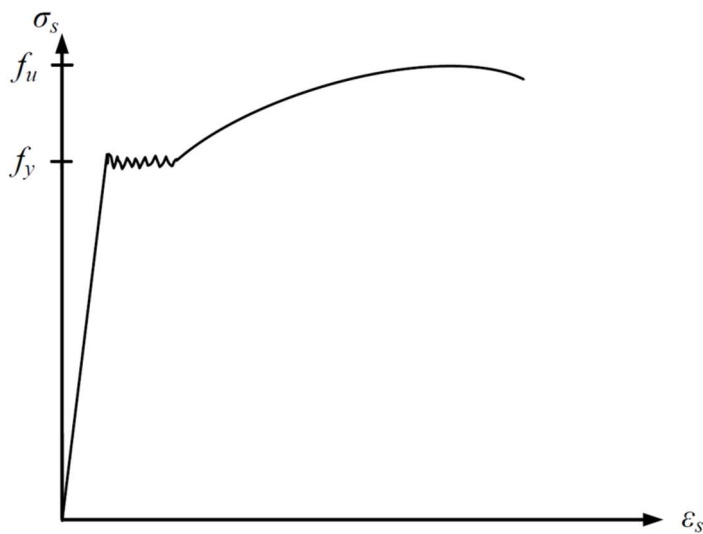


Figure 3.2 Typical stress-strain relation for reinforcing steel in tension (hot-rolled bar)

From Figure 3.2 some characteristic properties are clear. Up to the yield strength is reached the material could be considered as elastic and it has a linear relationship between stress and strain. When the stress has reached and exceeded the yield strength, plastic deformations arise. Figure 3.2 also demonstrates that the plastic deformation of hot-rolled steel is of a considerable magnitude. With this in mind, it is possible to define simplified stress-strain relations. In Eurocode 2, CEN (2004), two alternate models are presented that can be used in normal design situations. These are illustrated in Figure 3.3.

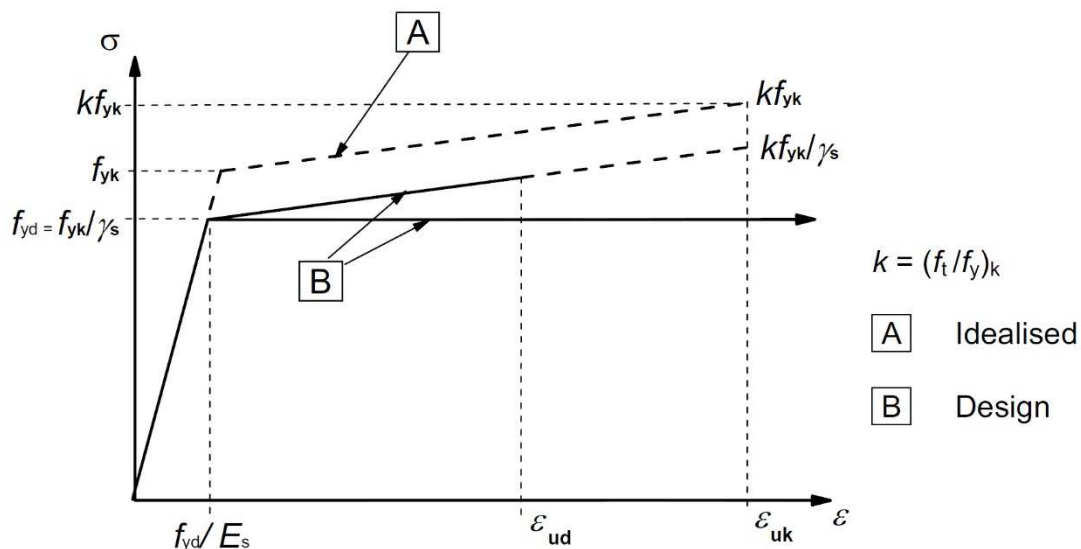


Figure 3.3 Idealised design stress-strain relations according to Eurocode 2 for reinforcing steel, from CEN (2004)

Both models involve the same linear elastic behaviour, defined by the modulus of elasticity E_s , for strains below the yield strain. For strains exceeding the yield strains, one model uses a horizontal top branch without a strain limit, while the other model uses an inclined top branch with a strain limit.

3.1.3 Typical behaviour of reinforced concrete

Reinforced concrete structures loaded until failure demonstrate a highly non-linear behaviour. This is clearly demonstrated by the typical moment-curvature relation of a reinforced concrete section shown in Figure 3.4. This behaviour (of a concrete structure) can be divided into four characteristic stages: uncracked, cracked, yielding and failure.

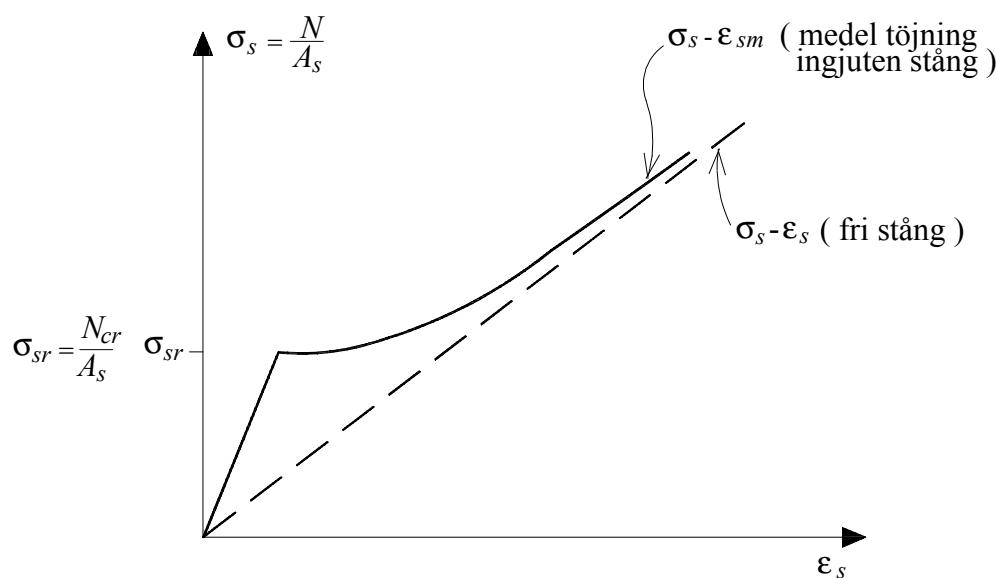


Figure 3.4 Typical moment-curvature relation for a reinforced concrete section

In the uncracked stage reinforcement has little influence on the behaviour and the response is often assumed to be linear elastic. When the first crack appears, the cracked stage is entered, the stiffness is decreased and the reinforcement influences the behaviour to a large extent. The yielding stage is entered when either reinforcement or concrete reaches yielding then after a certain plastic deformation, especially for sections with a ductile behaviour, concrete or steel reaches its ultimate strain and the section fails. For more information regarding these stages and the behaviour under loading of reinforced concrete, reference is made to Engström (2011b) regarding continuous beams and Engström (2011c) regarding slabs.

The cracking and crack control treated in this thesis is limited to the service state. Since yielding should be avoided in the service state, only the uncracked and cracked stages are likely to be of interest. Consequently, yielding and failure stages are related to the ultimate limit state. More information about the cracking process and service state behaviour under loading can be found in Section 3.5.2.

3.1.4 Interaction between reinforcement and concrete

Since reinforced concrete is a composite material, where reinforcement and concrete are attached, there is an obvious need for interaction and transfer of forces between them. As illustrated in Figure 3.5 a force is transferred by means of stresses acting along the surface area of the reinforcement bar within a certain transmission length. These stresses are called bond stresses and are usually denoted τ_b .

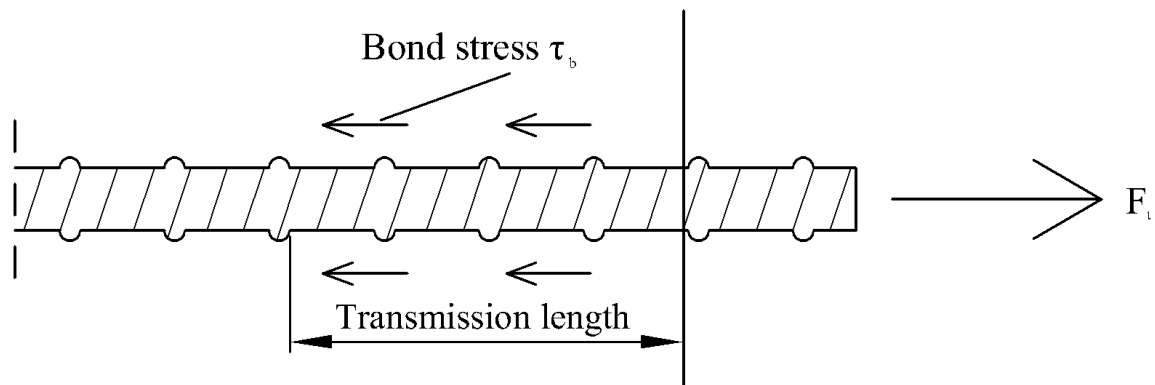


Figure 3.5 Transfer of force between a reinforcing bar and concrete

3.1.4.1 Physical components of bond stresses

From a physical point of view bond stresses depend on different contributions. For low needs of force transfer, bond stresses are mainly resisted by adhesion. The cement paste of the concrete surrounding the reinforcement virtually functions as glue. For increasing needs of force transfer and consequently also higher bond stresses, the effect of adhesion decomposes. At this stage force transfer is mainly due to shear key effect, Engström (2011e).

Irregularities of the surface area give rise to the shear key effect. The surface of a reinforcement bar always has some irregularities and a certain roughness. This is true even for plain bars, although they are no longer used as reinforcement in structural concrete, Engström (2011e). Instead bars with intentionally deformed surface shape, commonly by added ribs, are used to enhance the roughness and consequently improve mechanical engagement with the surrounding concrete. The shear key effect between a reinforcement bar and its surrounding concrete causes inclined principle stresses, in both compression and tension, in close proximity to the bar. If the stresses in tension reach the tensile strength of the concrete, inclined cracks originating from the ribs occur, as illustrated in Figure 3.6.

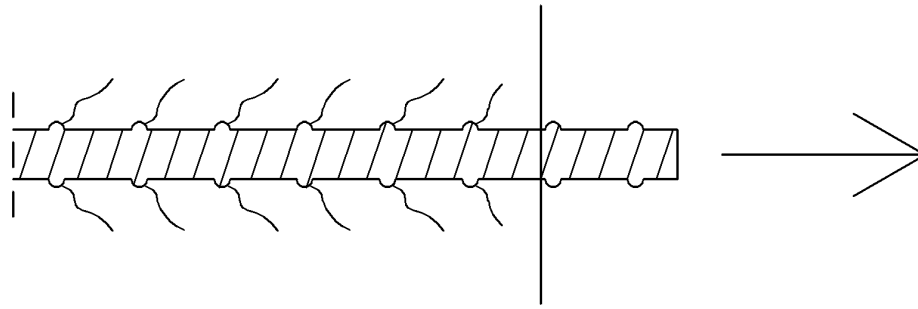


Figure 3.6 Inclined cracks due to shear key effect at the interface of an anchored reinforcement bar

When the inclined cracks occur, the reinforcement is anchored within the concrete by inclined compressive forces. The horizontal component of this inclined force can be regarded as the bond stress acting along the reinforcement bar. These inclined forces acts in three-dimensional compressed cone shaped shells, as illustrated in Figure 3.7. These shells arise between the inclined cracks originating from the ribs, visualised in Figure 3.6. These are balanced by a tensile stress ring in the concrete in order to maintain equilibrium, Tepfers (1973).

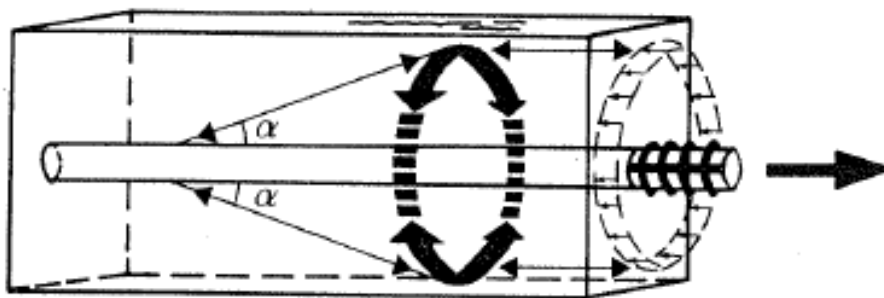


Figure 3.7 Compressive forces acting in three-dimensional shells at anchorage of a reinforcement bar, from Tepfers (1973)

It should be noted that different types of anchorage failure could occur, if reinforcement detailing is inadequate. Examples of such failures are pull-out failure and splitting failure, both of which are illustrated in Figure 3.8. Although important in structural design, anchorage failures have not been considered in this project. For more information about anchorage failures reference is made to Engström (2011e).

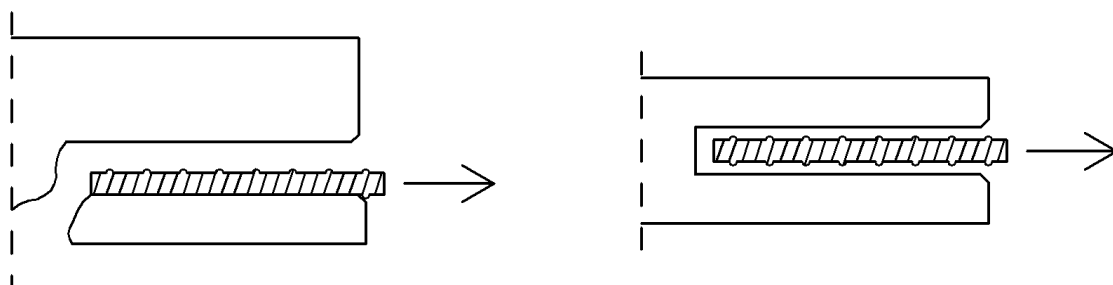


Figure 3.8 Examples of anchorage failure, to the left; splitting failure and to the right; pull-out failure

3.1.4.2 Bond stress – slip relation

A bond stress at a section is always associated with a certain local slip of the reinforcement bar in relation to the surrounding concrete in the same section. For instance, if a force is applied directly to the bar, while no external load is applied on the concrete, a strain difference between the two arises due to the relative elongation of the reinforcement. This strain difference is evened out along the transmission length. Thus, if a load is applied to the end of a reinforcement bar, the concrete and steel strains are equal one transmission length away from the loaded end.

Furthermore, the actual extension of the transmission length is dependent on the load level. As mentioned earlier a bond stress is always associated with a certain local slip, which implies that a bond stress-slip relation exists. Such a relation can be found experimentally by using a pull-out test where a centrally placed reinforcement bar with a short embedment length is loaded in tension. The principle of the test is illustrated in Figure 3.9.

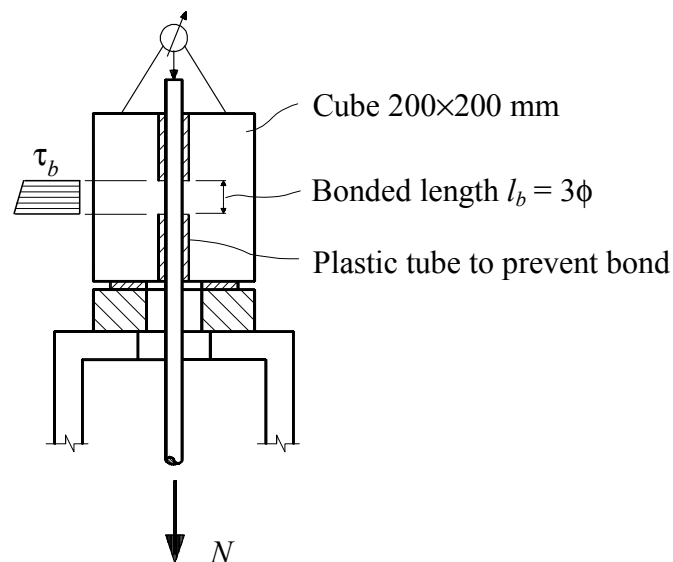


Figure 3.9 Principle of a pull-out test of reinforcement

By measuring the force applied to the reinforcement bar and the displacement of the bar in relation to the concrete surface, a bond stress-slip relation can be determined. Due to the short embedment length the force can be assumed to cause a uniformly distributed bond stress over the surface area, Engström (2011a). The results from a series of such experiments are illustrated in Figure 3.10, together with a figure illustrating the bond mechanisms at different slips in a typical manner.

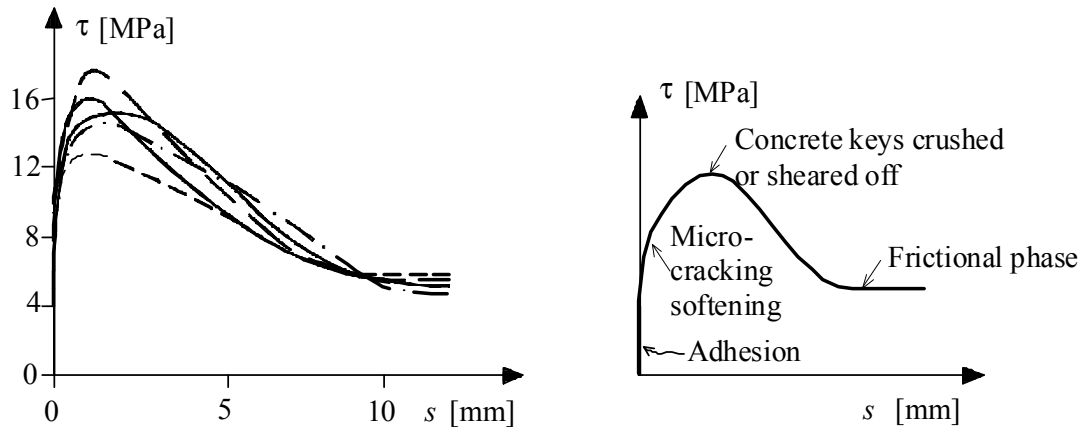


Figure 3.10 Experimental and schematic bond stress-slip curve, from Engström (2011a)

Based on such experiments an idealised relation between bond stress and slip has been suggested in the CEB-FIP Model Code 1990, CEB (1993), see Figure 3.11.

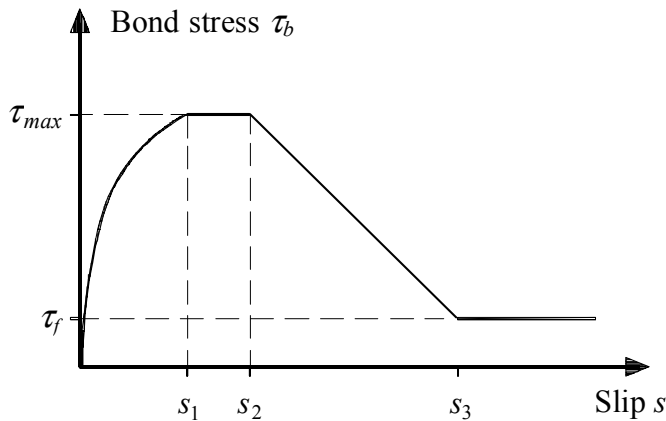


Figure 3.11 Model for bond stress-slip relation according CEB-FIP Model Code 1990

As indicated in Figure 3.11, a certain local slip s is required to reach the maximum bond stress. However, in normal service state the actual slip rarely reaches this value. This means that using only the first branch of the curve could be enough in service state analysis. According to Engström (2011a) this can be mathematically expressed as

$$\tau_b(s) = 0,22 \cdot f_{cm} \cdot s^{0,21} \quad (3.1)$$

where f_{cm} is the mean concrete compressive strength for concrete
 s is the slip

It should be noted that neither the bond stress nor the local slip is constant along the length of a reinforcement bar. Consider a reinforcement bar load axially at its end. For small loads, exemplified in Figure 3.12a, bond stresses only exist along part of the length of the embedded bar. In this case the transmission length needed is smaller than the available embedded length. Since the steel strain decreases along the transmission length, the bond stress and consequently also the local slip are different in different sections of the bar. It is obvious that the maximum slip (and steel strain) occurs at the

loaded end and that no slip exists at the end of the transmission length. Consequently, the bar does not move as a rigid body and different bond mechanisms may act in different sections regions along the bar.

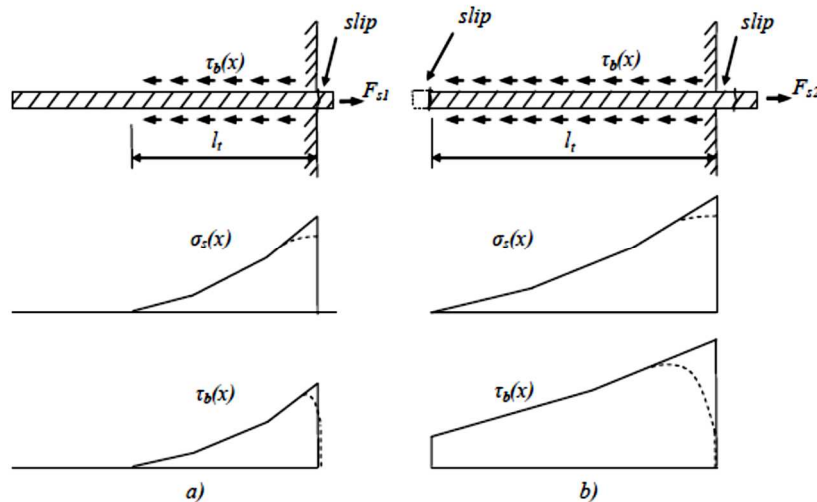


Figure 3.12 Stress distribution along the embedment length of a reinforcement bar
a) small load, less than the embedded length is activated
b) large load, embedded length is shorter than a fully developed transmission length

Figure 3.12b illustrates a case where the embedded length is shorter than a fully developed transmission length. Consequently the transmission length must be equal to the embedded length. In this case the bond stress will be non-zero at the end of the transmission length and slip occurs, but of different magnitudes, at both ends of the bar. Thus the extent of the transmission length, bond stresses and slip might vary greatly depending on the conditions in different situations. Note that the concept of transmission length is important with regard to crack distribution, which is treated in Section 3.5.2.

3.1.5 Interaction between concrete and concrete

3.1.5.1 Shear effect

The interaction between two concrete layers cast at different times depends on many different factors. According to fib Model Code 2010, fib (2013), the interaction depends of three main contributions. These are adhesion/interlocking, shear friction and dowel action.

The adhesive bond and mechanical interlocking depend on several different parameters, for instance strength classes of both concretes and the surface roughness. Adhesion can develop along a smooth surface, but the mechanical interlocking effect needs a sufficient surface roughness to develop, see the principle in Figure 3.13. If the shear deformation is small, the adhesion and interlocking effect can have a significant influence on the shear resistance, but if the deformation increases, this effect decreases due to the loss of bond and failure of upstanding parts in the surface.

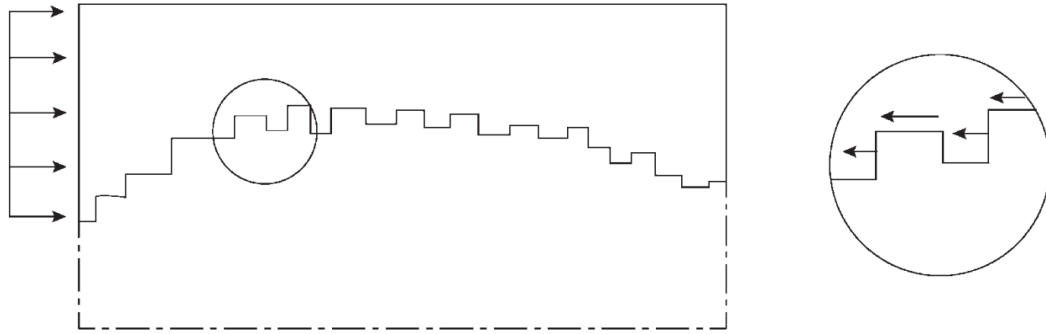


Figure 3.13 Principle of adhesion/interlocking, fib (2013)

Shear friction resistance can appear when the interface is exposed to a compression force perpendicular to the interface, see Figure 3.14. The shear friction depends on the roughness of the surface, the rougher surface the larger the shear friction.

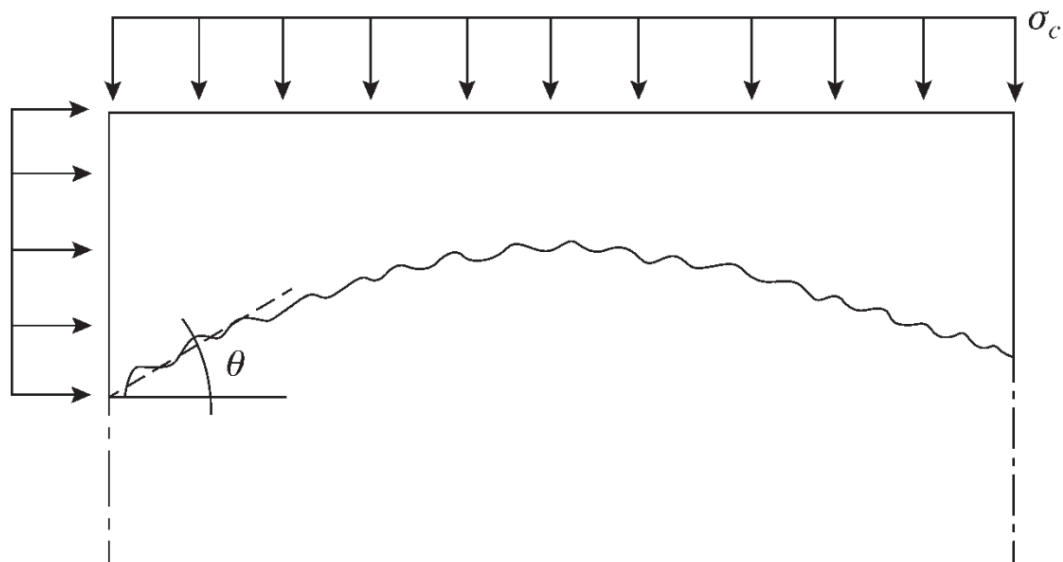


Figure 3.14 Principle of shear friction, fib (2013)

The dowel action is the resistance of connectors, such as transverse reinforcement bars and dowels, through bending action. If the shear slip is very large, a plastic deformation of the connector appears and a kinking effect can be observed. For the principle of the dowel effect, both for bending and kinking, see Figure 3.15.

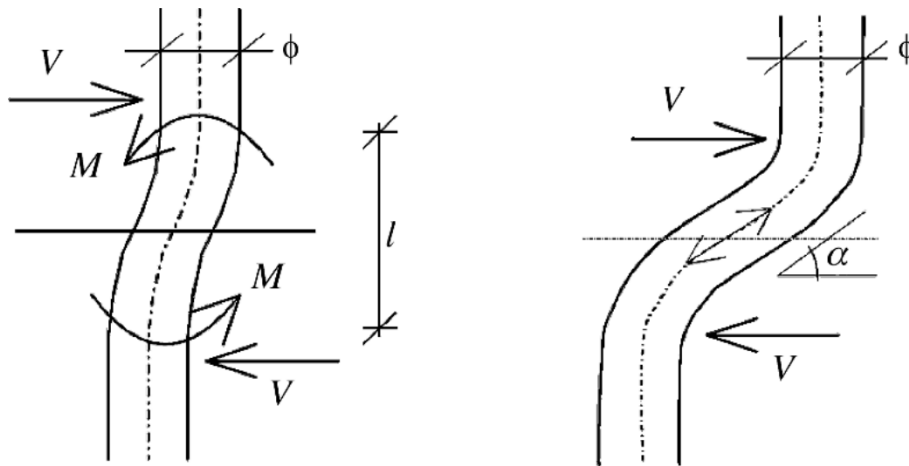


Figure 3.15 Principle of dowel action, shear resistance through bending on the left and kinking effect on the right, fib (2013)

Beside the dowel action a tensile force in the reinforcement due to the roughness of the surface is going to appear, see Figure 3.16. In real structures this tensile force have a large influence on the dowel action and due to it, the kinking effect may not even appear due to tensile failure before in the reinforcement bars.

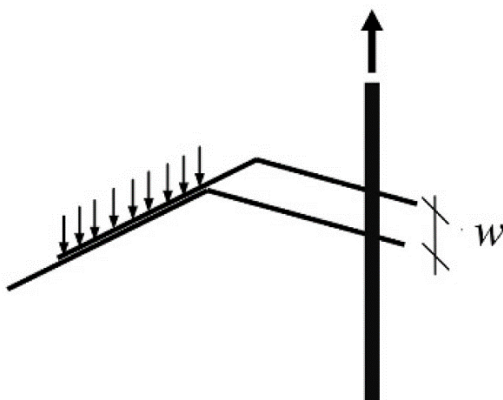


Figure 3.16 Principle of tensile force in the reinforcement bar due to the roughness of the surface, fib (2013)

Model Code 2010 proposes the following equation for the shear resistance of an interface which takes these effects into account.

$$\tau_{fu,d} = \tau_a + \mu \cdot (\rho \cdot \kappa_1 \cdot f_y + \sigma_n) + \kappa_2 \cdot \rho \cdot \sqrt{f_y \cdot f_{cc}} \leq \beta_c \cdot v \cdot f_{cc} \quad (3.2)$$

where	τ_a	is the shear resistant from adhesion/interlocking, see Table 3.1
	μ	is the friction coefficient, see Table 3.1
	ρ	is the reinforcement ratio of bars crossing the interface
	κ_1	is interaction (“effectiveness”) factor, see Table 3.1
	f_y	is the yield strength of the reinforcement
	σ_n	is the (lowest) normal compressive stress applied
	κ_2	is the interaction coefficient for flexural resistance, see Table 3.1
	f_{cc}	is the concrete compression strength
	β_c	is a reduction coefficient for the strength of inclined compression struts, see Table 3.1
	v	is the effectiveness factor for the concrete, see Equation 3.3

Table 3.1 Factors for calculation of the shear resistance at interfaces between concrete and concrete

Surface roughness	τ_a [MPa]	μ	κ_1	κ_2	β_c
Very rough	~2,5-3,5	1,0-1,4	0,5	0,9	0,5
Rough	~1,5-2,5	0,7-1,0	0,5	0,9	0,5
Smooth	-	0,5-0,7	0,5	1,1	0,4
Very smooth	-	-	0	1,5	0,3

The effectiveness factor for the concrete is according to fib Model Code 2010

$$v = 0,55 \cdot \left(\frac{30}{f_{ck}} \right)^{1/3} < 0,55 \quad (3.3)$$

where f_{ck} is the characteristic compressive strength inserted in MPa.

3.1.5.2 Shear stress to shear slip relation

The CEB-FIP Model Code 1990, CEB (1993), proposes an indicative relation between the shear stress and the shear slip at an interface between two different concrete layers. This relation is illustrated in Figure 3.17. As appears from the figure the relation between shear stress and shear slip is linear for a shear stress not exceeding half of the ultimate shear stress, i.e. $0,5 \cdot \tau_{fu,d}$. At that point the shear slip is

$0,05 \cdot s_u$. When the shear stress exceeds $0,5 \cdot \tau_{fu,d}$, the non-linear phase of the relation is entered.

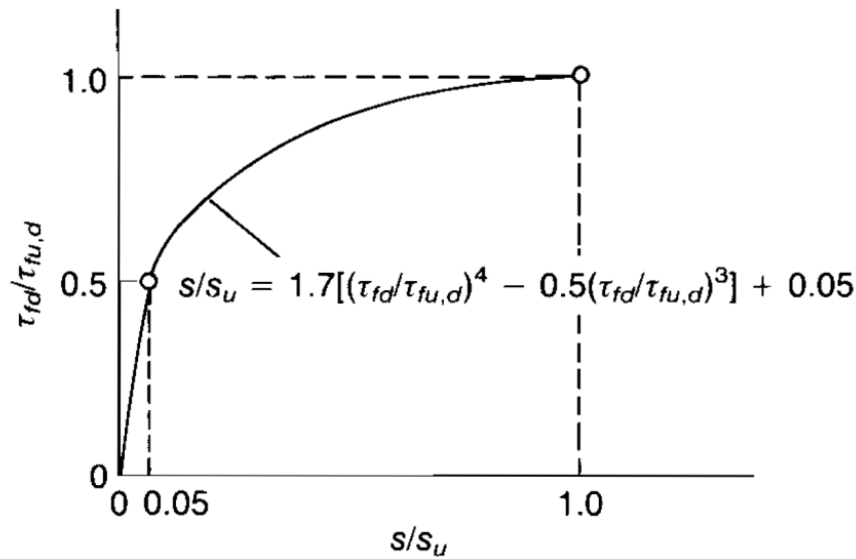


Figure 3.17 Shear-stress-slip relation for interaction between concrete and concrete, from CEB (1993)

For stresses lower than $0,5 \cdot \tau_{fu,d}$ a linear relation is used and that relation is expressed as

$$\tau_{fd} = 5 \cdot \tau_{fu,d} \cdot s \quad (3.4)$$

where τ_{fd} is the shear stress at the interface
 $\tau_{fu,d}$ is the ultimate shear stress at the interface
 s is the slip

For stresses exceeding $0,5 \cdot \tau_{fu,d}$, the non-linear relation expressed as

$$s / s_u = 1,7 \left[\left(\tau_{fd} / \tau_{fu,d} \right)^4 - 0,5 \left(\tau_{fd} / \tau_{fu,d} \right)^3 \right] + 0,05 \quad (3.5)$$

where s_u is the ultimate slip

The ultimate slip s_u , according to CEB-FIP Model Code 1990, should be taken as 2,0 mm.

3.1.6 Fibre reinforced concrete

Fibre reinforcement is an alternative, or complementary, approach to reinforce concrete structures. Although different in behaviour and applications the basic principle of fibre reinforcement is the same as for reinforcement in general, i.e. to compensate for the low tensile strength and low ultimate tensile strain of plain concrete. Fibre reinforced concrete (FRC) consists of a concrete matrix surrounding the fibre reinforcement, which makes it a composite material. These fibres are usually, but not always, added already during mixing.

The addition of fibres can greatly influence the properties of concrete. However, this influence varies significantly depending on such parameters as the material, shape, amount and distribution of the fibres. In general, the greatest influence of fibres is on the post-cracking behaviour. This is demonstrated in Table 3.2, which contains general values of mechanical properties of cement paste, normal and high strength concrete and fibre reinforced concrete respectively. The properties presented in the table are; compressive strength f_c , tensile strength f_t , modulus of elasticity E , fracture energy G_f and characteristic length l_{ch} (indicates material brittleness; low values indicate brittle nature and vice versa).

Table 3.2 Material properties of various concrete types, data from Löfgren (2005)

Material	f_c [MPa]	f_t [MPa]	E [GPa]	G_F [Nm/m ²]	l_{ch} [mm]
Cement paste	10-25	2,0-10,0	10-30	≈10	5-15
Normal strength concrete	20-80	1,5-5,0	25-40	50-150	200-400
High strength concrete	>80	4,0-5,5	40-50	100-150	150-250
Fibre reinforced concrete	20-80	1,5-5,0	25-40	>500	>1000

By studying the different values for normal strength concrete and fibre reinforced concrete in Table 3.2, some observations can be distinguished. The compressive strength, tensile strength and the modulus of elasticity are within the same ranges. However, the fracture energy and characteristic length are significantly increased for FRC compared to those of normal strength concrete, implying that FRC is considerably more ductile than ordinary concrete. Thus, in general, adding fibres to concrete mainly influence the post-cracking behaviour. However, it should be noted that there is a difference in behaviour impact depending on the size of the fibres added. It is possible to distinguish between microfibres and long fibres. The addition of long fibres, such as normal steel fibres, mostly influences the post-cracking behaviour. However, the addition of microfibres might affect the pre-cracking behaviour, where only micro-cracks exist, and could improve the tensile strength of concrete to some extent, Löfgren (2005). This is described further in Section 3.5.4.

Since the addition of fibres in concrete mostly affects the post-cracking behaviour, fibres are often used as secondary reinforcement for crack control. A positive consequence of this is that the amount of primary reinforcement (conventional steel bars) might be somewhat reduced.

There are a vast number of materials that are more ductile than concrete and thus represent possible alternatives for fibre reinforcement. However, there are a number of fibre types carrying considerably higher commercial weight than others. According to Purnell (2010) these commercially significant fibre types are polymer, steel, natural, glass, carbon and asbestos fibres. It should be pointed out that the use of asbestos fibres has declined to near zero due to the now widely known health

concerns. The most commonly used fibres are steel fibres, which have been used during a considerable time. Besides the material there are several possible cross-sectional shapes and geometries of fibres that can be used. For instance, the cross-section of a fibre could be circular, rectangular, triangular or irregular, while the fibre geometry could be straight, twisted, bow shaped or have special end shapes such as hooks, paddles and knobs, Löfgren (2005). This is illustrated in Figure 3.18 and Figure 3.19 respectively.

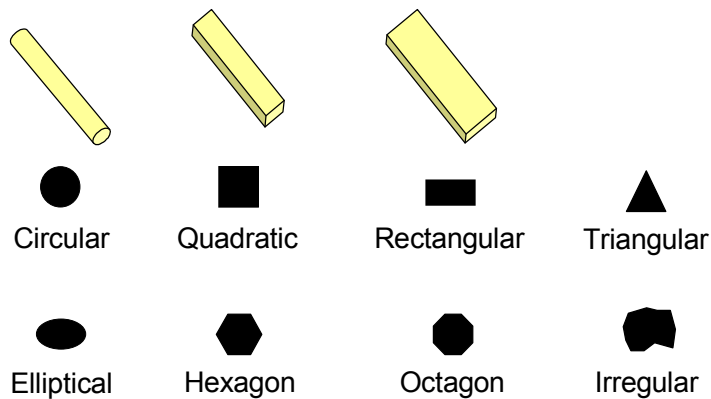


Figure 3.18 Different cross-sections for fibre reinforcement

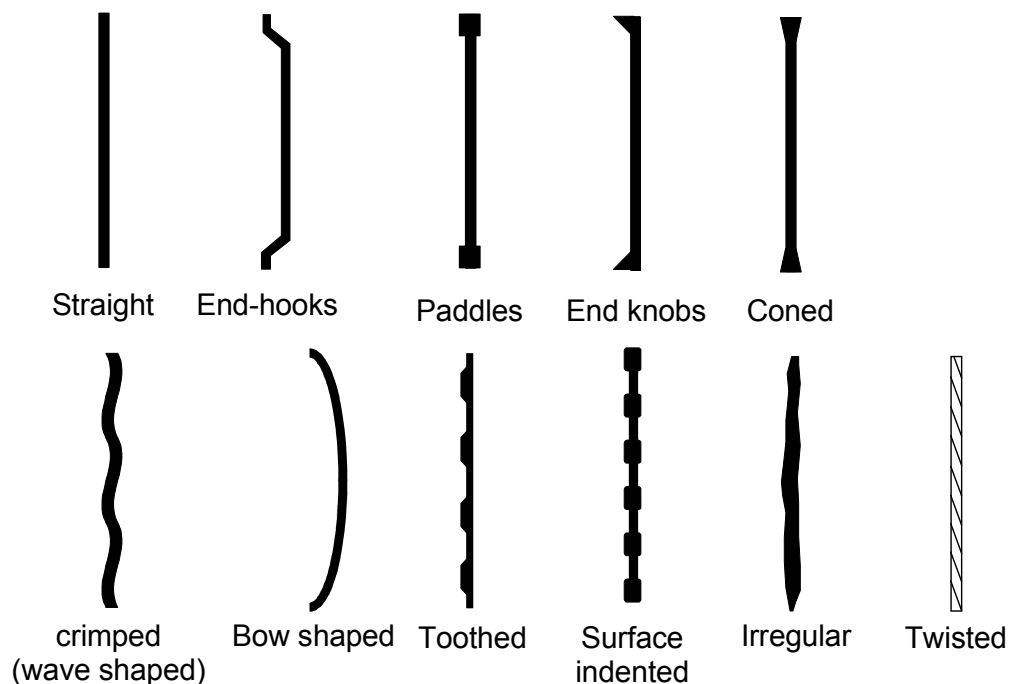


Figure 3.19 Different fibre geometries

As presented above, the influence on concrete behaviour varies greatly depending on the type of fibre used. Consequently different fibres are used for different purposes. Löfgren (2005) points out that some fibres are used to prevent concrete spalling during a fire, while others are being used to reduce plastic shrinkage or to improve the toughness of concrete and to reduce crack widths. Thus, fibre reinforced concrete can

be used for numerous different applications. Some of the main applications where FRC is preferred today are listed below, Purnell (2010).

- Components with thin sections (insufficient cover thickness for conventional reinforcement bars), such as roofing and cladding products.
- Industrial flooring, tunnel linings, marine structures and blast-restraint structures etc. where considerable and/or unpredictable localised deformations are expected.
- Crack control with regard to restrained shrinkage and thermal strain.

According to Purnell (2010), due to the distribution of its reinforcement, FRC excels in distributing cracking due to restrained intrinsic deformations (such as thermal and shrinkage strain). Thus FRC might potentially show a great influence on crack control with regard to restraint stresses in concrete walls. Cracking of fibre reinforced concrete is treated in Section 3.5.4.

3.2 Restraint

3.2.1 Stress-dependent strain and stress-independent strain

Strains in concrete can arise from numerous different reasons. Each strain occurring can be classified as either stress-dependent or stress-independent. It is important to distinguish them during design and analysis of concrete structures. The sum of all stress-dependent and stress-independent strains represents the total strain.

All strains occurring as a consequence of applied or imposed stress are called stress-dependent strains. Such strains might occur directly at loading or during time after load application. Hence, they can be immediate or time-dependent. Consider a concrete member loaded in compression. At loading the member deforms immediately. This deformation subsequently increases with time due to creep (see Section 3.4). All deformations occurring in this case are stress-dependent, but only the creep deformations are time-dependent.

All strains occurring without any applied stress are called stress-independent strains. These strains, if allowed to develop freely without restraint, only result in deformations and no stresses are generated. Stress-independent strains are generated from effects such as shrinkage (see Section 3.3) and thermal expansion or contraction. It should be noted that stress-independent strains can develop over a considerable period of time, just as stress-dependent strains due to creep. If any restraints, internal or external, are present in a concrete member subjected to stress-independent strains, free deformation is prevented. This generates stresses which in turn generate stress-dependent strains. Engström (2011a)

3.2.2 Restraint degree

Concrete structures always have a certain need for movement, which could originate from a variety of different causes. For instance, movements can originate from stress-dependent strains such as external loading as well as stress-independent strains such as shrinkage. If a concrete structure is in any way prevented from free movement, a restraint exists. The term restraint degree, denoted R , defines to what extent the

need for movement is prevented. If a structure's movement is completely prevented, full restraint exists and the restraint degree is equal to one. As opposed, if a structures movement is completely free, no restraint exists and the restraint degree is equal to zero. Thus, the restraint degree varies between zero and one. Traditionally, restraint degree is defined by means of imposed strains, as expressed in the following equation

$$R = \frac{\text{actual imposed strain}}{\text{imposed strain in case of full restrain } t} \quad (3.6)$$

When a need for movement is prevented, a certain stress-dependent strain occurs. This strain is equal to the actual imposed strain. If a full restraint exists, all stress-independent strains are prevented and thus the imposed strain must be equal to this stress-independent strain. Equation 3.6 might then be expressed by means of stress-dependent and stress-independent strains, as defined below, Engström (2011a).

$$R = \frac{\text{actual stress dependent strain}}{\text{-(stress independen } t \text{ strain)}} \quad (3.7)$$

However, the formulations of Equation 3.6 and Equation 3.7 are not well suited when a combination of internal and external restraints are to be expressed by means of a restraint degree. Instead the restraint degree is better expressed using restraint forces, defined as follows

$$R = \frac{\text{actual imposed force}}{\text{imposed force in case of full restrain } t} = \frac{N}{N_{\max}} \quad (3.8)$$

The restraint degree of a concrete member depends on both the stiffness of its boundaries (external restraint) and the stiffness of the member itself. Effects that decrease the stiffness of a member or its boundaries, such as creep and cracking, consequently also decrease the restraint degree. Thus, the actual restraint degree in a member varies over time, Engström (2011a).

This section only provides a general definition of the restraint degree. The equations provided can be applied to different situations of restraint, examples of applications related to external and internal restraints are treated in Section 3.2.3 and Section 3.2.4 respectively.

3.2.3 External restraints

Whenever a structure is hindered from free movement externally, at its supports or boundaries, the restraint is classified as an external restraint. Consider, for instance, a concrete wall being cast against an existing concrete slab. At its base the wall is attached to the slab and is consequently prevented from free movement there. Thus an external restraint exists. Note that the magnitude of such restraint varies within the height of the wall and that the restraint degree varies accordingly. At the connection between the wall and the slab, the wall is more or less fully fixed.

Figure 3.20 provides an example of how the restraint degree can vary across the height of a wall with a fixed base boundary and with its remaining edges free.

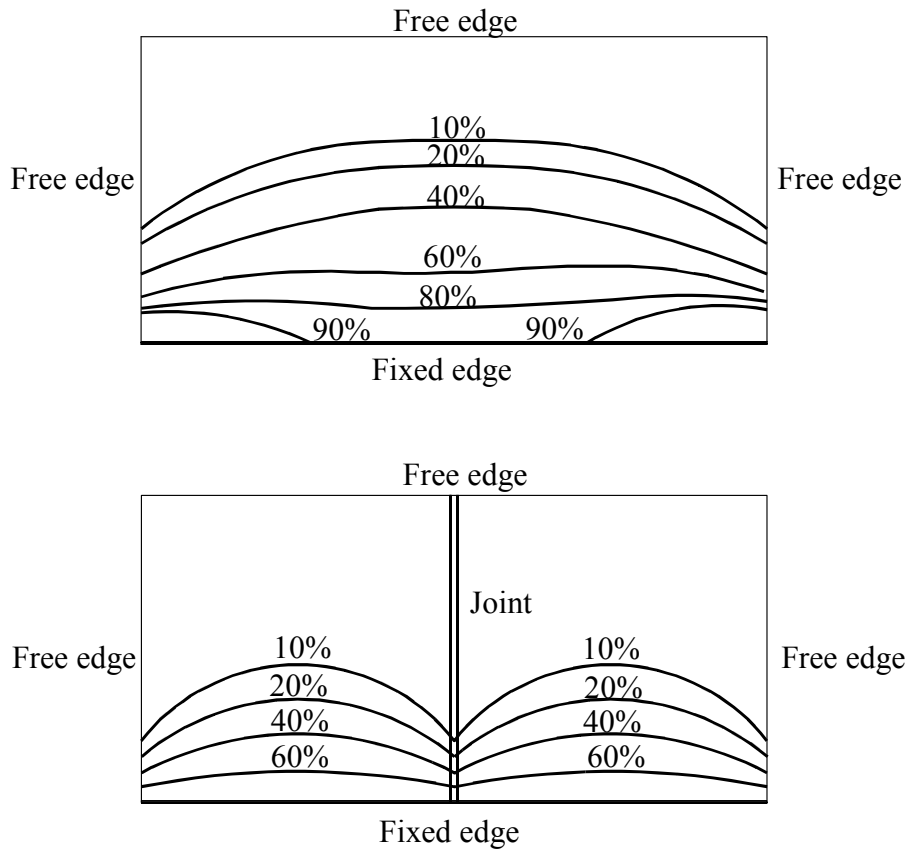


Figure 3.20 Variation of restraint degree within a wall with a fixed bottom boundary, from Engström (2011a)

The distribution of the restraint degree within such a wall depends on the relation between its length and height. When the length increases in relation to the height, the restraint increases. This variation is illustrated in Figure 3.21, which can be used to determine the restraint degree at different heights within such a wall.

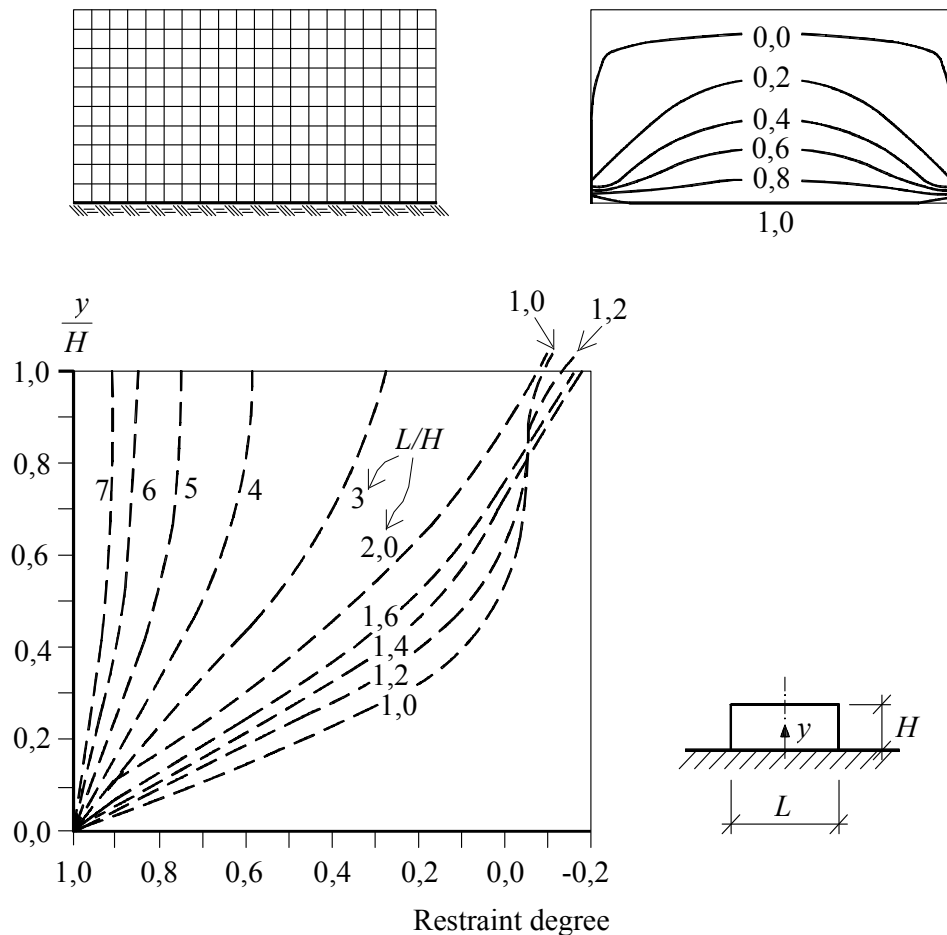


Figure 3.21 Variation of restraint degree in a wall with a fixed bottom boundary depending on the length to height ratio, Engström (2011a)

The influence of external restraints on the restraint degree within a structure varies greatly depending on parameters such as boundary conditions, size and the existence of joints. A boundary can be free, fixed or partially restrained and different boundaries on the same structure might have entirely different boundary conditions. If a joint exists, the restraint decreases at and near the joint compared to if there was no joint present.

In case of partial restraint the boundaries providing such restraint are flexible. The restraint degree of such a boundary is always greater than zero and smaller than one. In reality all boundaries other than those that are completely free are to some extent flexible. However, in calculations some boundaries can be assumed completely free or fixed. For a prismatic concrete member where the short ends have flexible boundaries, the partial restraint can be treated by defining a support stiffness, denoted S . Assuming a linear variation with constant stiffness the support stiffness can be defined as

$$S = \frac{N}{n} \quad (3.9)$$

where N is the normal force
 n is displacement of each support

Equations 3.6-3.8, presented in Section 3.2.2, are used to define the restraint degree. These form a basis for expressing the restraint degree in different cases of external

restraint. For instance, consider the long term response of a plain concrete member exposed to externally restrained shrinkage. The restraint degree of such a member can be expressed as, Engström (2011a).

$$R_{ext} = \frac{N}{N_{max}} = \frac{\varepsilon_{ct} E_{c,ef} A_c}{-\varepsilon_{cs} E_{c,ef} A_c} = \frac{\varepsilon_{ct}}{-\varepsilon_{cs}} \quad (3.10)$$

where N is the normal force
 ε_{ct} is the concrete tensile strain
 $E_{c,ef}$ is the effective Young's modulus of concrete, see Section 3.4
 A_c is the concrete area
 ε_{cs} is the concrete shrinkage strain

For a prismatic member with partially restrained ends with support stiffness S , it is possible to define the restraint degree by stiffness relations, as expressed below, Engström (2011a).

$$R_{ext} = \frac{1}{1 + 2 \cdot \frac{E_{cm} A_c}{S \cdot l}} \quad (3.11)$$

where E_{cm} is the mean Young's modulus for concrete
 A_c is the concrete area
 S is the support stiffness, see Equation
 l is the length of the member

3.2.4 Internal restraints

Internal restraints are defined by the situation when different parts of a cross-section of a concrete member cannot move freely in relation to each other, i.e. different needs for movement do not fit within the cross-section. Stresses are generated as a consequence of internal restraint. However, these stresses are eigenstresses, which must balance each other out within the cross-section.

Stress-independent strains might demonstrate both linear and non-linear variations within a cross section. The difference is of great importance with regard to internal restraint. If the variation is non-linear, internal restraint and eigenstresses are generated. Due to the fact that a linear variation will allow all parts of the cross section to fit together, no eigenstresses develop. A need for curvature is generated instead. Stresses, but not eigenstresses, will however be generated, if the need for curvature is prevented by an external restraint.

Internal restraint can originate from several causes and one of the most common is reinforcement. When reinforced concrete shrinks, the reinforcement provides an internal restraint, preventing the concrete from free shrinkage movement. The restraint degree can then be expressed as

$$R_{\text{int}} = \frac{F_{cs}}{-\varepsilon_{cs} E_{c,ef} A_{I,ef}} = \frac{\varepsilon_{ct}}{-\varepsilon_{cs}} \quad (3.12)$$

where F_{cs} is the shrinkage force acting on the reinforced concrete section, defined as $F_{cs} = |\varepsilon_{cs}| E_s A_s$

ε_{cs} is the shrinkage strain of the concrete

$E_{c,ef}$ is the effective Young's modulus of concrete, see Section 3.4

$A_{I,ef}$ is the effective cross sectional area of state I, see Engström (2011b)

ε_{ct} is the concrete tensile strain

E_s is the Young's modulus of the reinforcement steel

A_s is the cross sectional area of the reinforcement steel

Most real structures are exposed to internal and external restraints simultaneously which could increase the difficulty of the analysis. There are also cases when the same restraint can be considered as either external or internal depending on how the concrete member is considered. The following example of such a case is obtained from Svensk Byggtjänst (1994). Consider a wall cast against an existing wall. If only the newly cast wall is considered, the connection to the existing wall provides an external restraint. However, if the wall as a whole is considered, there will be an internal restraint at the section where the new wall was cast against the existing wall.

3.3 Shrinkage

The shrinkage of concrete starts already in the fresh concrete and is an ongoing process during long time. The final value of the total shrinkage strain $\varepsilon_{cs}(\infty)$ in concrete is usually in the magnitude of $0,1 \cdot 10^{-3}$ too $0,5 \cdot 10^{-3}$ depending on the surrounding environment. This relatively small strain can have a significant impact on the cracking of concrete.

There are mainly two different sources of shrinkage, drying shrinkage and autogenous shrinkage. According to Eurocode 2, CEN (2004), the total time dependent shrinkage strain can be expressed as follows

$$\varepsilon_{cs}(t) = \varepsilon_{cd}(t) + \varepsilon_{ca}(t) \quad (3.13)$$

where $\varepsilon_{cs}(t)$ is the total shrinkage strain

$\varepsilon_{cd}(t)$ is the drying shrinkage strain

$\varepsilon_{ca}(t)$ is the autogenous shrinkage strain

3.3.1 Drying shrinkage

The mechanism for drying shrinkage is the exchange of moisture between concrete and its ambient environment. Depending on how much moisture there is in the environment the concrete can either swell or shrink. However, swelling of concrete is quiet rare. In general the drying shrinkage develops under long time. The

development of the shrinkage is depending on various parameters, for example the thickness of the structure and if the structure is able to dry out at all the faces or not.

If a concrete member, for instance a wall or a slab, is subjected to one sided drying, the shrinkage in the concrete is not going to be uniform throughout the structure. For example in a slab where the concrete is cast against a permanent steel sheet, see Figure 3.22, the shrinkage strain varies non-linearly, Engström (2011a).

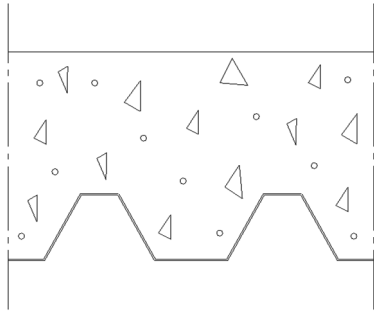


Figure 3.22 Concrete slab cast against a permanent steel sheet

Engström (2011a) provides an example of a non-linear shrinkage strain distribution in case of a 170 mm thick slab exposed to one sided drying. The shrinkage strain then varies non-linearly between $0,149 \cdot 10^{-3}$ in the top and $0,06 \cdot 10^{-3}$ in the bottom of the slab, see Figure 3.23. The mean value of the strain is $0,08 \cdot 10^{-3}$. However, in Eurocode 2 the method for shrinkage strain only predicts the mean value of the shrinkage strain in the section and not its distribution.

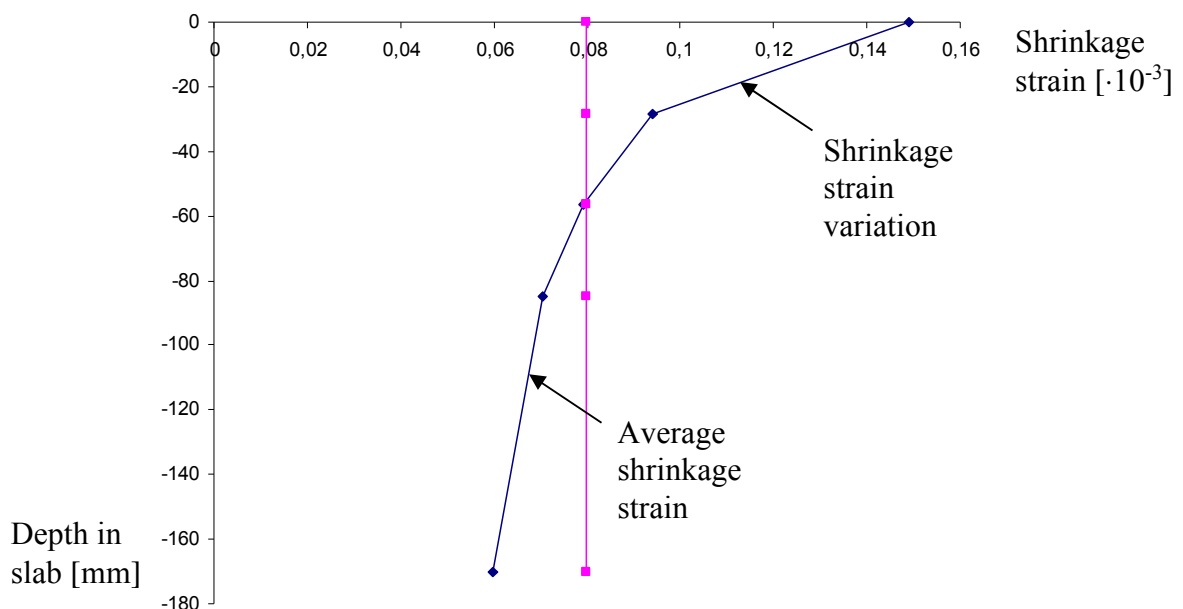


Figure 3.23 Plot of shrinkage strain versus the depth of the slab in Figure 3.22

The drying shrinkage strain is in Eurocode 2 expressed as

$$\varepsilon_{cd}(t) = \beta_{ds}(t, t_s) \cdot k_h \cdot \varepsilon_{cd,0} \quad (3.14)$$

where $\beta_{ds}(t, t_s)$ is time function for drying shrinkage development
 k_h is a coefficient depending on h_0 (notional size), see Table 3.3
 $\varepsilon_{cd,0}$ is a reference value of the shrinkage strain

Table 3.3 Values for k_h (linear interpolation between values)

h_0 [mm]	k_h
100	1,0
200	0,85
300	0,75
≥ 500	0,70

The notional size of the cross section is defined below.

$$h_0 = \frac{2A_c}{u} \quad (3.15)$$

where A_c is the concrete cross-sectional area
 u is the perimeter of the part of the cross section that is exposed to the atmosphere

The time function $\beta_{ds}(t, t_s)$ for the development of the drying shrinkage is defined as

$$\beta_{ds}(t, t_s) = \frac{(t - t_s)}{(t - t_s) + 0,04\sqrt{h_0^3}} \quad (3.16)$$

where t is the actual age of the concrete in days
 t_s is the age of concrete (in days) at the beginning of drying shrinkage (normally this is at the end of curing)
 h_0 is the notional size inserted in mm

The reference value of the shrinkage strain is presented in Eurocode 2 for different concrete strength classes and types of cement.

3.3.2 Autogenous shrinkage

Autogenous shrinkage appears due to the chemical reaction, hydration, under the hardening process of the concrete. This type of shrinkage develops under a shorter time period than the drying shrinkage. Almost 50% of the autogenous shrinkage has develop after only 10 days. The hydration process consumes water and this is not dependent of any exchange of moisture with the surroundings. Because of this there is a positive effect of autogenous shrinkage, the concrete becomes dryer in the early stage.

In concrete with low water/cement ratio there is a low permeability and therefore it is harder for moisture to be transported within the concrete. With the slow transportation rate of moisture, drying shrinkage mainly appears on the surface of the concrete, while the autogenous shrinkage is the most significant shrinkage in the centre of the cross-section. This can lead to a non-uniform shrinkage distribution across the cross-section.

The autogenous shrinkage strain is expressed in Eurocode 2 as

$$\varepsilon_{ca}(t) = \beta_{as}(t) \cdot \varepsilon_{ca}(\infty) \quad (3.17)$$

where $\varepsilon_{ca}(\infty)$ is the final autogenous shrinkage depending on the concrete strength class
 $\beta_{as}(t)$ is the time function for the development autogenous shrinkage

The final autogenous shrinkage strain is defined as

$$\varepsilon_{ca}(\infty) = 2,5(f_{ck} - 10) \cdot 10^{-6} \quad (3.18)$$

where f_{ck} is the characteristic compressive strength of the concrete in [MPa]

The time function of the autogenous shrinkage is expressed as

$$\beta_{as}(t) = 1 - \exp(-0,2 \cdot t^{0,5}) \quad (3.19)$$

where t is the actual age in days

3.4 Creep

When concrete is subjected to stress it deforms. This deformation can be divided in two parts. The first part of the deformation is the instant elastic deformation, which takes place directly when the stress is applied, and the second part is a time dependent creep deformation, see Figure 3.24. Note that the total stress dependent deformation of concrete subjected to stress is the sum of the elastic deformation and the creep deformation. The time dependent creep deformation is an ongoing process for a long time. It can be assumed to have reached its final value after around 70 years, Engström (2011d).

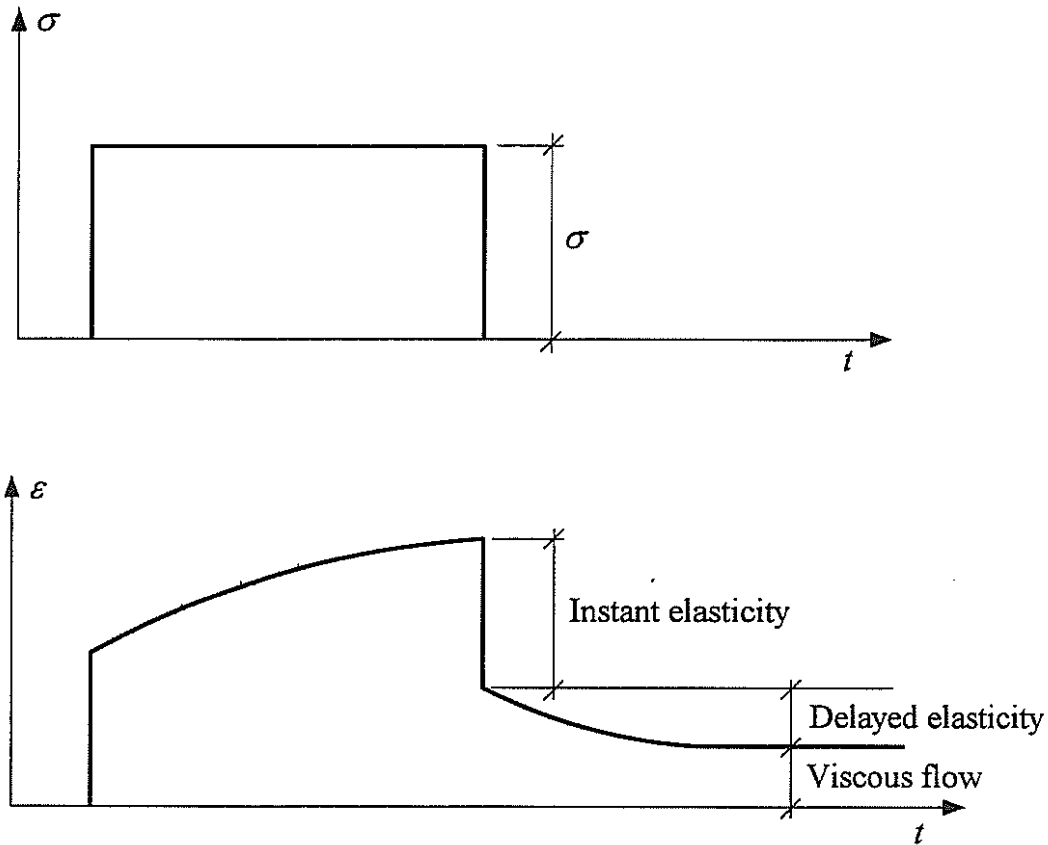


Figure 3.24 Instant and time dependent deformations due to loading

The magnitude of the creep deformation depends on the age of the concrete when the stress is applied. For instance, if the concrete is subjected to a stress at an early age, the creep is going to be larger than if it is subjected to the same stress later on. The creep coefficient is therefore related to both the actual age and the age when the stress was applied.

The creep strain in Eurocode 2, CEN (2004), is expressed as follows

$$\epsilon_{cc}(t, t_0) = \varphi(t, t_0) \frac{\sigma_c}{E_c} \quad (3.20)$$

where $\varphi(t, t_0)$ is the creep coefficient
 t is the actual age considered
 t_0 is the age of the concrete when it's loaded
 σ_c is the concrete stress
 E_c is the Young's modulus

In Equation (3.20) the creep strain is proportional to the concrete stress. However, when the concrete stress exceeds $0,45 f_{ck}$, Eurocode 2 states that non-linear creep should be considered.

The creep coefficient in Eurocode 2, not accounting for non-linear creep, is expressed as

$$\varphi(t, t_0) = \beta_c(t, t_0) \cdot \varphi_0 \quad (3.21)$$

where φ_0 is the notional creep coefficient
 $\beta_c(t, t_0)$ is the time function for development of creep during time

The notional creep coefficient is determined as

$$\varphi_0 = \varphi_{RH} \cdot \beta(f_{cm}) \cdot \beta(t_0) \quad (3.22)$$

where φ_{RH} is a factor that consider the relative humidity in the creep
 $\beta(f_{cm})$ is the factor that consider the concrete strength of concrete
 $\beta(t_0)$ is a factor that consider the age of the concrete when it is loaded

Equation (3.22) usually results in a value between 1 and 3 under normal service conditions. In an indoor environment the creep coefficient and hence also creep deformation is going to be larger than in a moist outdoor environment. How the creep develops under time is considered with the time function $\beta_c(t, t_0)$ which is determined as

$$\beta_c(t, t_0) = \left(\frac{(t - t_0)}{(\beta_H + t - t_0)} \right)^{0,3} \quad (3.23)$$

where t is the actual age of concrete in days
 t_0 is the age of concrete in days at loading
 $t - t_0$ is the non-adjusted duration of the loading
 β_H is a function depending on the relative humidity and the notional size (h_0 in mm)

For a complete calculation procedure see Eurocode 2, CEN (2004).

In a structure that is subjected to restraint related stresses, for example due to prevented shrinkage, creep has a positive effect on the uncracked concrete. The prevented deformation in the concrete results in a tensile stress. Under time the creep effect results in a reduction of the tensile stress in the concrete and an increase of the stress in the reinforcement, Engström (2011a).

When performing analysis according to Eurocode 2, creep can be considered by means of an effective modulus of elasticity. Since stiffness-dependent parameters, e.g. deflection, are time dependent, so is the effective modulus of elasticity. Hence, for the time of interest, the creep coefficient is calculated and subsequently the effective modulus of elasticity is calculated as defined below.

$$E_{c,ef} = \frac{E_c}{1 + \varphi(t, t_0)} \quad (3.24)$$

where E_c is the Young's modulus of concrete

For a constant stress level creep deformations can be considered directly according to the method described above. However, the stress level in a real structure is rarely constant and creep deformations should be determined with regard to the varying stress levels during time. Since the creep coefficient is dependent on the concrete age

at the time of load application, each load change corresponds to a unique creep coefficient. There are several approaches of how to consider creep under varying stress, Engström (2011a) defines four such approaches.

The first and simplest approach to consider creep under varying stress is based on the first creep function and ignores the loading history. Using this approach, an effective modulus of elasticity, as defined by Equation (3.24), is calculated where the creep coefficient $\varphi(t, t_0)$ is defined based on the age of the first load application. Then the concrete strain at the age t is related by Equation (3.20) to the stress acting at the same time. It should be noted that this approach overestimates the creep deformations, if the stress increases over time and, consequently, underestimates the creep deformations, if the stress decreases over time. The second approach is almost identical to the first approach, but the creep coefficient is multiplied by a relaxation factor in order to decrease the overestimated effects.

A third approach is to calculate an effective creep coefficient as a weighted average of several creep functions. This approach considers the load history and a unique creep function is determined for each load increment. Calculation of the effective creep coefficient is performed as

$$\varphi_{ef}(t, t_0) = \frac{\sum_i \varphi_i(t, t_i) \cdot \sigma_{ci}}{\sum_i \sigma_{ci}} \quad (3.25)$$

where $\varphi_{ef}(t, t_0)$ is the effective creep coefficient
 $\varphi_i(t, t_i)$ is the creep function related to load increment i
 σ_{ci} is the stress increment of i

The fourth approach considered is the superposition method. Using this approach different stress contributions are considered using their own respective creep coefficient. This is exemplified for three stress contribution in the following equation

$$\varepsilon_{cc}(t) = (1 + \varphi(t, t_1)) \frac{\sigma_1}{E_c} + (1 + \varphi(t, t_2)) \frac{\sigma_2}{E_c} + (1 + \varphi(t, t_3)) \frac{\sigma_3}{E_c} \dots \quad (3.26)$$

where σ_i is the stress component i
 $\varphi(t, t_i)$ is the creep function related to load increment i

At time t_1 the stress changes and the stress component σ_1 is considered using a unique creep coefficient for the time t_1 , i.e. $\varphi(t, t_1)$. Each change of stress can then be considered by an additional stress component with a corresponding creep coefficient. A decrease in stress is easily considered by adding a negative stress component.

The superposition method is preferably used numerically, where in case of continuously varying stress three or four time steps are usually enough for an adequately accurate estimation. Increasing the number of time steps increases the accuracy of the calculation, Engström (2011a).

3.5 Cracking process

It is important to empathise that reinforcement cannot be used to prevent cracking, with the exception or prestressing. Due to its low tensile strength concrete cracks already at small tensile strains. Since there is an interaction between the materials, the strains should match (assuming full interaction and no local slip). Thus before concrete cracking the steel stresses are limited by the low tensile strain dictated by the concrete. With these small stresses the reinforcement is only utilised to a small degree of its capacity and has a limited influence on an uncracked concrete member, as mentioned in Section 3.1.3. However it is also important to empathise that despite not being able to prevent cracking, reinforcement is necessary in order to ensure good crack control.

3.5.1 Cracking of plain concrete

In order to understand the complex cracking processes of reinforced concrete, a good starting point is the cracking process occurring when a plain concrete specimen is loaded until tensile failure in a uniaxial deformation controlled test. Figure 3.25 illustrates different stages of such a test.

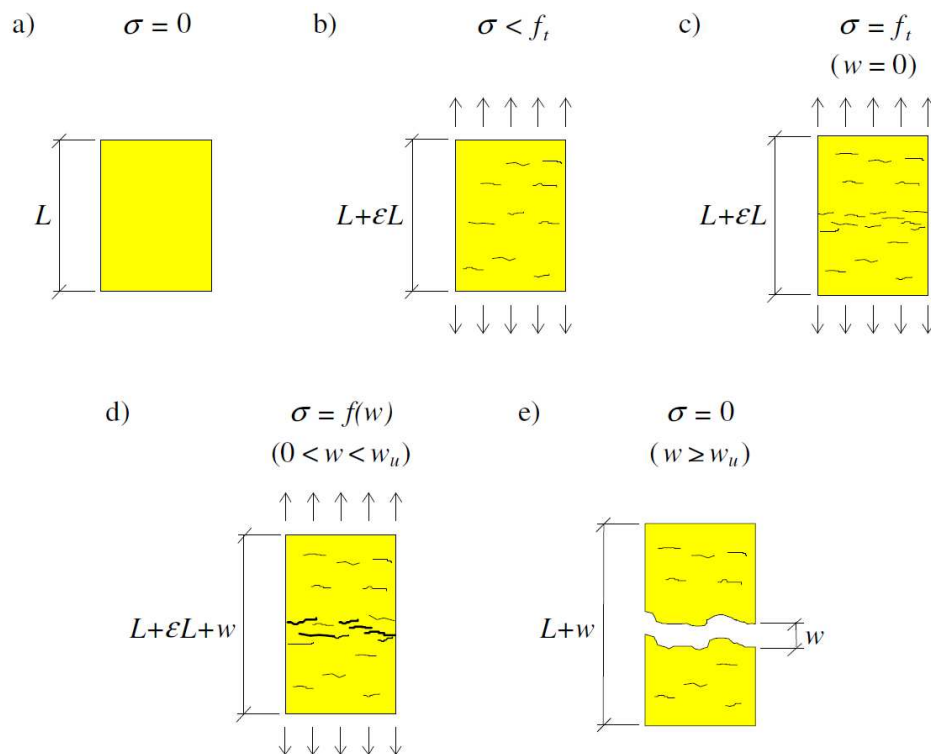


Figure 3.25 Uniaxial, deformation controlled, tensile test of plain concrete, from Plos (2000)

In stage a) the specimen is unloaded and unstrained. This stage is the starting point of the test and the deformation is applied gradually until the failure in stage e) is obtained. As the deformation increases within stage b), keeping stresses lower than the tensile capacity, microcracks are forming at local weak spots in the specimen. Then the deformation is increased further and stresses in the specimen reach the

tensile capacity and thus, in stage c), deformations are localising in the weakest section of the specimen by connecting of microcracks. This means that a fracture zone is formed and that the maximum stress is reached. After this stage, when the deformation increased beyond that generating the maximum stress, stage d) is entered. Here parts of the specimen outside of the fracture zone become unloaded, while the deformation within the fracture zone increases as the stress decreases. After additionally increasing the imposed deformation, the specimen finally separates into two pieces and stresses can no longer be transferred across the crack. Thus the failure of stage e) is obtained, Plos (2000).

The resulting data from such a test can be used to generate an average stress-strain relation for the tested concrete. By simply dividing the applied deformation by the specimen length, the corresponding strain is obtained. However, since the deformations are localised to the fracture zone and not uniformly distributed over the specimen length, the average strain will vary depending on the specimen length for the same applied deformation. This is possible to overcome by subdividing the measured stress-displacement relation, illustrated in Figure 3.26a, into two separate relations as illustrated in Figure 3.26b. The left curve in Figure 3.26b represents a stress-strain relation for the elastic parts outside the fracture zone, while the right curve represents the stress-crack opening relation for the displacement within the fracture zone. It should be noted that this is an additional deformation to the overall strain of the specimen which takes place within the fracture zone. The area underneath the stress-crack opening curve (Figure 3.26b right) represents the important parameter fracture energy, denoted G_f , which expresses the energy needed for the fracture process, Plos (2000).

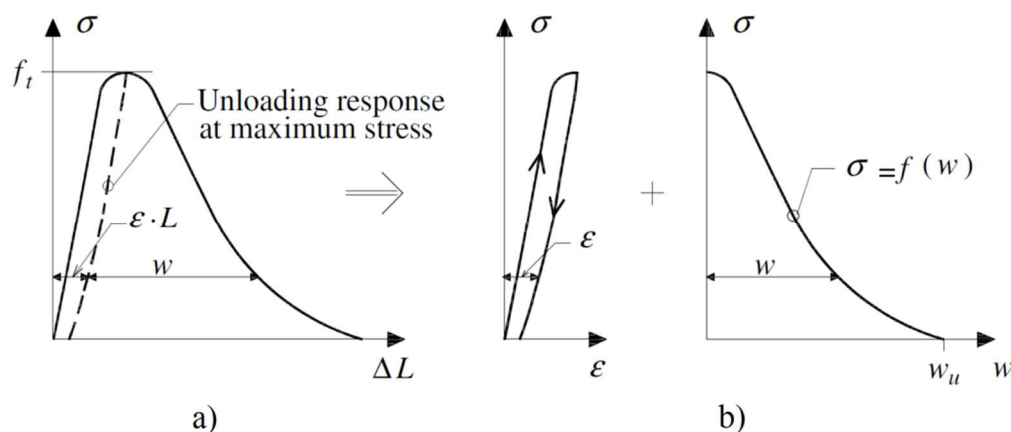


Figure 3.26 Stress-strain relation divided into stress-strain and stress-crack opening relations, based on Plos (2000)

3.5.2 Cracking of reinforced concrete

As noted above, reinforcement is needed for crack control. However, when a concrete structure is reinforced as opposed to being plain, the behaviour changes significantly. The typical behaviour of reinforced concrete is briefly exemplified in Section 3.1.3 using an example of a beam section loaded in bending. As presented there it is only the service state that is of interest with regard to crack control. The cracking process in a reinforced concrete member subjected to pure tensile loading is illustrated by its

average response in Figure 3.27. The two theoretical stages of the service state can be distinguished; the uncracked stage (state I) and cracked stage (state II).

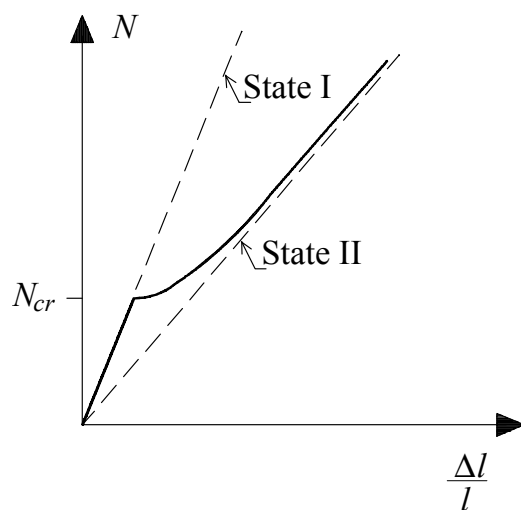


Figure 3.27 Load-displacement relation for a reinforced concrete member (or region) subjected to pure tensile loading

From no load up until the first crack appears the member is in the uncracked stage and all tensile stresses in the concrete are below the tensile capacity. In this stage the reinforcement has little influence on the overall behaviour, which can be considered as linear. Thus the behaviour is almost the same as assumed in a state I model, meaning linear elastic behaviour, where the entire concrete section and reinforcement are considered for the sectional parameters.

When the load is increased enough for the first crack to appear, the crack formation stage is entered and the stiffness is significantly decreased. Theoretically, a concrete member can be fully cracked instantly when the cracking load is reached. In reality though a certain load increase is needed to reach the fully cracked stage due to irregularities between different parts of the member. Generally this load increase is assumed to about 30%, Engström (2011a). While increasing the load in the crack formation stage, more and more cracks appear until the member is fully cracked and the stage of stabilised cracking is reached. Then theoretically no further cracks can be initiated and the final crack pattern has been obtained. In this stage the crack widths increases in correlation to the increasing load.

Studying the load-displacement curve in Figure 3.27, it is observed that the curve never reaches but only approaches the line representing state II (cracked section). This is due to the effects of tension stiffening. In a concrete member (or region), there are uncracked regions between cracks. Thus, the overall average response of a cracked concrete member only approaches the state II-line since not all sections are cracked.

A thin reinforced member load axially, illustrated in Figure 3.28, explains the cracking process and why there is a certain distance between cracks. Opposite ends of the reinforcement bar are directly loaded. As stated in Section 3.1.4, a transfer of forces takes place along the transmission length. For a sufficiently high load enough force is transferred for the tensile stress in the concrete to reach its tensile capacity. Hence, the maximum value of the transmission length is now obtained and the first

crack appears. When a crack occurs, a concrete stress can no longer exist at the crack interface. However, at a certain critical distance away from the first crack, enough force has been transferred to generate the cracking stress in the concrete and a new crack can occur. Consequently, there is a minimum distance between two cracks or one crack and a loaded end needed to generate a new crack. The crack spacing in a fully cracked member (stabilised cracking) can vary between one and two transmission lengths. Hence, if the distance between two cracks exceed two transmission lengths, a new crack could be formed.

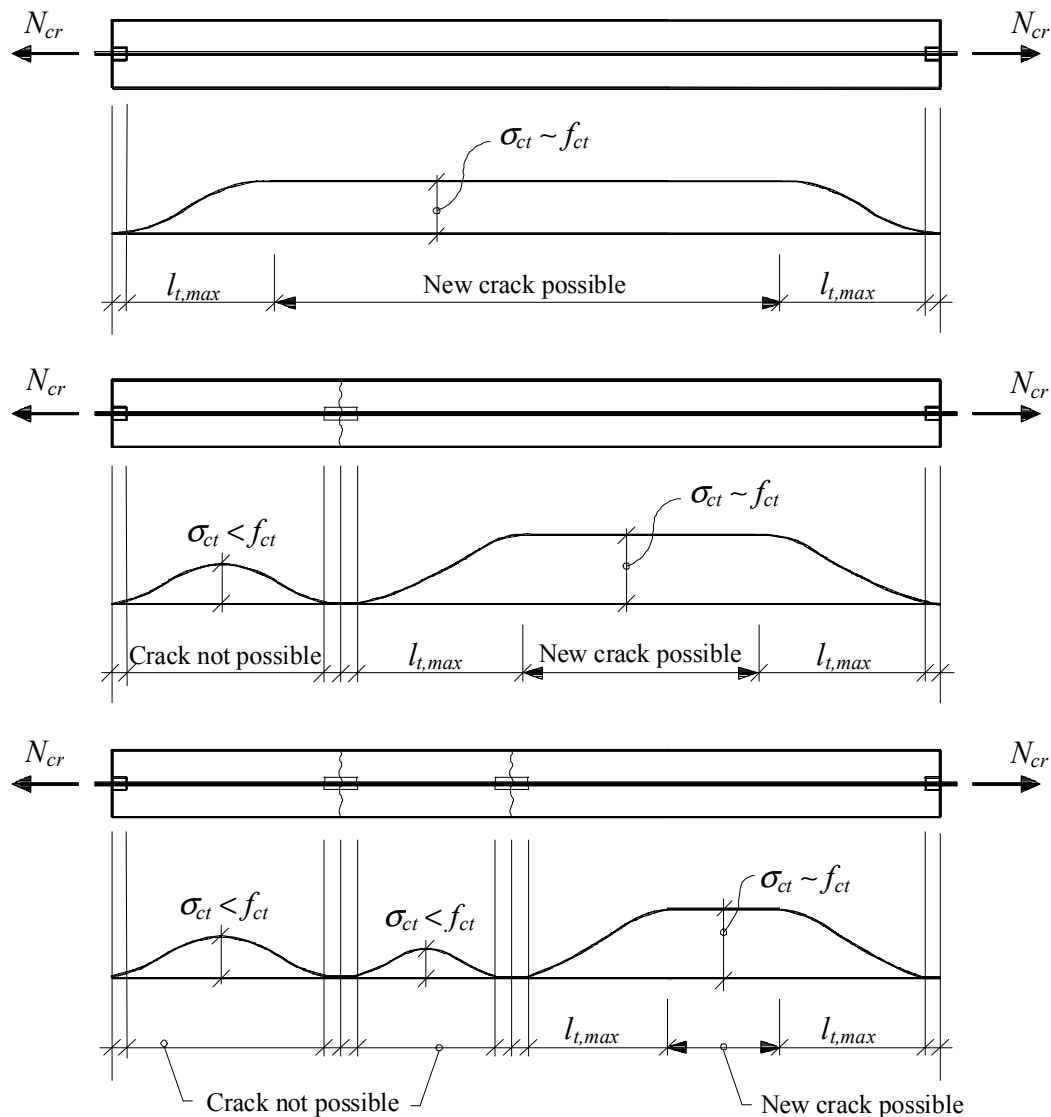


Figure 3.28 Crack development of a thin concrete member in pure tension, from Engström (2011a)

3.5.3 Effective area in thick reinforced members

The cracking of reinforced concrete members treated above is restricted to thin concrete members. In such members the concrete stress is generally assumed to be uniformly distributed over the cross section at the end of the transmission length. This is possible since the transmission length is significantly greater than the width of such

member. However, for thick reinforced concrete members, such as many real structures, this is not possible to achieve with reasonable accuracy. For thick members contributing parts of the cross-section with regard to crack development are limited and the concept of effective area is important.

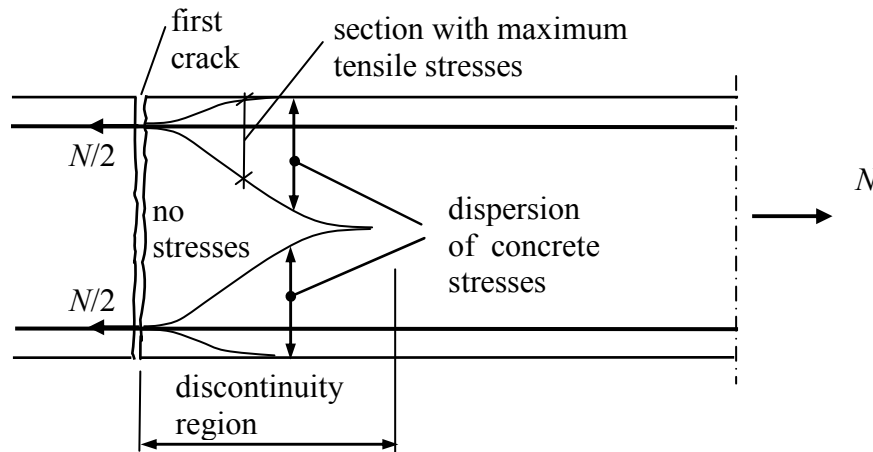


Figure 3.29 Stress spreading in a thick concrete member, from Engström (2011a)

Consider the thick member illustrated in Figure 3.29. Due to the separation of the concrete in the first crack, which is a through crack, the concrete at the crack section is stress free and the entire load is carried by the reinforcement bars. Behind the cracked section forces are transferred from the reinforcement bars into the concrete, which increases the concrete stress in a similar way as for thin members. Due to the thickness of the member though, the distribution of stresses within the concrete is non-uniform, creating a discontinuity region. As illustrated in the figure the cross-sectional area over which the stresses are dispersed increases with increasing distance from the crack. Since an increased area decreases the stress, the maximum concrete stress will occur before the stresses are completely dispersed. Thus, the next crack will occur in a section where only a limited part of the area is utilised. This concrete area is called the effective area and is limited by the height of the effective area. Figure 3.30 illustrates how the effective concrete area is defined in both CEB-FIP Model Code 1990 and Eurocode 2. As illustrated only parts of the cross section in close proximity of the reinforcement are accounted for. Note that when the height of the effective area is larger or equal to half of the cross sectional height, the member should be considered as a thin member.

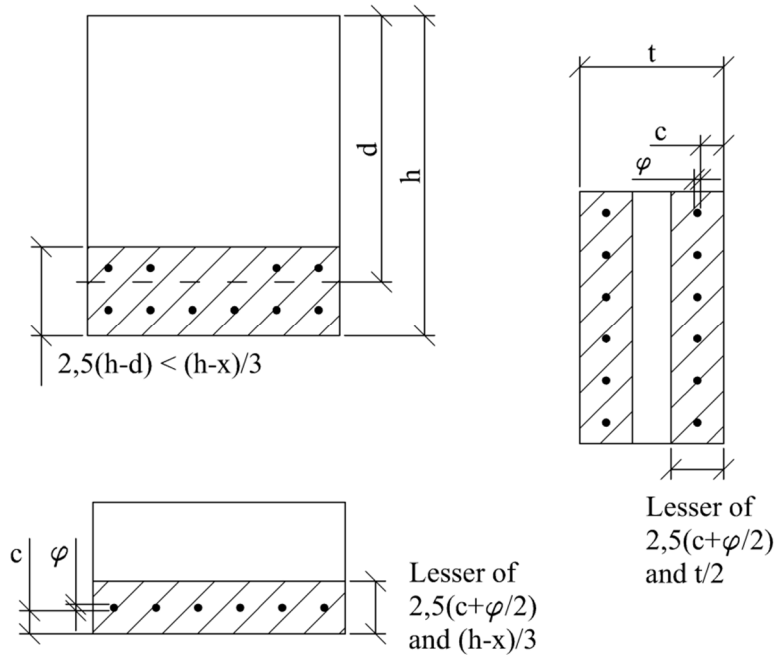


Figure 3.30 Effective concrete area in different types of cross sections according to Eurocode 2, CEN (2004)

The effective concrete area has an important consequence, which is illustrated in Figure 3.31. The first crack is a through crack, since the member is uncracked before it appears and the reinforcement has little influence at that time. However, the subsequent cracks are not through cracks, they develop within the effective concrete area of the member. Thus, the effective concrete area is important to consider in order to ensure proper crack control.

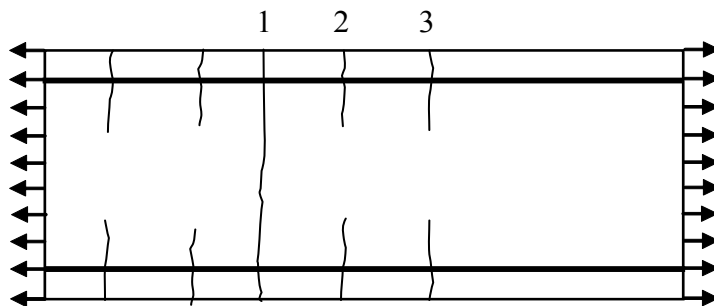


Figure 3.31 Cracking of a thick concrete member, from Engström (2011a)

3.5.4 Cracking of fibre reinforced concrete

The main difference between the cracking processes in plain concrete and fibre reinforced concrete (FRC) is due to effects of fibre bridging. When cracks occur in FRC they are bridged by fibres, which up to a certain limit, hold the cracks together. This is in principle not different from how ordinary reinforcement bars work. However, due to the distributed nature and the relatively large amount of fibres, the cracking process of FRC could differ considerably from those of plain and reinforced concrete. A good starting point for understanding the cracking process of FRC is a

uniaxial tensile test. The result from such test is used to obtain a stress-crack opening relation, illustrated in Figure 3.32.

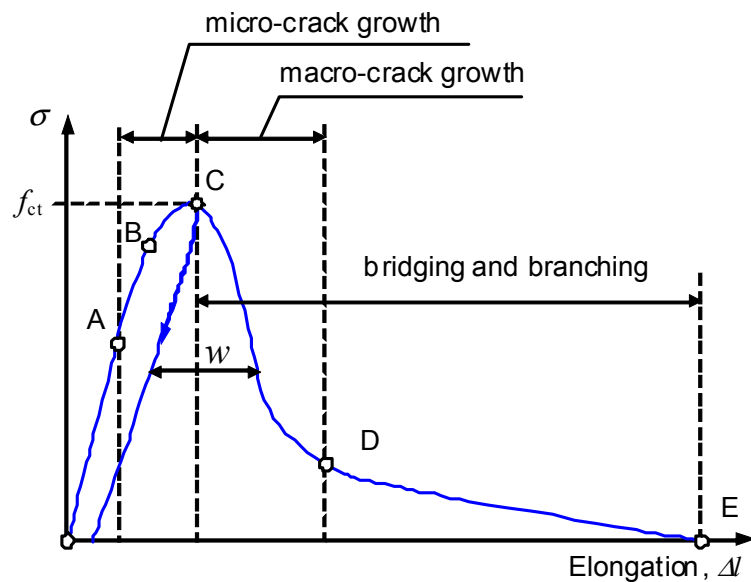


Figure 3.32 Typical stress-elongation curve for fibre reinforced concrete, from Löfgren (2005)

The processes of the test and how the stress-crack opening relation is obtained is described for plain concrete in Section 3.5.1 and are not different from that of FRC. During such a test of FRC a few different stages can be distinguished. The limits between those stages are marked in Figure 3.32. In the early stages micro-cracks are formed at the cement paste and aggregate interfaces (A), and subsequently propagate within the concrete (B). When the tensile capacity is reached (C), micro-cracks connect with each other and forms larger macro-cracks.

It is important to distinguish between micro- and macro-cracking. Concrete, regardless of how and if it is reinforced, generally contains a large number of micro-cracks. Some of these arise before loading due to internal restraint from aggregates and reinforcement, when concrete is exposed to stress-independent strains (e.g. shrinkage and thermal expansion or contraction). When a load subsequently is applied, the number of micro-cracks increases. Before any macro-cracks arise concrete is considered uncracked and is in the pre-cracking stage. Consequently, when the first macro-crack appears, the concrete is cracked and is in the post-cracking stage. After the maximum stress is reached (C), macro-cracks are propagating through the specimen (D). A consequence of this is a stress decrease. Finally, the specimen separates (E). The area under the curve between C-E corresponds to the fracture energy of the specimen.

Different fibres influence the pre- and post-cracking stages of FRC differently. Possible effects of adding microfibres are illustrated in Figure 3.33. Due to the small size of microfibres there is a relatively high number of them present for a given fibre content. Thus it is likely that when micro-cracks arise and propagates, they are bridged by microfibres. Consequently the formation of micro-cracks could be

somewhat delayed and the tensile strength slightly increased. Certain requirements should be fulfilled for microfibres to demonstrate this influence, such as high aspect ratio and stiffness, Löfgren (2005).

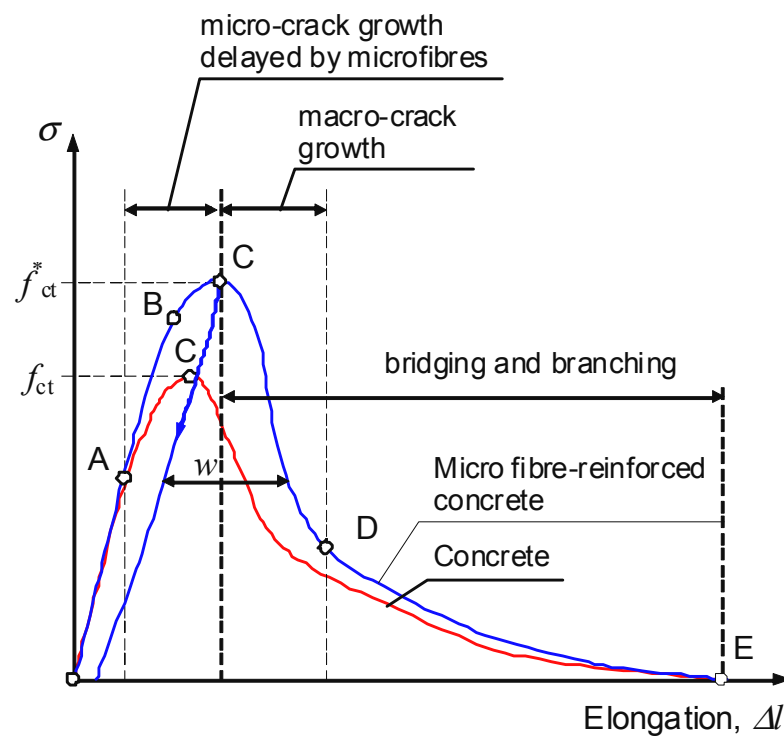


Figure 3.33 Typical stress-elongation relation for fibre reinforced concrete and plain concrete, from Löfgren (2005)

Due to the small size of microfibres their impact on the post-cracking stage (macro-cracking) is limited. Hence, an unstable growth of macro-cracks will dominate the behaviour when the post-cracking stage is reached, since microfibres are not able to bridge macro-cracks. However, by adding long fibres it is possible to bridge macro-cracks and to some extent control the post-cracking behaviour. By adding a mixture of microfibres and long fibres it should be possible to produce FRC with slightly increased tensile strength as well as improved post-cracking behaviour. Figure 3.34 and Figure 3.35 illustrates fibre bridging of cracks by microfibres and long fibres respectively, Löfgren (2005).

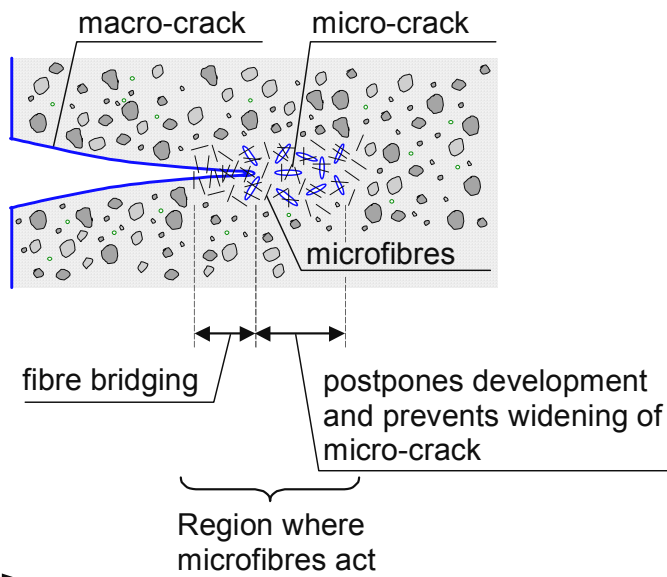


Figure 3.34 Fibre bridging by micro-fibres, from Löfgren (2005)

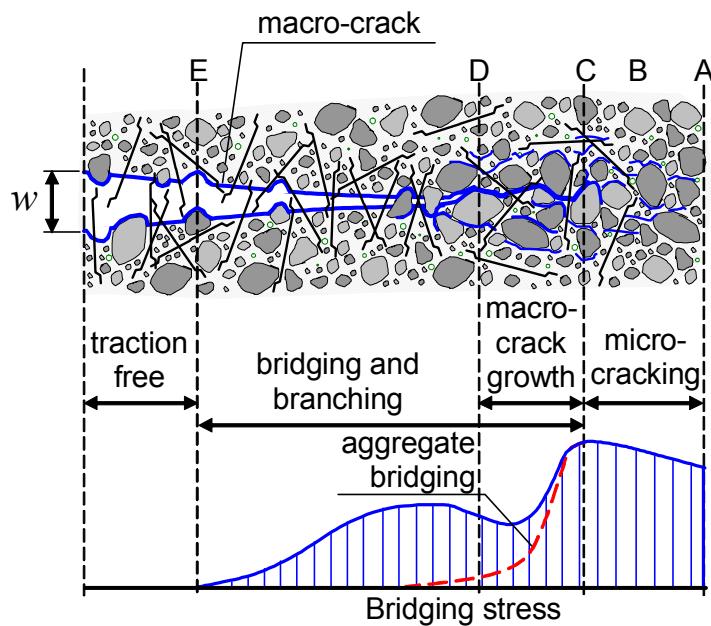


Figure 3.35 Fibre bridging by macro-fibres (long fibres), from Löfgren (2005)

Due to fibre bridging more energy is required in the fracture process in an FRC specimen than in a plain concrete specimen. This is demonstrated by Figure 3.36. The area under the curve for FRC is considerably greater than the area for concrete, implying that the fracture energy is considerably higher and that the material response is more ductile for FRC than for concrete. Furthermore Figure 3.36 demonstrates that the FRC response results from the combined actions of its components, concrete and fibres.

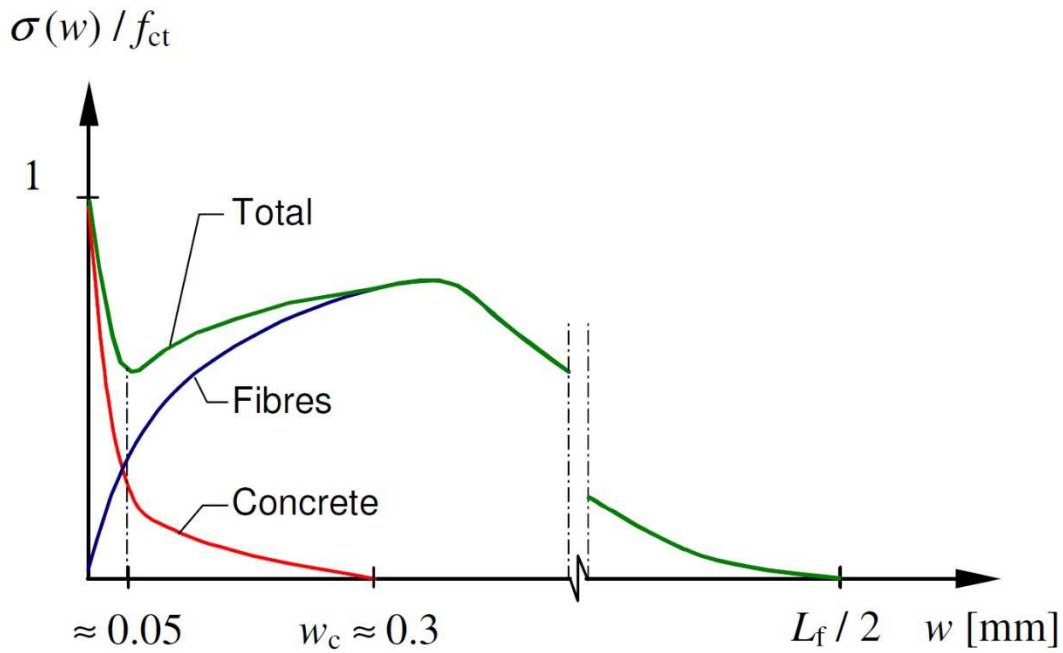


Figure 3.36 Typical stress-crack opening relation for fibre reinforced concrete, from Löfgren (2005)

Thus, it is of great importance with regard to the fracture energy which fibres that are used. According to Löfgren (2005) examination of fractured FRC specimens with steel fibres has shown that fibre pull-out is the primary cause of failure. Hence, the more energy needed to pull out a specific fibre type, the greater the fracture energy of the FRC. Figure 3.37 illustrates a pull-out test of a single fibre. As supported by the force-deformation diagram in the figure more energy is needed to pull out a fibre with an end hook than a straight fibre.

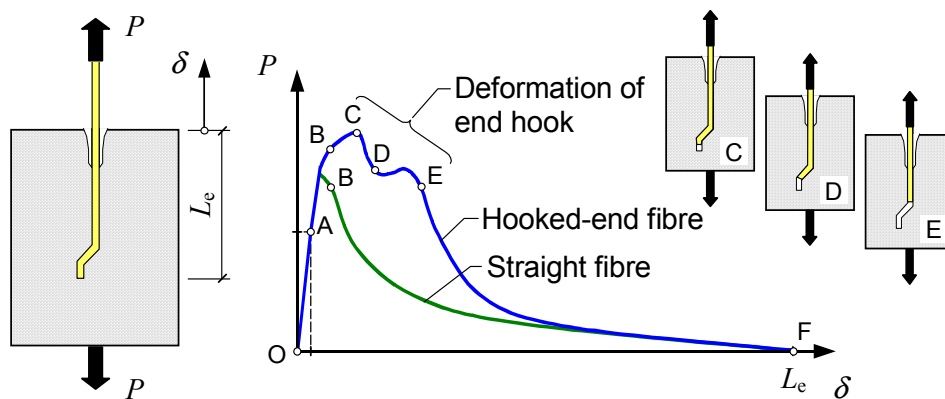


Figure 3.37 Fibre pull-out test, from Löfgren (2005)

This section deals with FRC based on normal strength concrete. If high strength concrete is used instead, the behavior of the FRC would be different. For instance, in a uniaxial tensile test of FRC with normal strength concrete, a single macro-crack governs the tensile failure. After the maximum stress (crack opening stress) is reached the stress decreases. However, for FRC with high strength concrete additional hardening and a slight stress increase could take place after the cracking stress is reached (pseudo-strain hardening). Furthermore, since the strength of the cement

paste and the aggregates are similar in high-strength concrete, cracks could propagate through aggregates as well as through concrete. Propagation through aggregates is unlikely in normal strength concrete since the aggregates are considerably stronger than the cement paste. For additional information about this and fibre reinforced concrete in general, reference is made to Löfgren (2005).

3.5.5 Crack widths

Crack widths can be specified as characteristic or mean crack widths. Furthermore crack widths vary depending on if long term effects are considered or not. In general, the design criterion requires a characteristic crack width not exceeding a specified limit, as expressed mathematically below.

$$w_k \leq w_{\text{lim}} \quad (3.27)$$

where w_k is the characteristic crack width
 w_{lim} is the specified limit of the characteristic crack width

The actual value of the limiting characteristic crack width depends on, for instance, ambient conditions and how cracks influence the considered concrete member. Values are specified in design codes such as Eurocode 2, CEN (2004), or BBK 04, Boverket (2004).

Besides using characteristic values, crack widths can also be calculated or measured using a mean value. The relation between mean and characteristic crack width depends on the loading conditions. For a concrete member subjected to restraint loading such a relation can be estimated as expressed below. Engström (2011a).

$$w_m = \frac{w_k}{1,3} \quad (3.28)$$

where w_m is the mean crack width

When calculating and measuring cracks it is important to distinguish between long term response and short term response. Crack widths are not constant in time and becomes larger when long-term effects are considered. However, uncertainties exist regarding the magnitude of the difference between short and long term response. A reasonable estimate might be that the mean crack width increases by a magnitude of 1,2 if long-term effects (sustained loading) are considered. Engström (2011a).

$$w_{m,sus} \approx 1,2 \cdot w_m \quad (3.29)$$

where $w_{m,sus}$ is the mean crack width including long term effects

Throughout this project, references are made to both mean and characteristic crack widths. However, only short-term effects are accounted for.

3.6 Crack control

Appropriate crack control is often an essential part of ensuring the durability of a concrete structure. There are however, different approaches to how the needed reinforcement amount should be calculated. This section presents the approaches used

in Eurocode 2, CEN (2004), and BBK 04, Boverket (2004), as well as two proposed alterations to the approach given in Eurocode 2.

3.6.1 According to Eurocode 2

Eurocode 2 gives an equation for calculation of the minimum reinforcement amount required for crack control in a concrete structure. This equation is derived from an equilibrium condition between steel and concrete forces just before cracking and is expressed as

$$A_{s,\min} \cdot \sigma_s = k_c \cdot k \cdot f_{ct,eff} \cdot A_{ct} \quad (3.30)$$

where	$A_{s,\min}$	is the minimum reinforcement area in the tensile zone
	A_{ct}	is the concrete area subjected to tension just before the first crack forms
	σ_s	is the steel stress allowed just after cracking, if the crack width is limited see Table 3.4 and Table 3.5, else use f_{yk}
	k_c	is a coefficient which takes the stress distribution just before cracking into account and of the change of the lever arm =1,0 for pure tension for other situations see Eurocode 2
	k	is a coefficient which allows for the effect of non-uniform self-equilibrating stresses, which lead to a reduction of restraint forces =1,0 for web height or flange width ≤ 300 mm =0,65 for web height or flange width ≥ 800 mm values in between may be interpolated
	$f_{ct,eff}$	is the mean tensile strength of concrete at the actual age when cracking is expected

Using this equation, it is possible to limit the crack width to a certain value by limiting the steel stress σ_s . If there is no requirement on the maximum allowed characteristic crack width, the steel stress can be set to the yield strength of the reinforcing steel. The maximum allowed steel stress, for a certain characteristic crack width, depends on the bar diameter and the bar spacing. Table 3.4 defines the steel stress and bar diameter for a certain characteristic crack width, while Table 3.5 defines the steel stress and bar spacing for a certain characteristic crack width.

Table 3.4 Maximum allowed steel stress for different bar size and characteristic crack widths

Steel stress [MPa]	Maximum bar size [mm]		
	$w_k = 0,4 \text{ mm}$	$w_k = 0,3 \text{ mm}$	$w_k = 0,2 \text{ mm}$
160	40	32	25
200	32	25	16
240	20	16	12
280	16	12	8
320	12	10	6
360	10	8	5
400	8	6	4
450	6	5	-

Table 3.4 is based on the following assumptions according to Eurocode 2; $c = 25$ mm; $f_{ct,eff} = 2,9$ MPa; $h_{cr} = 0,5$; $(h-d) = 0,1h$; $k_1 = 0,8$; $k_2 = 0,5$; $k_c = 0,4$; $k = 1,0$; $k_t = 0,4$ and $k' = 1,0$.

The maximum allowed bar diameter obtained in the tables should according to Eurocode 2 be modified depending on the type of load. In the case of bending, the bar diameter should be modified as

$$\phi_s = \phi_s^* (f_{ct,eff} / 2,9) \frac{k_c \cdot h_{cr}}{2 \cdot (h - d)} \quad (3.31)$$

While in case of tension, the bar diameter should be modified as

$$\phi_s = \phi_s^* (f_{ct,eff} / 2,9) \frac{h_{cr}}{8 \cdot (h - d)} \quad (3.32)$$

where ϕ_s is the adjusted maximum bar diameter
 ϕ_s^* is the maximum bar diameter according to Table 3.4
 h is the depth of the section
 h_{cr} is the depth of the tensile zone just before cracking
 d is the effective depth of the centroid of the outer layer of reinforcement

Table 3.5 Maximum allowed steel stress for different bar spacing and crack widths

Steel stress [MPa]	Maximum bar spacing [mm]		
	$w_k = 0,4 \text{ mm}$	$w_k = 0,3 \text{ mm}$	$w_k = 0,2 \text{ mm}$
160	300	300	200
200	300	250	150
240	250	200	100
280	200	150	50
320	150	100	-
360	100	50	-

3.6.2 According to BBK 04

In the Swedish handbook for concrete structures BBK 04, Boverket (2004), a different calculation method is used for the minimum reinforcement amount required for crack control. This equation is, just as the method in Eurocode 2, based on an equilibrium condition between steel and concrete forces. However, in BBK 04 the equilibrium just after the first cracking is used. The equation is defined as

$$A_s \cdot \sigma_s \geq A_{ef} \cdot f_{cth} \quad (3.33)$$

where A_s is the reinforcement area
 A_{ef} is the effective concrete area, see BBK 04 Figure 4.5.5
 σ_s is the steel stress f_{yk} but not greater than 420 MPa
 f_{cth} is $1,5 \cdot f_{ctk}$

In Equation 3.33 the effective area of the concrete A_{ef} shall be used. The concept of effective area is explained in Section 3.5.3. In BBK 04 the steel stress σ_s is not limited regarding either the crack width, bar diameter or bar spacing. These differences usually result in a lower minimum amount of crack controlling reinforcement compared to Eurocode 2. It should however be noted that Equation 3.33 does not take any crack widths limitations in consideration and therefore the resulting minimum reinforcement amount does not limit the crack widths to a certain specified value.

3.6.3 Other

Different proposals of how to change the approach given in Eurocode 2 have been published. Two of these proposals are presented here. The first proposal is a change in

the German national annex, Normenausschuss Bauwesen (NABau) im DIN (2012), while the second proposal comes from Björnberg and Johansson (2013).

3.6.3.1 Changes in the German national annex

In the national annex of Eurocode 2 in Germany (DIN EN 1992-1-1/NA) there is a modified expression for the minimum reinforcement area (Equation 3.30). According to Normenausschuss Bauwesen (NABau) im DIN (2012) it is expressed as

$$A_{s,min} = f_{ct,eff} \cdot A_{c,eff} / \sigma_s \geq k \cdot f_{ct,eff} \cdot A_{ct} / f_{yk} \quad (3.34)$$

where $A_{c,eff}$ is the effective concrete area, see Figure 7.1 in CEN (2004)
 k is according to Equation (3.30), but multiplied by 0,8 for internal effects

The equation above consists of two parts, where the left part uses the effective area of the concrete section and no reduction term such as k is to be used. If a certain characteristic crack width is demanded, the steel stress is reduced according to Table 3.4 and Table 3.5. This part should then be greater than the right part and the only difference from Equation (3.30) is that here the yield strength of the reinforcement is always used regardless of the crack width demand.

The k factor in Equation (3.30) is modified in the German annex as well. If the concrete stress originates from an internal restraint, a reduction of 0,8 for the k factor should be used, see Figure 3.38. If the concrete stress instead originates from external loading or external restraint, no reduction of the k factor is allowed.

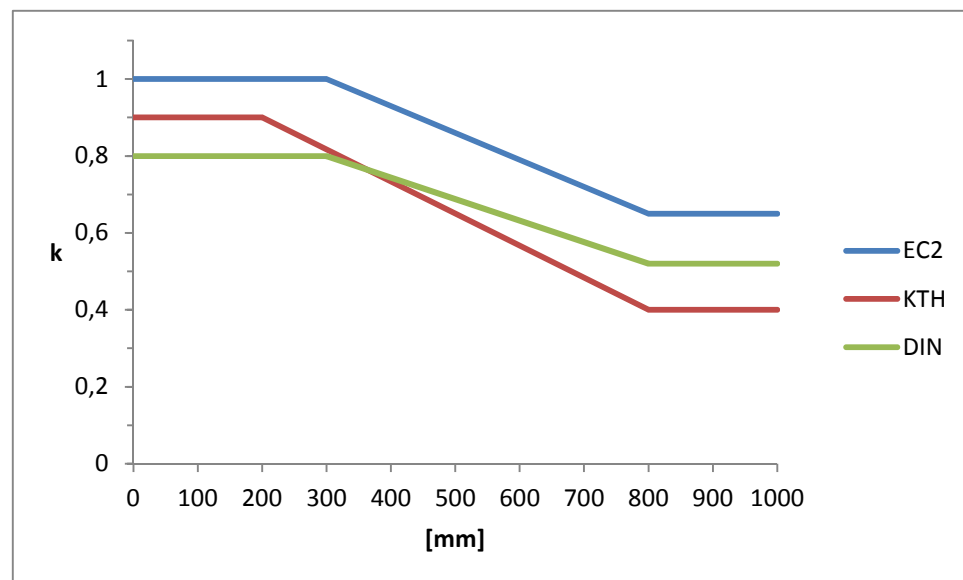


Figure 3.38 Variation of the k -factor in different calculation methods

3.6.3.2 Proposal from Björnberg and Johansson

In the master's thesis from Björnberg and Johansson (2013) at KTH changes to the equation for the minimum reinforcement amount in Eurocode 2 are proposed. The

proposed changes to the equation in Eurocode 2 affect the k factor in the equation. As in Eurocode it is dependent of the height of the structure. Björnberg and Johansson propose that the k factor shall be 0,9 if the height is less than 200 mm and 0,4 if the height is greater than 800 mm, see Figure 3.38. The proposed changes are based on a parametric study performed using the finite element software Atena.

4 Analysis of existing objects

4.1 Introduction

In order to provide a basis for comparison between modelling results and reality, as well as for drawing conclusions of cracking in cellar walls subjected to restrained deformations, cellar walls in two existing buildings have been investigated and their cracks documented. In this chapter the investigation method is described and observations made from the studied objects are evaluated and summarised. All references related, in any way, to visited objects, which could be used to identify the objects, have been anonymised throughout this chapter.

In the subsequent sections regarding each of the studied objects, Sections 4.3 and 4.4, cracks are classified depending on their respective crack width. A crack was denoted as either very small, small, large or very large. This classification is based on a visual inspection and not on actual measurements of the crack width. Hence, all cracks found during visual inspections can be classified without being measured and all walls, not only those studied in detail, could be classified based on the state of cracking. The implications of the four crack denotations are defined in Table 4.1. These denotations are used throughout this chapter.

Table 4.1 Classifications of cracks from visual inspection

Crack denotation	Implication	Crack width (approximate range)
Very small	Barely visible at close range	< 0,05 mm
Small	Clearly visible at close range	0,05-0,2 mm
Large	Clearly visible from distance	0,2-0,5 mm
Very large	Clearly visible and noticeably large	> 0,5 mm

To be able to compare the measured data between different cracks within the same wall or compare the overall cracking of a wall with other walls or simulations a mean value is needed. Therefore all the measured points in each individual crack was summarised to a mean value for each specific crack as expressed below

$$w_{m,crack} = \frac{\sum w}{n} \quad (4.1)$$

where w is the crack width
 n is the number of measuring points in each crack

The mean value for each crack is then summarised to a mean value for a certain section, for example a wall, as

$$w_{m,wall} = \frac{\sum w_{m,crack}}{i} \quad (4.2)$$

where $w_{m,crack}$ is the mean crack width for each crack
 i is the number of cracks in each section

4.2 Investigation method

A specific investigation method, used for all objects, was developed to achieve consistency between the investigations of the different objects. The primary part of each investigation was an on-site inspection where cracks were measured and documented. Each on-site inspection was complemented by studying relevant drawings and documents related to the design and construction of the building. An investigation protocol was developed and used consistently during each inspection, see Appendix A.1.

The two main objectives with the on-site inspections were to document the overall crack pattern at selected walls and to study individual cracks in those walls in greater detail. These objectives were pursued for each object using the same procedure, which is described in the following. First an overview of the cellar walls and their potential cracks was obtained by a visual inspection. With the overview obtained a certain number of walls were selected for a more detailed investigation. These selected walls were then carefully examined and all found cracks were marked. All found cracks were documented using coordinates and illustrations of their shape. This data was used to document the crack pattern of each selected wall.

A certain number of cracks in each selected wall were studied in greater detail. Depending on the number of cracks found in each wall, all or only a limited number of cracks were measured in greater detail. Each crack measured in greater detail was documented and measured using the same approach. A certain number of measurement points, depending on the length and the shape of the crack, were selected, usually five or six points were considered to be sufficient. The coordinates (in relation to a pre-decided reference point), crack width and reinforcement cover thickness of each point were measured and documented.

During these investigations a number of tools and instruments were used. Distances and coordinates were measured using a laser distance meter, yardstick and tape-measure. Cracks were measured using a crack width microscope, see Figure 4.1. The scale in the microscope is divided in tenths of a millimetre.



Figure 4.1 Crack width microscope

A cover thickness meter, Micro Covermeter by Kolectric Limited, was used to measure the concrete cover, see Figure 4.2. During the process of documentation cracks were marked with numbered notes and measurement points with tape before being photographed.



Figure 4.2 Micro Covermeter, used to measure the cover thickness

4.3 Object A

4.3.1 Object description

The first building that was studied, object A, is an office building in Gothenburg that was studied at February 26, 2014. The construction begun in 2011 and was finished in 2013. The cellar was cast during the summer of 2011 using in-situ cast concrete. A majority of the cellar is used as a parking garage, while remaining parts are used primarily for storage and housing of technical equipment. Building data for object A is briefly summarised in Table 4.2.

Table 4.2 Building data for object A

Building description and location	Office building in Gothenburg
Construction	2011-2013
Inspection date	2014-02-26
Casting of cellar walls	Summer of 2011
Cellar wall age	~ 2 years, 7 months
Primary cellar usage	Parking garage
Design code	BBK 04

Two of the exterior walls were selected for a more detailed investigation. The selected walls are denoted wall 1 and wall 2 and their respective location in the cellar is schematically illustrated in Figure 4.3. These walls were carefully documented with regard to cracks.

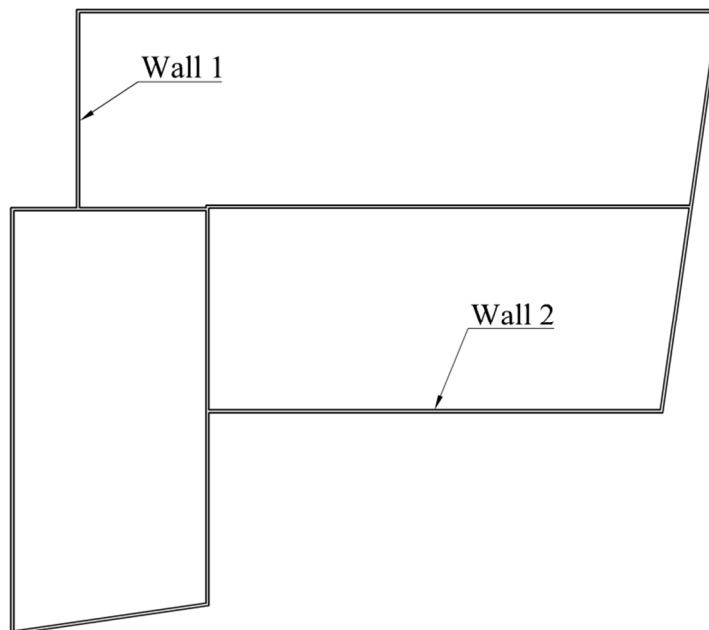


Figure 4.3 Layout of the cellar in object A

Since the building was in full operation at the time of inspection, there were some obstacles preventing a complete investigation of all walls in the cellar. Certain areas, mainly storage areas, technical rooms and a bicycle parking area, were inaccessible for investigation. Furthermore, parked cars partly prevented full access to wall 2. There were also installations, cable ladders and water pipes, mounted near the top of wall 2, which to some extent complicated the measuring procedure.

4.3.2 General observations

In the cellar of object A all in-situ cast walls accessible for inspection were found to have cracks. In general the cracks that were found during visual inspection of the walls were classified as very small or small, see Table 4.1, with some exceptions.

4.3.3 Wall 1

4.3.3.1 Design and detailing

General data for the design of the wall and the project is presented in Table 4.3.

Table 4.3 General data for concrete and reinforcing steel in object A

Concrete strength class	C35/45
Cover thickness	Outside 50 mm, inside 40 mm
Maximum water/cement ratio	0,45
Reinforcing steel	B500B and Nps 500

Wall number 1 is cast against a 450 mm thick ground slab resting on a pile foundation. The wall is connected to the slab via crossing reinforcement bars along both surfaces, see Figure 4.4. Prefabricated hollow-core floors as well as prefabricated wall elements are connected at the top of the wall. The floor and wall elements are connected through fasteners cast into the concrete.

The wall itself consists of cast in-situ concrete and has a thickness of 250 mm. There are longitudinal reinforcement bars distributed over the height of the wall, which are used for crack control. These reinforcement bars are evenly distributed over the height of the wall with extra bars added within the bottom 500 mm region, see Figure 4.4. The evenly distributed bars have a diameter of 12 mm and a spacing of 150 mm. The 5 extra bars in the bottom, at each side of the wall, have a diameter of 16 mm and a spacing of 100 mm.

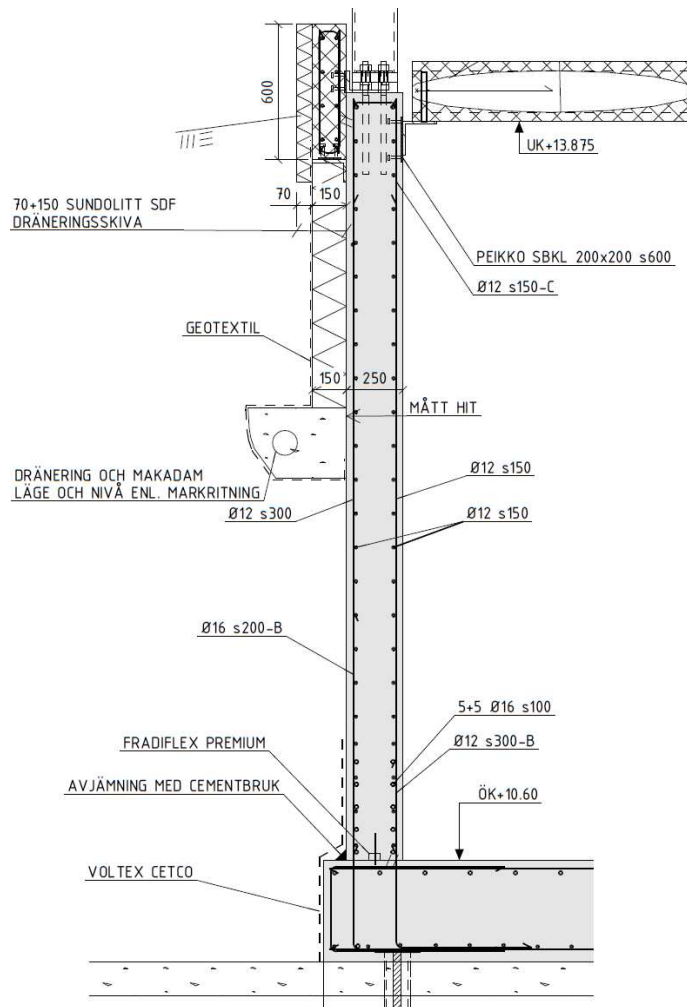


Figure 4.4 Detailing of wall 1 in object A [in Swedish], from building documentations

The wall was cast in two different sections, where one is 13,6 meters long, while the other is 2,6 meters, see Figure 4.5.

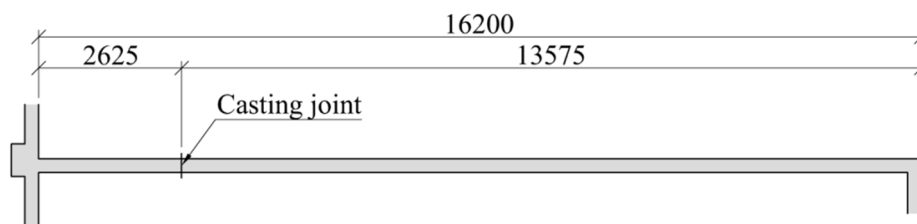


Figure 4.5 Longitudinal section of wall 1 in object A and location of casting joint

On the outside of the cellar wall the groundwater level varies between +11,3 meters and +12,7 meters. The slab is placed on +10,6 meters and the wall is therefore always subjected to a groundwater pressure. Hence the wall is designed to be watertight. According to BBK 04, Boverket (2004), the characteristic crack width should then not exceed 0,2 mm (in case of reasonable demands regarding tightness).

4.3.3.2 Observations

The overall length of this wall is rather short, although a large part of it is cast in the same casting step of 13,6 meters. On this wall only a smaller number of cracks and no particularly large cracks were found. A total of six cracks were found, and all of them are on the longer casting section. All cracks are marked with tape in Figure 4.6, Figure 4.7, Figure 4.8 and Figure 4.9.



Figure 4.6 Overview of wall 1



Figure 4.7 Closeup of cracks 1, 2, 3 and 4 at wall 1



Figure 4.8 Closeup of cracks 2, 3 and 4 at wall 1



Figure 4.9 Closeup of crack 5 and 6 at wall 1

The position, crack width and cover thickness were measured for all detected cracks. The resulting crack pattern obtained from the measurements is illustrated in Figure 4.10. In every dot in Figure 4.10 the crack width was measured. These measurements resulted in a mean crack width of 0,13 mm, and a characteristic crack width of 0,17

mm, for the whole wall, with a variation of the mean crack width of each individual crack between 0,08 mm and 0,2 mm. The maximum crack width measured in a single measurement point in the wall was 0,3 mm. For the complete results of the measurements see Appendix A.2.

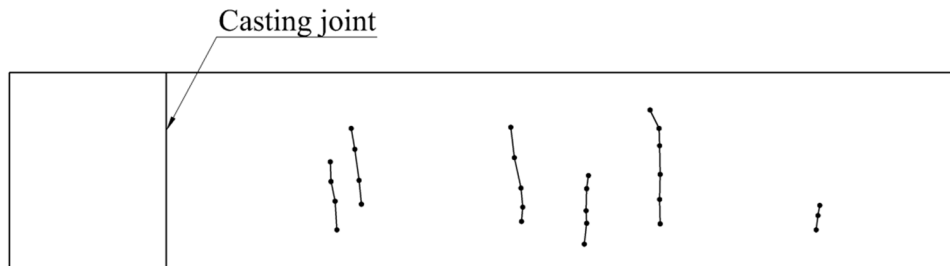


Figure 4.10 Crack pattern in wall 1, object A

4.3.4 Wall 2

4.3.4.1 Design

The design of wall 2 is almost equal to the design of wall 1, see Section 4.3.3.1. It is cast against a 450 mm thick pile-supported ground slab. The amount of bars crossing the interface between the slab and wall is slightly smaller than in wall 1, see Figure 4.11.

At its top the wall is connected to a floor plate composite floor with a cast in-situ top.. The wall is attached to this slab via reinforcement that is folded into the top side of the slab from the outside face of the wall, see Figure 4.11.

The reinforcement layout within the wall is exactly the same as in wall 1, see Section 4.3.3.1, with 12 mm bars spaced 150 mm and 5 extra 16 mm bars spaced 100 mm on each side in the bottom 500 mm region of the wall.

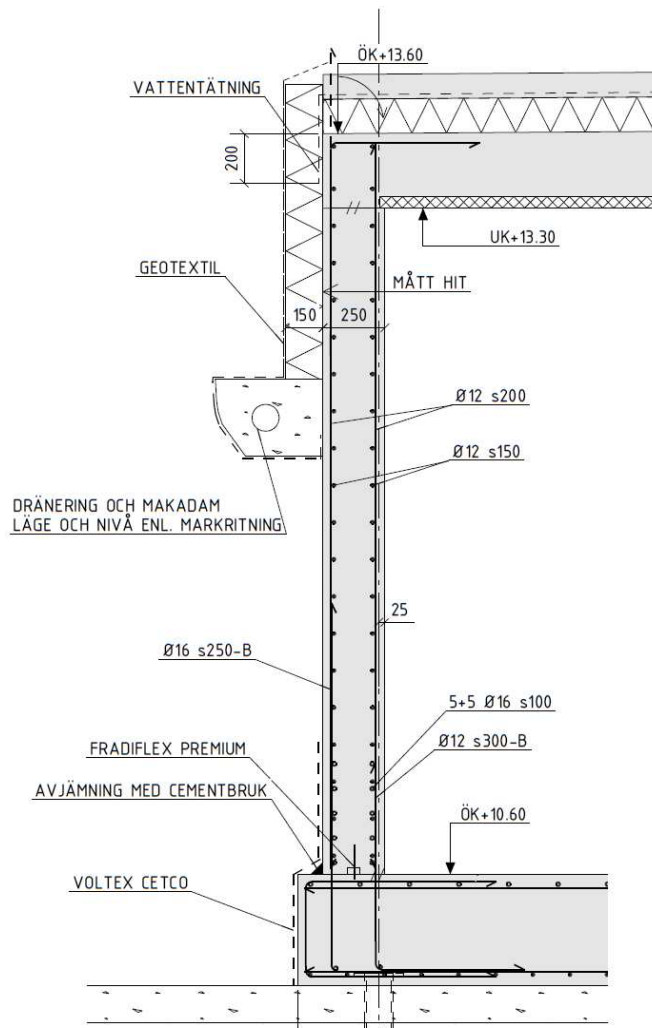


Figure 4.11 Detailing of wall 2 in object A [in Swedish], from building documentations

Wall 2 is cast in three different parts, one shorter part of 2,2 meters and two longer parts see Figure 4.12. Of the two longer parts, the middle part is 15,4 meters long and the right part, see Figure 4.12, is 19,6 meters long.

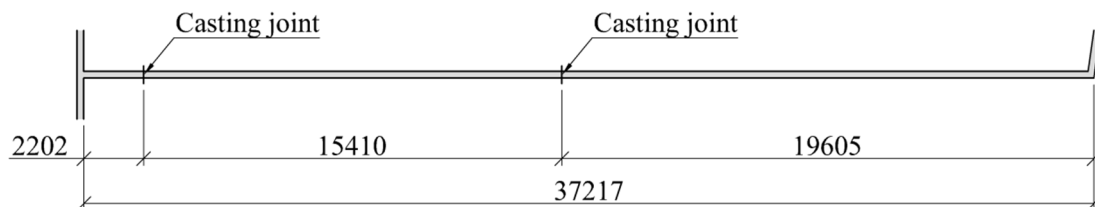


Figure 4.12 Longitudinal section of wall 1 in object A and locations of casting joints

Furthermore, wall 2 is subjected to the same level of groundwater pressure as wall 1, see Section 4.3.3.1, and is therefore also designed to be watertight. To ensure the water tightness of the structure, the characteristic crack width should, according to Boverket (2004), not exceed 0,2 mm.

4.3.4.2 Observations

In wall 2 there are several cracks that were considered to be larger cracks, see Table 4.1. On the parts of the wall that was accessible for examination 20 cracks were found. Most of the cracks had almost the same spacing. An overview of the wall is shown in Figure 4.13 and Figure 4.14.



Figure 4.13 Overview of the left part of wall 2, object A



Figure 4.14 Overview of the right part of wall 2, object A

The position of each crack was measured and the crack width and cover thickness were measured on every third crack, i.e. on seven cracks. The mean crack spacing was determined by measurements to 1,36 meters including all cracks. At four places the crack spacing can be assumed to not be representative for the mean crack spacing in a fully cracked section. One crack is positioned in a casting joint, which leads to an irregular spacing to neighbouring cracks. At two other places it is clear that the spacing is about double compared to the other cracks. With these spacing's excluded the mean crack spacing was determined to 1,21 meters.

In six out of seven cracks, where the crack widths were measured, the mean crack width for each crack varied between 0,18 mm and 0,25 mm. The seventh crack that was measured had a mean crack width of 0,6 mm, see Figure 4.15 for a picture of that crack. The average crack width when all measured cracks are included is 0,27 mm. With the seventh crack, with a crack width of 0,6 mm, excluded the average mean crack width of the remaining six cracks was 0,22 mm and a characteristic crack width of 0,28 mm.

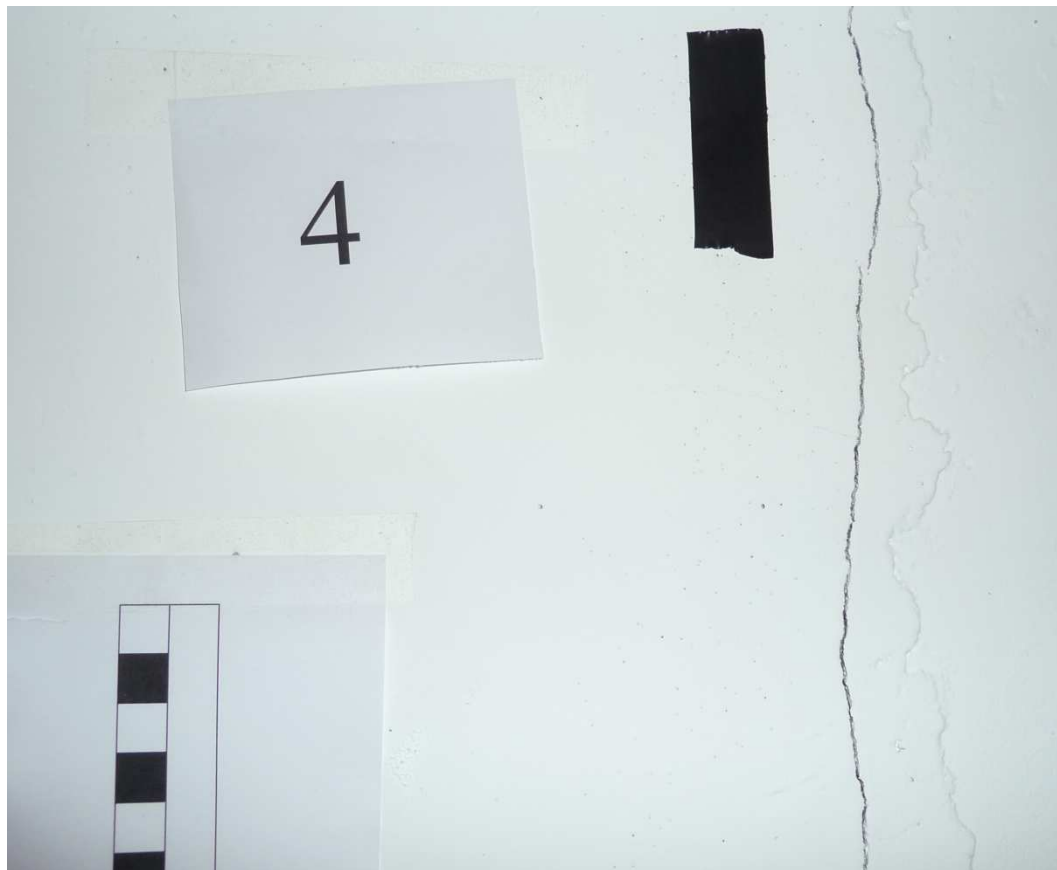


Figure 4.15 A very large crack in wall 2, object A

In this wall the observed characteristic crack width exceeds the maximum characteristic crack width of 0,2 mm according to BBK 04, Boverket (2004), for a structure that is subjected to a single sided water pressure. Even though the mean crack width exceeds the crack width limited according to BBK 04, there were no signs of any discolouration or flaking of the paint on the wall surface. For the complete results of the measurements see Appendix A.3.

4.3.5 Evaluation

By the overall visual inspection of the object the general appearance is that the amount of cracks and the crack widths are limited. The crack width in almost all outer cellar walls are approximately below 0,2 mm

In wall 2 the mean crack width exceeds the of all cracks in average 0,2 mm as stated in BBK 04, Boverket (2004), but still no sign of water leakage was observed. This may be due to various different reasons, for instance that the crack does not extend through the whole thickness of the wall. However, since the cellar walls are less than three years old, such deterioration might appear in the future.

One possible source of error in the conducted measurements can be the paint applied on the wall. If the crack existed before the paint was applied on the wall, the paint may reduce the crack width that was measured. It should also be noted that all the measurements were conducted by a visual reading on a scale in the crack microscope.

The total reinforcement area in the cross-section of wall 1 is 7 210 mm². According to BBK 04, see Section 3.6.2, the minimum reinforcement amount would correspond to 5 200 mm². This minimum area corresponds to the evenly distributed reinforcement bars with a diameter of 12 mm, see Figure 4.4. Thus the five bars in the bottom on each side are added beyond the demands in BBK 04. If this wall would be designed according to Eurocode 2, CEN (2004), with characteristic crack widths limited to 0,2 mm, it results in a reinforcement area of 13 600 mm². To satisfy this demand the reinforcement amount almost needs to be doubled compared to the provided amount in the wall. Wall 2 has a similar reinforcement layout and cover thickness. Therefore the result is similar to those of wall 1. The reinforcement area in the cross-section of wall 2 is 6 540 mm². According to BBK 04 the demand is 4 590 mm² and according to Eurocode 2, with a characteristic crack width of 0,2 mm the calculated reinforcement area is 12 000 mm².

4.4 Object B

4.4.1 Object description

The second object visited for inspection, object B, is an office building in Gothenburg that was studied on 4th of March 2014. Construction began in 2008 and was completed during 2010. Casting of the cellar took place during the summer and autumn of 2008 using in-situ cast concrete. The cellar has two floors, where the upper floor area is about two times larger than the lower floor area. Some parts of the cellar are used for technical equipment, loading of goods and storage. However a majority of the total floor space is used for parking. Some building data for object B is briefly summarised in Table 4.4.

Table 4.4 Building data for object B

Building description and location	Office building in Gothenburg
Construction	2008-2010
Inspection date	2014-03-04
Casting of cellar walls	Lower floor: Summer 2008 Upper floor: Autumn 2008
Cellar wall age	Lower floor: ~ 5 years, 7 months Upper floor: ~ 5 years, 4 months
Primary cellar usage	Parking garage
Design code	BBK 04

As schematically illustrated in Figure 4.16 and Figure 4.17 most of the outer walls were accessible for inspection. A limited part of one outer wall was selected for a more detailed investigation. This selected part was roughly 32 meters long. At the time of inspection the building was in full service. Consequently some obstacles, mainly parked cars, prevented complete wall access at certain locations. However, the selected wall part was free from parked cars. Although pipes fitted in the upper regions of the selected wall part slightly prevented full access and complicated measuring at heights near or above the pipe fittings.

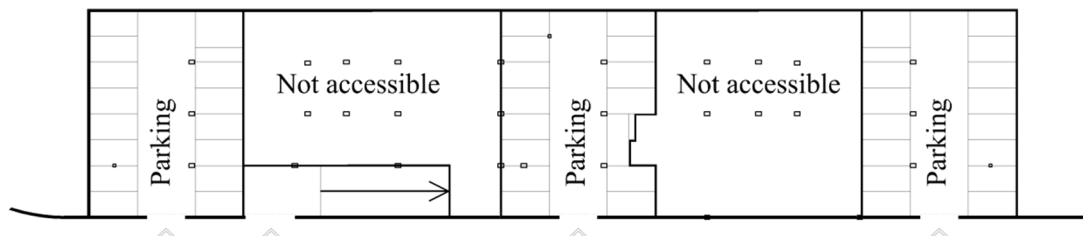


Figure 4.16 Plan drawing of lower cellar floor in object B

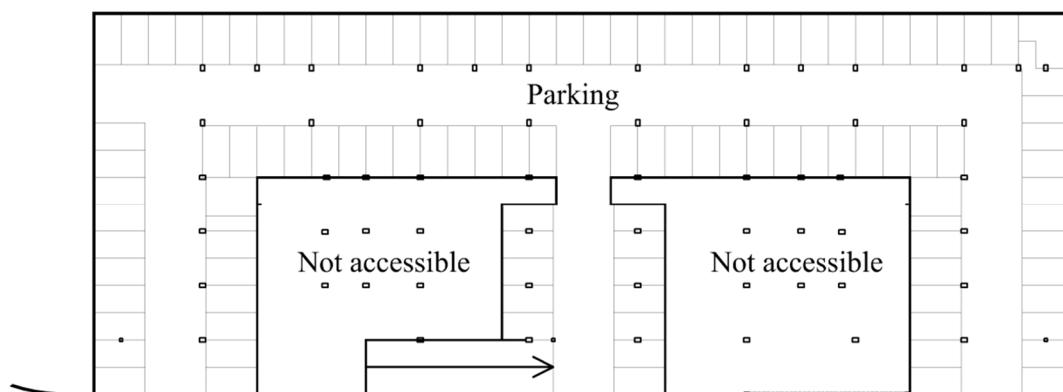


Figure 4.17 Plan drawing of upper cellar floor in object B

4.4.2 General observations

During the initial visual inspection cracks were found in all accessible outer walls. However, the distribution and widths of found cracks varied considerably between different walls. At the lower floor, all outer walls exhibited similar crack patterns. Only a few small and/or large cracks, see Table 4.1, were found in each wall. On the upper floor there were more cracks in the range of small and/or large cracks.

4.4.3 Wall 1

4.4.3.1 Design

General data for the design of the wall and the project is presented in Table 4.5.

Table 4.5 General data for concrete and reinforcing steel in object A

Concrete strength class	min. C30/37 max. C45/55
Cover thickness	Outside 30 mm, inside 40 mm
Maximum water/cement ratio	0,40
Reinforcing steel	B500BT

Wall 1 is cast against a 600 mm thick cast in-situ ground slab and the wall is connected to the slab via 12 mm reinforcement bars with a spacing of 300 mm at both faces of the wall. Above the wall there is a prefabricated hollow core floor spanning in the direction along the wall. The hollow core floor is connected to the wall via transverse reinforcement anchored in a concrete topping.

The wall is provided with 12 mm diameter reinforcement bars spaced 200 mm as horizontal reinforcement along the outside of the whole wall. On the inside of the wall there are 12 mm reinforcement bars with a spacing of 150 mm. In the bottom part of the wall there are six extra reinforcement bars at each side of the wall with a diameter of 16 mm and a spacing of 100 mm. Furthermore, in the top of the wall there are two

extra bars with a diameter of 16 mm on each side of the wall. Figure 4.18 illustrates this reinforcement arrangement.

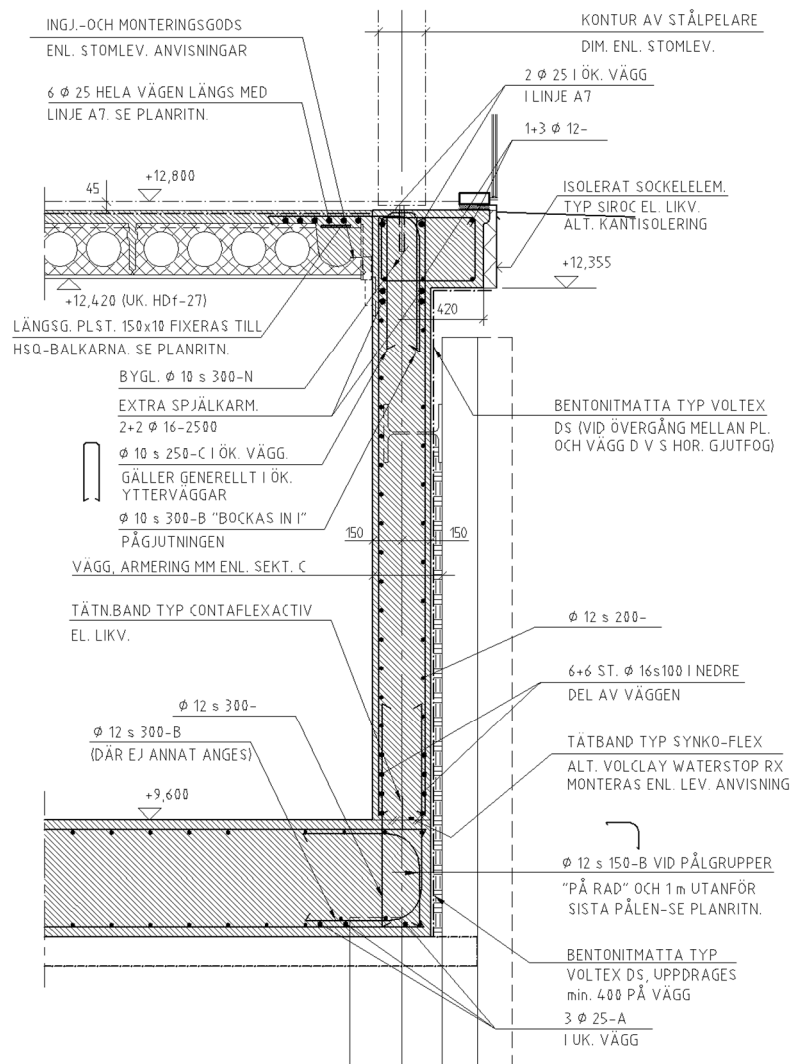


Figure 4.18 Detailing of wall 1 in object B [in Swedish], from building documentations

On the outside of the wall there is ground water pressure acting on the wall and therefore the concrete needs to be watertight. According to BBK 04, Boverket (2004), this results in to a maximum characteristic crack width of 0,2 mm.

The wall is cast against a retaining wall in steel acting as a permanent formwork. Because of this the cover thickness varies due to the cross-sectional shape of the retaining wall, see Figure 4.19. The retaining wall also provides a restraint of the wall.



Figure 4.19 Cross-sectional geometry of a retaining wall in steel

In the specifications for this object it is stated that for parts where watertight concrete shall be used, the concrete shrinkage shall be minimised. According to this the reference value for the shrinkage strain should not exceed $0,2 \cdot 10^{-3}$. This demand precedes any production related demands such as the ability to pump the concrete.

4.4.3.2 Observations

During the examination of the wall a total of 21 significant cracks were found, with the very small cracks excluded, in the selected wall part. These were all documented with regard to the crack distribution. Besides these significant cracks, several very small and short cracks were also found, see Table 4.1 for visual classification of cracks. The very small cracks found were excluded from the measurements and examinations of the wall. For photos of the wall, with tape which indicates the cracks, see Figure 4.21, Figure 4.22 and Figure 4.23 and for orientation of the different wall parts, see Figure 4.20.

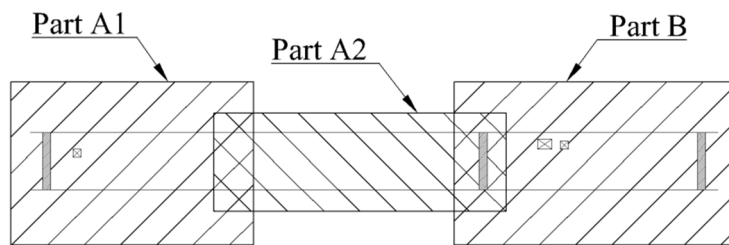


Figure 4.20 Orientation view for Figure 4.21, Figure 4.22 and Figure 4.23



Figure 4.21 Part A1 in wall 1, object B



Figure 4.22 Part A2 in wall 1, object B

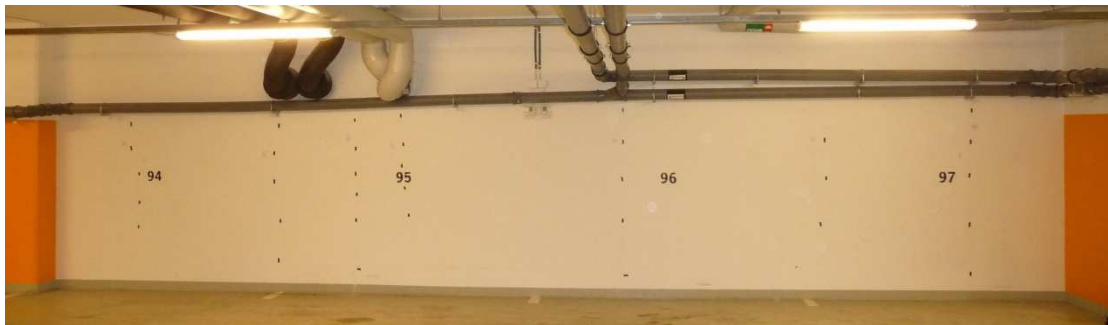


Figure 4.23 Part B in wall 1, object B

The crack pattern for all the 21 measured cracks can be seen in Figure 4.24. Over the almost 32 meter long wall no regular crack distribution was observed. To determine the average mean crack width for the wall every third crack, eight cracks in total, in the wall was measured. This resulted in an average mean crack width of 0,13 mm. After visually comparing the measured cracks with calculated average crack width in the examined wall section, two extra cracks were measured and included. The reason for this was that the first eight measured cracks were considered to not be representative for the average crack width. When the two extra cracks were included the average mean crack width was found to be 0,16 mm and the characteristic crack width then becomes 0,20 mm. In Figure 4.25 one example of a measured crack is illustrated.

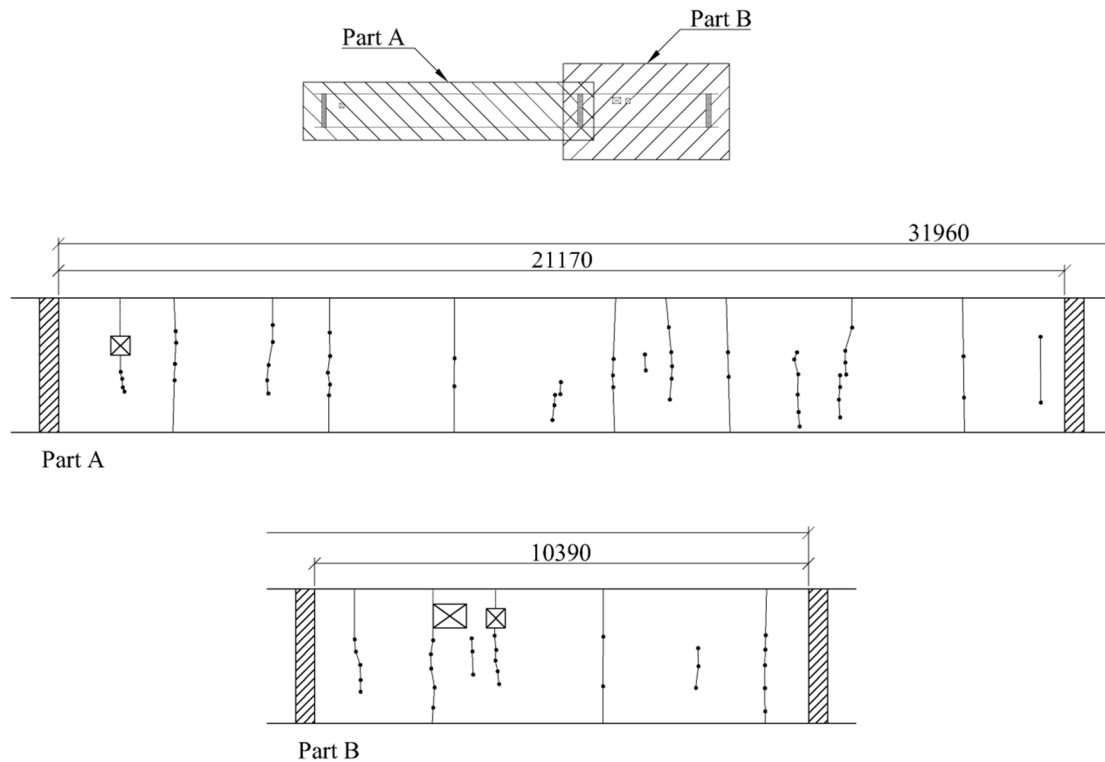


Figure 4.24 Crack pattern for wall 1, object B



Figure 4.25 Example of crack in wall 1, object B

Although the average crack width did not exceed 0,2 mm some discolouration and flaking of the paint were observed in the bottom part of several cracks. In some of them the mean crack width for that specific crack exceeded 0,2 mm. However, discolouration and flaking of the paint were also observed in cracks with a crack

width less than 0,2 mm as well. For the complete results of the measurements, see Appendix A.4.

4.4.4 Evaluation

During the visual inspection of the cellar walls the overall impression was good. In the lower floor no large or very large cracks were observed. In the upper cellar floor only a limited amount of large cracks and no very large cracks were found.

Even if the crack width in the wall is less than the 0,2 mm specified in BBK 04, Boverket (2004), signs of water leakage were observed in some of the cracks. It may be due to a larger crack width further into the section or maybe that the limit of 0,2 mm is too large in some situations.

In the detailed inspection of the wall several very small and short cracks were observed. Most of them were partly or completely covered in paint. Due to this they were formed before the paint was applied on the wall. Due to their limited size they were neither measured nor documented. One possible origin may be thermal or shrinkage effects in the early age concrete.

The actual reinforcement area in the cross-section of the wall is 6 150 mm². Calculations according to BBK 04 with a concrete strength class of C45/55 result in a required area of 4 120 mm². According to Eurocode 2, CEN (2004), the minimum reinforcement area is 19 630 mm². With a spacing of 200 mm and a characteristic crack width of 0,2 mm the steel stress is limited to 160 MPa.

5 Calculation model for numerical analysis

5.1 Introduction

In order to model the behaviour of a restrained concrete wall subjected to shrinkage, with respect to the cracking process, a Matlab program based on the direct stiffness method was developed. Both external, e.g. connecting walls and slabs, and internal, e.g. reinforcement, restraints are included in the model. Besides shrinkage the effects of creep are accounted for. Since shrinkage and creep are time-dependent parameters increasing over a considerable period of time, the calculation procedure is looped over a certain number of time steps during a certain pre-defined time period.

The program is based on a one-dimensional strip acting along the length of the considered concrete wall, see Figure 5.1. Since the model is one-dimensional, variations along remaining dimensions, height and width, are not possible to account for.

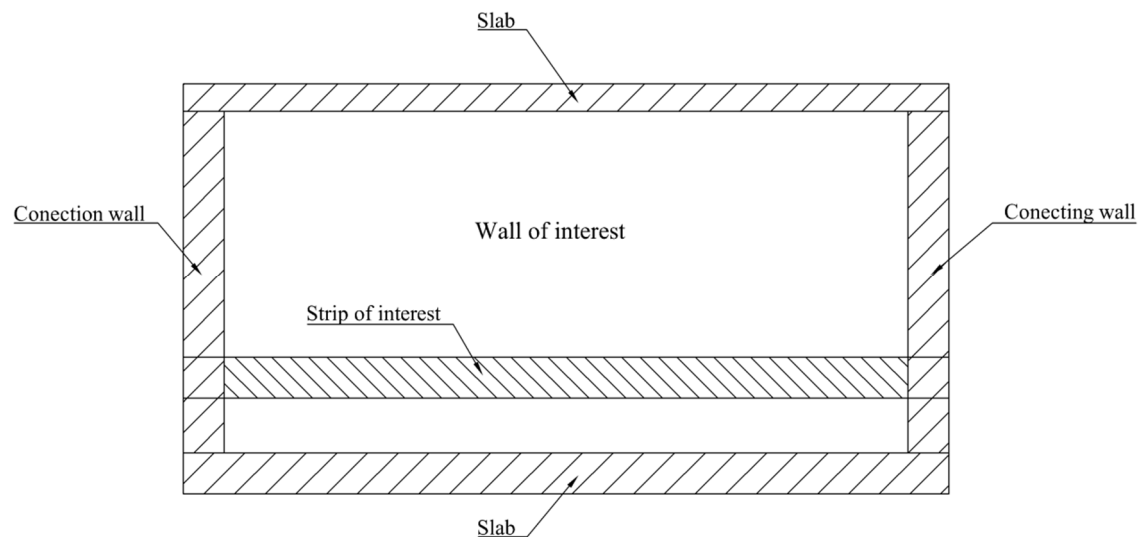


Figure 5.1 Schematic sketch of a strip in a wall

The program divides the considered wall segment into a number of elements, where all effects are considered to be distributed over the element length. Each element consists of two nodes where each node has one degree of freedom. Figure 5.2 illustrates the element and node distributions.

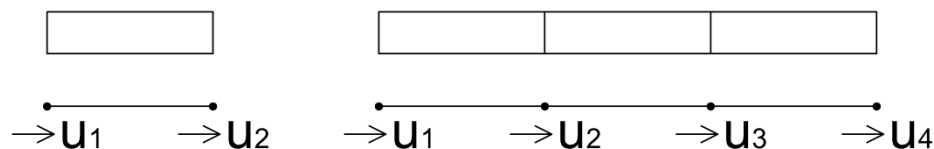


Figure 5.2 Schematic sketch showing degrees of freedom

Connections between the considered wall segment and its connecting elements are accounted for by means of spring stiffnesses. The external restraints acting in an individual node is summarised into a single spring element connected to that node. Figure 5.3 illustrates these connections between wall elements and their respective stiffnesses from external restraints by means of spring stiffnesses

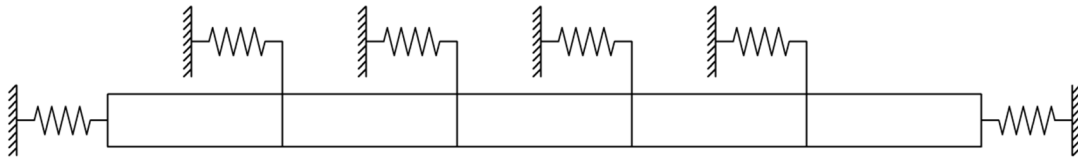


Figure 5.3 Modelling of external restraints acting on the calculation model

Besides the external stiffnesses described above internal stiffnesses from concrete, reinforcement and, when needed, cracks are accounted for in the calculation model. All stiffnesses are described further in Section 5.2.2.7.

Forces are applied to the system by first calculating the free shrinkage strain and applying it on the system as a shrinkage force. After applying this force stresses are calculated and, when the stresses are high enough, cracks are inserted. A crack is inserted into the model as a non-linear spring stiffness, as schematically illustrated in Figure 5.4. The insertion of cracks is treated further in Section 5.2.2.9.

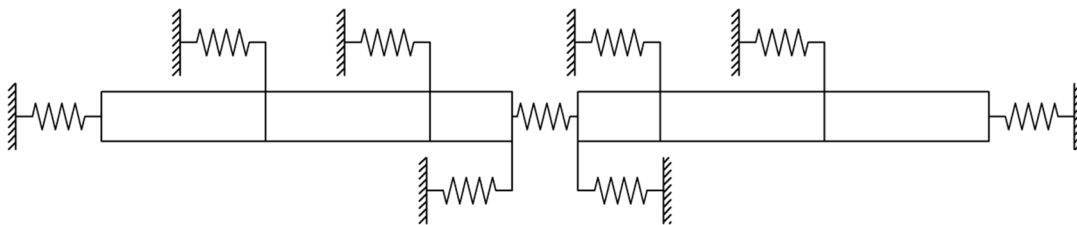


Figure 5.4 Model with a crack inserted in the centre element

After completion the program returns information about the cracking situation in the considered concrete member during circumstances defined by various input parameters. Most importantly, information about the crack distribution along with its crack widths and corresponding steel stresses are obtained. In section 5.2 the outline and structure of the program are described in greater detail, while all calculation results are presented in Chapter 5.3.4.

5.2 Program structure

5.2.1 Main program

In this section the structure and outline of the main program is described which is supported by 10 different function files, described further in Section 5.2.2. The Matlab-code for this program is presented in Appendix B.1. Using a flow chart Figure 5.5 and Figure 5.6 illustrate the main program's outline and when different supporting functions are called.

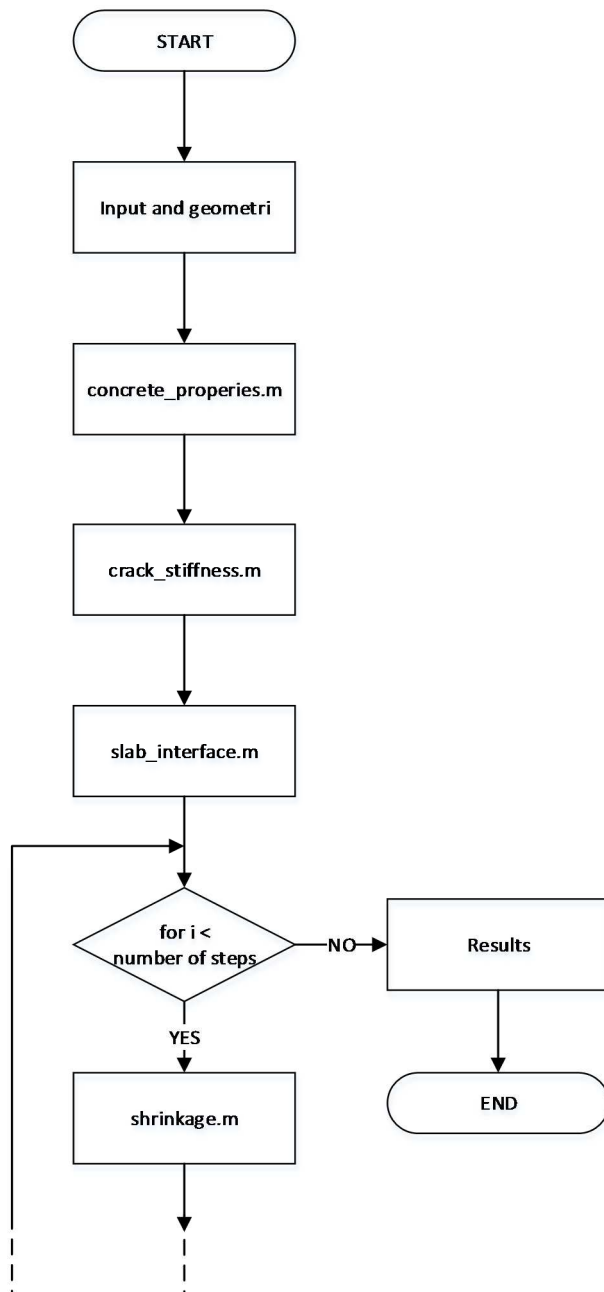


Figure 5.5 Flow chart of main program, part 1

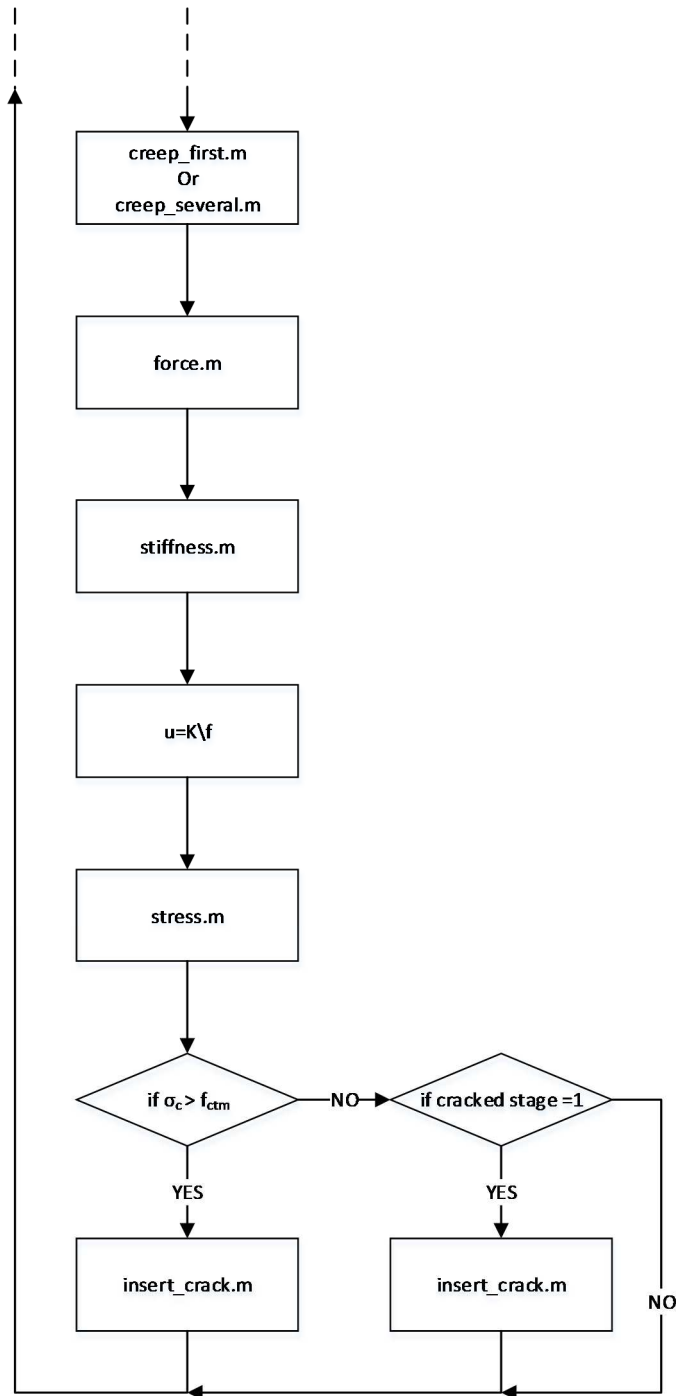


Figure 5.6 Flow chart of main program, part 2

Basically, the main program consists of an initial input and prerequisites section followed by an iterative calculation loop. In the initial part various input parameters are defined by the operator. Required input parameters include information about calculation time steps, parameters regarding concrete, reinforcement and support stiffness at connecting walls and variables controlling shrinkage, creep and shear response of the wall/slab interface.

With all required input parameters defined the main program defines geometric parameters, obtains concrete properties from *concrete_properties.m* (Section 5.2.2.1), calculates properties and stiffnesses of the wall/slab interface using *slab_interface.m*

(Section 5.2.2.2), calculates crack stiffness and steel stress parameters using *crack_stiffness.m* (Section 5.2.2.3) and preallocates various matrices, vectors and parameters.

After the definitions stated above, the main program initiates the iterative calculation loop covering a predefined time period using a predefined number of time steps. First, the shrinkage strain is calculated using the function file *shrinkage.m*, see Section 5.2.2.4. Afterwards the effects of creep are considered by obtaining a creep coefficient and calculating the effective Young's modulus. The creep coefficient can be calculated either based on the first creep function by using *creep_first.m* or based on a weighted average of several creep functions using *creep_several.m*, see Section 5.2.2.5. Section 3.4 further describes the effects of creep and the difference between the two alternative procedures possible in this program to take creep deformations into account.

At this stage the program generates the global force vector and the global stiffness matrix. Using *force.m*, see Section 5.2.2.6, a global force vector is assembled based on the free shrinkage strain and effective Young's modulus. Depending on if the member is cracked or uncracked, individual components of the force vector are calculated and assembled differently. After obtaining the force vector, individual components of the stiffness matrix are calculated and assembled using *stiffness.m*, Section 5.2.2.7. Just as for the force vector, the stiffness matrix is generated differently depending on the existence of cracks. With forces and stiffnesses obtained, the governing equation of the direct stiffness matrix, expressed below, can then be solved.

$$K \cdot a = F \tag{5.1}$$

where K is the global stiffness matrix
 a is the global displacement vector
 F is the global force vector

When solving the equation above, nodal displacements are obtained and stresses are then possible to calculate. Calling the function *stress_cracks.m*, see Section 5.2.2.8, concrete tensile stresses are calculated and returned to the main program. In short, stresses are calculated based on the part of the shrinkage strain that is prevented by external and internal restraints, i.e. the difference between the total strain and free shrinkage strain, see Section 3.2. If the calculated concrete stresses exceed the mean tensile strength, the member is considered to be cracked and a new crack is identified and inserted in the next step of the calculation loop. After cracking is initiated, *stress_cracks.m* also calculates crack widths and corresponding steel stresses at all existing cracks.

Cracks are identified directly in the main program by finding all elements where the concrete stress in the given time step exceeds the mean tensile strength. If several elements are identified, one is randomly chosen to be the new crack element. This simulates the fact that in a real member, a crack is initiated in the weakest section, see Section 3.4 and Section 5.2.2.9. When a crack element is chosen, *insert_crack.m*, see Section 5.2.2.9, is called to redefine and update matrices, vectors and parameters that need to change due to the appearance of cracks. By the completion of *insert_crack.m* calculations for the given time step are completed and the next time step is ready to be initiated. However, before ending the given time step, the current stress distribution along the member with the positions of all existing cracks are plotted and the

maximum concrete stress is printed in order to follow the calculation process during all iterations.

After the completion of all time steps results are extracted. The main results are crack distribution, crack widths and steel stresses in crack sections. It should be noted that at that time the program considers all nodes of the connecting slab to be fully fixed. However, the program is prepared to handle a non-fixed slab since a global displacement vector for slab nodes exists but is defined as a zero-vector in every time step.

5.2.2 Function files

5.2.2.1 Concrete properties

The function file *concrete_properties.m*, see Appendix B.2, returns values for five different concrete properties based on the strength class of the concrete considered. Eurocode 2, CEN (2004), tabulates all values used in this function. With the characteristic concrete strength inserted as input, *concrete_properties.m* returns mean value of Young's modulus, mean compressive strength, lower (5%-fractile) characteristic tensile strength, mean tensile strength and upper (95%-fractile) characteristic tensile strength. 14 different strength classes are possible to use as input in *concrete_properties.m*. The characteristic compressive strength of these classes is 12, 16, 20, 25, 30, 35, 40, 45, 50, 55, 60, 70, 80 and 90 MPa respectively.

5.2.2.2 Slab interface

Section 3.1.5.2 states an expression for the shear strength and a shear stress-slip relation for an interface between two concrete layers cast at different times. Utilising this expression and relation the function *slab_interface.m*, see Appendix B.3, returns parameters required to calculate the stiffness in a certain node along the wall/slab interface.

The first section of *slab_interface.m* calculates the shear strength according to the proposed procedure in fib Model Code 2010, while the second section, utilising the shear strength, calculates the linear and non-linear inclinations of the shear stress-slip relation from CEB-FIP Model Code 1990. In order to obtain the inclinations the curve is divided into small segments and the inclinations between end points of each segment are calculated. These inclinations together with limiting slip values of each segment, the shear strength, the slip limit of the linear branch and the ultimate slip are returned to the main program as output parameters.

A total of six input parameters are required in *slab_interface.m*. These are the surface roughness factor, characteristic concrete compressive strength, the lowest compressive stress resulting from a normal force at the interface (Appendix D.2), concrete contact area of the interface and the total reinforcement area of bars placed across the interface.

5.2.2.3 Crack stiffness

For each new crack appearing in the modelled concrete member, a special crack element is inserted, see Section 5.2.2.9. Such crack element consists of reinforcement

only as opposed to uncracked elements. Consequently the stiffness is different from that of an uncracked element. Values for this crack stiffness are calculated using the function *crack_stiffness.m*, see Appendix B.4.

Engström (2011a) gives an expression where the mean crack width is a function of the steel stress. This equation was derived using the bond stress-slip relation according to Jaccoud, see Equation 3.1, and is expressed as.

$$w_m = 0,420 \left(\frac{\phi \cdot \sigma_s^2}{0,22 \cdot f_{cm} \cdot E_s \left(1 + \frac{E_s}{E_c} \cdot \frac{A_s}{A_{cf}} \right)} \right)^{0,826} + \frac{\sigma_s}{E_s} \cdot 4\phi \quad (5.2)$$

where w_m is the mean crack width
 ϕ is the reinforcement bar diameter inserted in mm
 σ_s is the steel stress
 f_{cm} is the mean concrete compressive strength
 E_s is the Young's modulus of reinforcing steel
 A_s is the reinforcement area
 E_c is the Young's modulus of concrete
 A_{cf} is the effective concrete area

According to Engström (2011a) part of this equation can on the safe side be assumed equal to one as

$$\left(1 + \frac{E_s}{E_c} \cdot \frac{A_s}{A_{cf}} \right) \approx 1 \quad (5.3)$$

This assumption is utilised in *crack_stiffness.m*, which reduces Equation 5.2 to the expression below.

$$w_m = 0,420 \left(\frac{\phi \cdot \sigma_s^2}{0,22 \cdot f_{cm} \cdot E_s} \right)^{0,826} + \frac{\sigma_s}{E_s} \cdot 4\phi \quad (5.4)$$

The relation between steel stress and mean crack width presented by the equation above is obviously non-linear. Hence the stiffness, represented by the inclination of the curve, exhibits a non-linear variation. In order to obtain corresponding inclinations the curve is divided into numerous small segments, where the inclination of each segment is assumed to be linear between its end points. These inclinations are returned to the main program, along with limiting crack width values, as output parameters which are later used to assemble the global stiffness matrix, see Section 5.2.2.7.

Besides these inclinations, *crack_stiffness.m* returns a matrix containing intervals of crack widths and corresponding steel stresses, which are calculated using the same procedure as for the inclinations. This matrix is later used to determine the steel stress in each crack element, see Section 5.2.2.8.

The input required for *crack_stiffness.m* is limited to four parameters. These are reinforcement bar diameter, mean concrete compressive strength, Young's modulus of reinforcing steel and total reinforcement area.

5.2.2.4 Shrinkage

During the calculation procedure shrinkage is introduced by means of a shrinkage strain, which is calculated according to the method defined in Eurocode 2, CEN (2004), see Section 3.3. The function file *shrinkage.m*, see Appendix B.5, returns the free shrinkage strain at a given concrete age based on seven input parameters. These are current age, age when drying starts, relative humidity of surroundings, characteristic concrete compressive strength, cement class, concrete cross-sectional area and the cross sectional perimeter exposed to drying. The concrete shrinkage strain is, as stated in Section 3.3, time dependent. Hence, the shrinkage strain must be recalculated in each time step. It should be noted that uniform shrinkage is assumed.

5.2.2.5 Creep

Creep can be considered using two alternative approaches. Each approach uses separate function files denoted *creep_first.m*, see Appendix B.6, and *creep_several.m*, see Appendix B.7, respectively. Which approach to be used is decided by means of an input parameter in the main program. Both approaches calculate a creep coefficient which in turn is used to calculate an effective Young's modulus of concrete.

The approach in *creep_first.m* is based on the first creep function. Thus a creep coefficient based on the concrete age at the first load application is recalculated in each time step. Thus this approach ignores the loading history of the considered concrete member. According to Engström (2011a) the effects of creep will be overestimated for an increasing stress and underestimated for a decreasing stress.

The second approach, used in *creep_several.m*, is based on several creep functions. During each time step the load changes and a load increment can be determined. In this approach each such load increment has its own creep coefficient depending on the concrete age when the load increment is introduced. An effective creep coefficient is then calculated as a weighted average of the creep coefficients for all load increments, as expressed below.

$$\varphi_{ef} = \frac{\sum (\sigma_i \cdot \varphi_i)}{\sum \sigma_i} \quad (5.5)$$

where φ_{ef} is the effective creep function (weighted average)
 φ_i is the individual creep function of each stress increment
 σ_i is the stress increment of each time step

Both of these approaches are treated in Section 3.4. Regardless of the chosen approach the individual creep coefficients are calculated using the equations defined in Eurocode 2, which are treated in Section 3.4. In order to calculate creep coefficients seven input parameters are required. These are current concrete age, concrete age when drying starts, relative humidity of surroundings, characteristic concrete compressive strength, concrete cross-sectional area, the cross-sectional perimeter exposed to drying and cement class. However, *creep_several.m* requires two

additional input parameters, Young's modulus of concrete and a vector containing shrinkage strains for each time steps in order to calculate stress increments.

5.2.2.6 Force

A global force vector is assembled using the function *force.m*, see Appendix B.8, according to the procedure explained throughout this section. Since each concrete element shrinks, the shrinkage force mentioned in Section 5.1 should be applied on each concrete element considered in the model. A local force vector for each such element can be expressed accordingly.

$$F_{element} = f_{element} \begin{bmatrix} 1 \\ -1 \end{bmatrix} \quad (5.6)$$

where $F_{element}$ is the local element force vector
 $f_{element}$ is the force according to the equation below

$$f_{element} = \varepsilon_{cs} \cdot E_{c.ef} \cdot A_c \quad (5.7)$$

where ε_{cs} is the free shrinkage strain
 $E_{c.ef}$ is the effective Young's modulus of concrete with regard to creep
 A_c is the concrete cross-sectional area

Note that the shrinkage applied is that of free shrinkage, see Section 5.1, and that the effective Young's modulus is used. Furthermore, note that internal restraints are implemented as stiffnesses directly into the stiffness matrix, see Section 5.2.2.7, and not by using the force vector. When the local force vectors of each element are assembled into a global force vector for an uncracked section, all force components besides both end nodes cancel each other out and the resulting global force vector becomes

$$F_{global} = f_{element} \begin{bmatrix} 1 \\ 0 \\ \vdots \\ 0 \\ -1 \end{bmatrix} \quad (5.8)$$

where F_{global} is the global force vector
 $f_{element}$ is the element force

Thus force components only have to be added in the first and last positions of the global force vector while the member remains uncracked. However, when the cracked stage is initiated by the appearance of a first crack, the force vector has to be defined differently from the uncracked stage. Since cracking to some degree reduces the restraints on the member, the shrinkage force should consequently decrease. This reduction is calculated as an equivalent strain based on the sum of all crack widths and the local force vector for a concrete element is then defined accordingly.

$$F_{element} = f_{element} \begin{bmatrix} 1 \\ -1 \end{bmatrix} \quad (5.9)$$

where $F_{element}$ is the local element force vector
 $f_{element}$ is the force according to the equation below

$$f_{element} = (\varepsilon_{cs} - \varepsilon_w) \cdot E_{c.ef} \cdot A_c \quad (5.10)$$

where ε_{cs} is the free shrinkage strain

$$\varepsilon_w = \sum_{i=1}^{n_{cracks}} w_{crack} / L_{total}$$

w_{crack} is the mean crack width

L_{total} is the total length of the wall

n_{cracks} is number of cracks

$E_{c.ef}$ is the effective Young's modulus of concrete

A_c is the concrete cross-sectional area

Since cracking divides a concrete member into several smaller concrete members held together by reinforcement, the force vector contains more non-zero components compared to the uncracked stage. At each crack a force component remains and the global force vector for the cracked stage is expressed accordingly, as illustrated by Figure 5.7.

$$F_{global} = f_{element} \begin{bmatrix} 1 \\ 0 \\ \vdots \\ 0 \\ -1 \\ 1 \\ 0 \\ \vdots \\ 0 \\ -1 \end{bmatrix} \quad (5.11)$$

where F_{global} is the global force vector
 $f_{element}$ is the element force

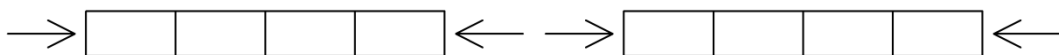


Figure 5.7 Forces on model with one crack

The function file *force.m* requires eight input parameters in order to return the global force vector. These are shrinkage strain, effective Young's modulus of concrete,

cross-sectional concrete area, number of nodes, variable defining cracked or uncracked stage, cracked element numbers, all crack widths and the total length of the considered concrete member.

5.2.2.7 Stiffness

As stated in Section 5.1 stiffnesses are introduced by means of spring elements acting in the nodes of each element, see Figure 5.3. Consequently, all element parameters are considered as uniformly distributed over each element. Within the calculation program stiffnesses are calculated using a function file denoted *stiffness.m*, see Appendix B.9, which returns a global stiffness matrix to the main program. Since cracking drastically changes the stiffness of a concrete member, see e.g. Section 3.1, the individual components of the global stiffness matrix are calculated differently depending on if the member is uncracked or cracked.

For an uncracked member the global stiffness matrix contains four different stiffness components. These are plain concrete, reinforcing steel, connecting walls and interface to the connecting slab. The global stiffness matrix for a cracked member contains these four components as well as the additional component expressing the crack stiffness.

Concrete and reinforcement stiffnesses are obtained according to the principle of a rod element, since the model is one-dimensional. The local stiffness matrix for one element, containing concrete and reinforcement stiffnesses only, can then be expressed as, Dahlblom and Olsson (2010).

$$K_{element} = k_{element} \begin{bmatrix} 1 & -1 \\ -1 & 1 \end{bmatrix} \quad (5.12)$$

where $K_{element}$ is the local element stiffness matrix
 $k_{element}$ is the element stiffness

The element stiffness $k_{element}$ in the equation above is expressed as

$$k_{element} = \frac{E_c \cdot A_c}{L} + \frac{E_s \cdot A_s}{L} \quad (5.13)$$

where E_c is the Young's modulus of concrete
 A_c is the cross-sectional area of concrete
 E_s is the Young's modulus of reinforcing steel
 A_s is the cross-sectional area of reinforcement
 L is the initial element length

Stiffnesses from connecting elements, walls and slabs, are obtained differently from concrete and reinforcement stiffnesses. As illustrated by Figure 5.3 these stiffnesses are only connected to two nodes where one is not a part of the considered concrete member. Consequently, these stiffnesses only consist of components of the diagonal of the stiffness matrix, as exemplified below using a global four-node system.

$$K_{global} = \begin{bmatrix} S_{wall.left} + k_{slab.1} & 0 & 0 & 0 \\ 0 & k_{slab.2} & 0 & 0 \\ 0 & 0 & k_{slab.3} & 0 \\ 0 & 0 & 0 & S_{wall.right} + k_{slab.4} \end{bmatrix} \quad (5.14)$$

where K_{global} is the global stiffness matrix
 $k_{slab.i}$ is the slab interface stiffness at node i
 $S_{wall.left}$ is the support stiffness of the left connecting wall
 $S_{wall.right}$ is the support stiffness of the right connecting wall

In the exemplifying expression above $S_{wall.left}$ and $S_{wall.right}$ are the support stiffnesses for the left and right connecting walls respectively. The topic of support stiffness is briefly treated in Section 3.2.3. The diagonal elements $k_{slab.1}$ to $k_{slab.4}$ denote the interface stiffness at the connecting slab in each node. Note that since the interface stiffness depends on the nodal slip, see Section 3.1.5 or 5.2.2.2, the actual stiffness in one node might be different from that of another node. Actual stiffness values at the interface to the connecting slab nodes are obtained using the function *slab_interface.m*, see Section 5.2.2.2.

As stated in Section 3.1 a crack element contains a different stiffness from that of an uncracked element. The local stiffness matrices for crack elements are generated using the same principle as for the matrices for concrete and reinforcement stiffness. A local stiffness matrix for a crack element is exemplified below, where the value of k_{crack} is obtained from the function *crack_stiffness.m*.

$$K_{crack.local} = k_{crack} \begin{bmatrix} 1 & -1 \\ -1 & 1 \end{bmatrix} \quad (5.15)$$

where $K_{crack.local}$ is the local element stiffness matrix for a crack element
 k_{crack} is the crack element stiffness

All local stiffness matrices, for all elements and all stiffness components, are finally assembled into the global stiffness matrix which, of its individual components, has the unit of N/m. Note that the assembly process differs slightly for an uncracked and a cracked member. In an uncracked member contributions from concrete, reinforcement and the interface to the connecting slab are included in every element. For a cracked member contributions from concrete, reinforcement and the interface to the connecting slab are ignored in the crack elements.

In order to return the global stiffness matrix, *stiffness.m* requires the following input: support stiffness of left connecting wall, support stiffness of right connecting wall, initial element length, effective Young's modulus of concrete, Young's modulus of steel, concrete cross-sectional area, total horizontal reinforcement area, number of nodes, number of elements, parameter defining cracked or uncracked stage, wall thickness, global wall displacement vector, global slab displacement vector, linear inclination (stiffness) for interface to connecting slabs, non-linear inclinations (stiffnesses) for interface to connecting slabs, ultimate interface slip, linear limit of slab slip, cracked element numbers, non-linear inclinations (stiffnesses) of the crack opening-relation and the number of slab restraints considered.

5.2.2.8 Stresses and crack widths

The function file *stress_cracks.m*, see Appendix B.10, calculates concrete stresses in all uncracked elements and steel stresses and crack widths in any existing cracks. These values are then returned to the main program. Required input parameters for *stress_cracks.m* are uncracked element numbers, global wall displacements, global wall/slab interface displacements, initial element length, current shrinkage strain, effective Young's modulus for concrete, yielding strength of reinforcing steel, cracked element numbers, diameter of horizontal reinforcement bars, mean concrete compressive strength and Young's modulus of reinforcing steel.

Concrete stresses are, regardless of if the member is in the cracked or uncracked stage, calculated using the imposed stress-dependent strain. Figure 5.8 illustrates three different shrinkage strain situations of a concrete member. In the first situation no shrinkage strain has occurred and consequently the member is stress free. In the second situation the member shrinks but is free from restraint. Thus free shrinkage occurs and no stress arises since the total concrete strain is equal to the free shrinkage strain. However, in the third case the concrete member shrinks with restraint present. Since free shrinkage cant occur due to the restraint, an imposed stress-dependent strain, ϵ_c , exists. It is this strain which generates the tensile stress occurring in a restrained concrete member that shrinks, which can be expressed mathematically as

$$\sigma_{concrete} = -(\epsilon_{c,tot} - \epsilon_{cs}) \cdot E_{c,ef} \quad (5.16)$$

where ϵ_{cs} is the free shrinkage strain
 $\epsilon_{c,tot}$ is the total concrete strain

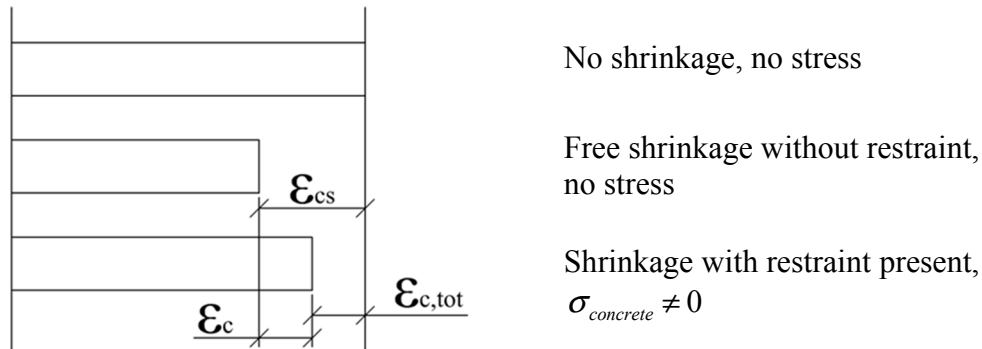


Figure 5.8 Illustration of imposed stress-dependent strain

Concrete stresses in uncracked elements, which are returned to the main program as an output parameter, are calculated using the equation above where the total concrete strain is calculated using the displacements obtained by solving Equation (5.1). When the first crack appears and the member enters the cracked stage, *stress_cracks.m* also calculates crack widths and corresponding steel stresses.

Crack widths are calculated as the difference in global displacement between the two nodes in each crack element. Since the initial length of an inserted crack element, see Section 5.2.2.9, is zero, this displacement difference is equal to the element length. After obtaining the crack width the corresponding steel stress is calculated using the

steel stress matrix obtained from *crack_stiffness.m*, see Section 5.2.2.3. During the course of a while-loop and using Equation (5.4), a steel stress is first guessed and then increased until the crack width obtained using Equation (5.4) matches (approximately) the one calculated using the displacement vector. It is possible to solve Equation (5.4) exactly through Matlab commands. However, such a solution running once for each crack in each out of possibly thousands of time steps are not feasible with regard to the calculation time required. Additionally the fault caused by the while-loop iteration is of limited significance.

The last part of *crack_stiffness.m* contains warning functions for yielding reinforcement, negative reinforcement strain (compression) and negative concrete strains. Note that in this case a negative concrete strain would imply that the actual shortening of the considered concrete member exceeds the free shrinkage strain, which, of course, is unreasonable. The reason being that the imposed strain considered here is the difference between the total deformations and the free shrinkage, as stated earlier in this section.

5.2.2.9 Crack insertion

When, or if, the calculated tensile stress in a concrete element exceeds the mean tensile strength of the considered concrete, that element is considered to be cracked. Since all effects are accounted for as uniformly distributed over the course of the element length, each new crack is assumed to take place in the middle of the now cracked element. In a real concrete member cracking is initiated in the weakest part within parts where stresses are sufficiently high, which is not necessarily in the middle. However, while element lengths are kept small enough, this approximation remains reasonable. Furthermore, it would not be possible to analyse the stresses within a single element using this model, since all actions are considered as uniformly distributed over an element length.

If the calculated tensile stress exceeds the mean tensile strength in more than a single element, an element that cracks is chosen randomly from the elements with sufficiently high tensile stress. In a way that is an approximation of the fact that cracks occur in the weakest section in a real concrete member.

In the main program the function *insert_crack.m*, see Appendix B.11, is called in every time step, when the cracked stage is entered. Depending on if a new crack is initiated in the ongoing time step or not, all or only a limit part of the function is utilised. During every call to *insert_crack.m* the transmission length is calculated, using the equations below, for each crack based on the steel stress of each crack. The concept of transmission length is treated in Section 3.1.4. In short, in a crack all forces are transferred across by the reinforcement bars only and in sections near the crack some of the forces are gradually transferred to the concrete. After a certain length strain compatibility between the reinforcement and the surrounding concrete is achieved. That is the end of the transmission length.

Based on the calculated transmission lengths of all cracks, elements are divided into different regions. The first type of region is the transmission region, in which a crack element along with its adjacent elements within its calculated transmission length are included. Each crack has such a region, while the other type of region contains all remaining elements. When, in each time step, concrete stresses are compared to the mean tensile strength to evaluate if a new crack should be inserted, only elements not

included in a transmission region are considered. All regions are updated in *insert_crack.m* in each time step.

$$w_{net} = 0.420 \cdot \left(\frac{\phi \cdot \sigma_s^2}{0.22 \cdot f_{cm} \cdot E_s \cdot \left(1 + \frac{E_s}{E_c} \cdot \frac{A_s}{A_{ef}} \right)} \right)^{0.826} \quad (5.17)$$

Where ϕ is the bar diameter inserted in [mm]
 σ_s is the steel stress
 f_{cm} is the mean concrete compression strength

$$l_t = 0.433 \cdot \frac{\phi \cdot \sigma_s}{0.22 \cdot f_{cm} \cdot w_{net}^{0.21} \cdot \left(1 + \frac{E_s}{E_c} \cdot \frac{A_s}{A_{ef}} \right)} + 2 \cdot \phi \quad (5.18)$$

Engström (2011a) states that, on the safe side, parts of the denominator of the upper equation can be assumed equal to 1, as expressed below.

$$\left(1 + \frac{E_s}{E_c} \cdot \frac{A_s}{A_{ef}} \right) \approx 1 \quad (5.19)$$

This assumption is utilized in *insert_crack.m*. Thus Equations (5.17) and Equation (5.18) are reduced to the expressions below, which are used in *insert_crack.m*.

$$l_t = 0.433 \cdot \frac{\phi \cdot \sigma_s}{0.22 \cdot f_{cm} \cdot w_{net}^{0.21}} + 2 \cdot \phi \quad (5.20)$$

$$w_{net} = 0.420 \cdot \left(\frac{\phi \cdot \sigma_s^2}{0.22 \cdot f_{cm} \cdot E_s} \right)^{0.826} \quad (5.21)$$

If a new crack is to be initiated during a certain time step, *insert_crack.m* runs a special part of the program. This part is placed before the part described above and updates various parameters with respect to the initiated crack. The parts updated are the number of elements and nodes, the cracked element vector containing the cracked element numbers, the crack time vector saving the time step where each crack first occurs and its corresponding element number, an initial guessed value of steel stress in the new crack is added in the steel stress vector to enable calculation of the transmission length and, finally, the displacement vectors with respect to the newly inserted crack element.

After completion *insert_crack.m* returns updated parameters concerning the cracking situation of the considered concrete member. These parameters are cracked element numbers, element numbers for elements part of a transmission region and remaining elements respectively, number of elements, number of nodes, global displacement vectors for wall and wall/slab interface and a vector containing the time steps of

cracking. The input required for these outputs to be generated is the number of elements and nodes, the number of the newly appeared crack (zero if no new crack is initiated in a certain time step), cracked element numbers, total number of cracks, steel stresses in cracks, mean concrete compressive strength, Young's modulus of reinforcing steel, horizontal reinforcement diameter, initial element length, global displacement vectors for wall and wall/slab interface, time step of the newly appeared crack (zero if no new crack is initiated in a certain time step) and, finally, the already existing vector containing time steps of cracking.

5.2.3 Boundary conditions

Boundary conditions used in the calculation model are, as illustrated in Figure 5.3 and Figure 5.4, represented by spring stiffness's connected to rigid supports. Such spring stiffness is applied to each node within the one-dimensional strip. The actual stiffness value of each node depends on the external restraints connected to said node and is determined individually using the function file *stiffness.m*, Section 5.2.2.7.

Each spring is connected to two nodes, its rigid support and a node within the one-dimensional strip. Since the deformation of a rigid support always is zero, the row and column of the stiffness matrix, deformation vector and force vector corresponding to the node of a rigid support can be excluded from the calculation.

$$\begin{bmatrix} k_{11} & k_{12} \\ k_{21} & k_{22} \end{bmatrix} \begin{bmatrix} u_1 \\ u_2 \end{bmatrix} = \begin{bmatrix} f_1 \\ f_2 \end{bmatrix} \rightarrow [u_1 = 0] \rightarrow k_{22} \cdot u_2 = f_2 \quad (5.22)$$

where k_{ij} is the stiffness component of row i and column j
 u_i is the displacement of node i
 f_i is the force in node i

For further information regarding the derivation of the matrix and vectors above and boundary conditions in general, see e.g. Ottosen and Petersson (1992).

5.2.4 Deformation conditions

As stated in Section 5.2, the calculation model uses the direct stiffness method. The fundamental deformation condition on which the method is based is that all deformations should fit together, i.e. the sum of all deformations should be zero. In the case modelled in this project, this means that the sum of the deformation vector, see Section 5.2.1, should be zero. This corresponds to that the total deformation of the concrete member (elastic strain, shrinkage strain, creep strain and crack widths) is equal to the total deformation of both end supports (connecting walls) combined. Utilizing the direct stiffness method with properly defined boundary condition, no further deformation condition needs to be applied. For more information about the direct stiffness method and this fundamental deformation condition, reference is made to Ottosen and Petersson (1992).

5.3 Verification of the model

The verification of the calculation model is divided into four parts. In turn, verifications of the shrinkage strain calculation, creep coefficient calculations, the concrete stress calculation and the essential deformation condition are presented. In Section 5.3.1 the shrinkage strain calculation is verified by comparing results from the Matlab main program and its function file with analytical calculations performed using Mathcad. Subsequently the calculations of creep coefficient and concrete stress are verified in Section 5.3.2 and Section 5.3.3 respectively, each using the same aforementioned approach as for the shrinkage strain verification. Finally, the essential deformation condition of Section 5.2.4 is verified in Section 5.3.4. This verification is carried out by a tabulation of the sum of all deformations where the computational results are obtained by running the Matlab main program using a series of different input values.

5.3.1 Shrinkage strain

Calculations of the total shrinkage strain were verified by comparing Matlab results with analytical results. The complete verifying calculation can be found in Appendix C.1. Table 5.1 below illustrates results in form of total shrinkage strain after 2, 5, 15 and 50 years respectively from both analytical calculations and Matlab calculations. As seen in the table all values are identical to four decimals or more, implying the correctness of the shrinkage strain calculation performed by the function file *shrinkage.m*, see Section 5.2.2.4, in the main program.

Table 5.1 Shrinkage strains from analytical calculation and Matlab program

Years	Total shrinkage strain [-]	
	Analytical calculation	Matlab calculation
2	$3,4063 \cdot 10^{-4}$	$3,4063 \cdot 10^{-4}$
5	$3,8252 \cdot 10^{-4}$	$3,8252 \cdot 10^{-4}$
15	$4,0519 \cdot 10^{-4}$	$4,0519 \cdot 10^{-4}$
50	$4,1389 \cdot 10^{-4}$	$4,1389 \cdot 10^{-4}$

Figure 5.9 illustrates the shrinkage strain developments during five and 50 years respectively calculated using both Matlab calculations and analytical calculations. The figure clearly demonstrates the high resemblances between these calculations, implying the correctness of the shrinkage strain calculation. The plots of Figure 5.9 were generated by the verification calculation presented in Appendix C.1.

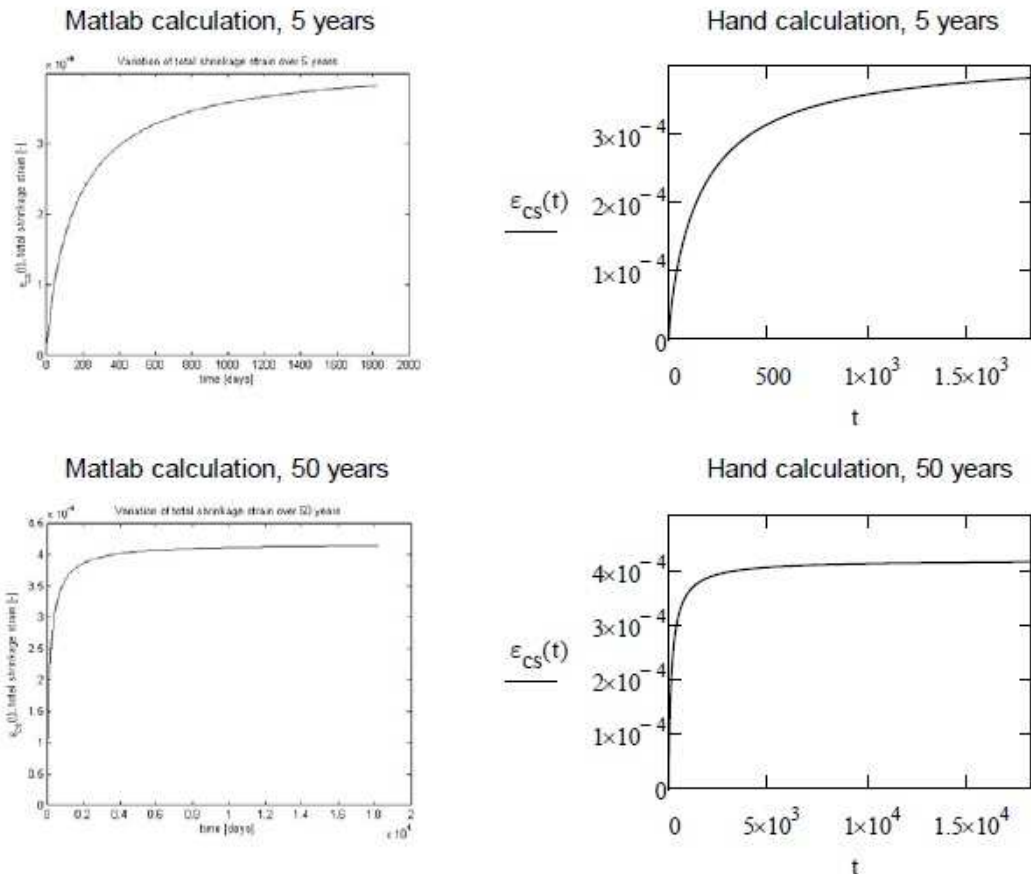


Figure 5.9 Shrinkage strain developments determined by analytical and Matlab-calculations

Since the values of Table 5.1 as well as the plots of Figure 5.9 all illustrate a very high correlation between the Matlab calculations of the main program and the analytical calculations, the shrinkage strain calculations were considered to be verified.

5.3.2 Creep coefficient

As stated in Section 5.2.2.5 there are two alternate approaches to consider creep in the calculation model. The first approach, verified in Section 5.3.2.1, calculates a creep coefficient from the first creep function, while the second approach, verified in Section 5.3.2.2, calculates an effective creep function as a weighted average of several creep functions (one for each load increment).

5.3.2.1 First creep approach

In order to verify the first creep approach, which calculates a creep coefficient using the first creep function, computational results from the Matlab program were compared with analytical calculations. The complete verifying calculation can be found in Appendix C.2. Creep coefficients were calculated after 2, 5, 15 and 50 years using analytical calculations and the function file *creep_first.m*, which is part of the main program. Table 5.2 displays the results of the calculations and the creep

coefficients are identical to at least four decimals, implying the correctness of the results.

Table 5.2 Creep coefficients from analytical and Matlab-calculations

Years	Creep coefficient [-]	
	Analytical calculation	Matlab calculation
2	2,1475	2,1475
5	2,2455	2,2455
15	2,2952	2,2952
50	2,3137	2,3137

Figure 5.10 illustrates the development of the creep coefficient over five and 50 years respectively, calculated both using Matlab and Mathcad (analytical). The high resemblance between the respective plots is clear, which implies that the Matlab program calculates the creep coefficients correctly.

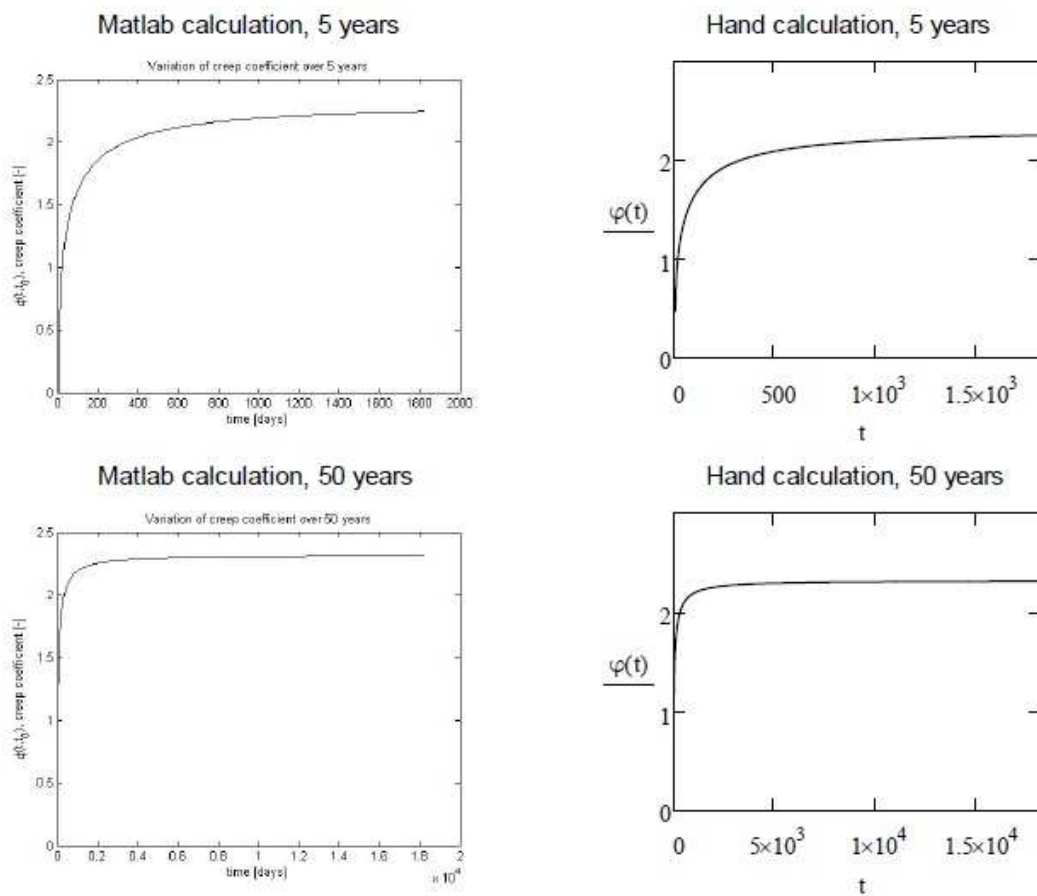


Figure 5.10 Development of creep coefficients during 5 and 50 years from both Matlab and analytical calculations

Since all values of Table 5.2 from analytical calculations and Matlab calculations match, and due to the high resemblance of the plots in Figure 5.10, the first creep approach was considered to be verified.

5.3.2.2 Effective creep coefficient using several creep functions

The second approach to creep was also verified by comparing the results from analytical calculations and the Matlab program. The complete calculation can be found in Appendix C.3. Using identical input an effective creep coefficient was calculated in both ways. Table 5.3 shows the results.

Table 5.3 *Effective creep coefficient for 100 days generated from hand calculation and Matlab using four load steps*

Concrete age [days]	Effective creep coefficients [-]	
	Analytical calculation	Matlab calculation
100	0,9755	0,9756

As seen in the Table the difference is 0.0001 between the analytical calculation and the value obtained in Matlab. This difference is insignificant and likely to be caused by a round off error. Thus, the second creep approach was considered to be verified.

5.3.3 Concrete stress

The calculation of concrete stresses was verified using a special case where the wall was fully fixed at its left and right edges and completely free at its top and bottom edges as illustrated by Figure 5.11. This case was used due to its simplicity. The complete calculation can be found in Appendix C.4.

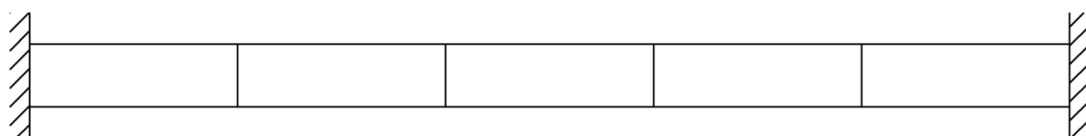


Figure 5.11 *Model for verification of concrete stress calculations in Matlab program*

In this special case the entire shrinkage strain is restrained and the stress distribution should be uniform over all elements. Consequently, the tensile stress due to restraints can be calculated as

$$\sigma_c = \varepsilon_{cs} \cdot E_{c,ef} \quad (5.23)$$

By changing the connecting wall and slab stiffnesses in the Matlab program an equivalent calculation model value was obtained. Table 5.4 contains the values of the calculated concrete stress obtained from Equation (5.23) and from the Matlab program.

Table 5.4 Results from analytical calculations and Matlab of concrete tensile stress after 100 days

Concrete age [days]	Concrete tensile stress [MPa]	
	Analytical calculation	Matlab calculation
100	2,2571	2,2571

The values in the table above demonstrate that the values are identical to four decimals or, possibly, more, which implies the correctness of the Matlab calculation. As previously stated the stress distribution should be uniform. Figure 5.12 illustrates the stress distribution obtained in the Matlab calculation, which is clearly uniform, implying the correctness of the result.

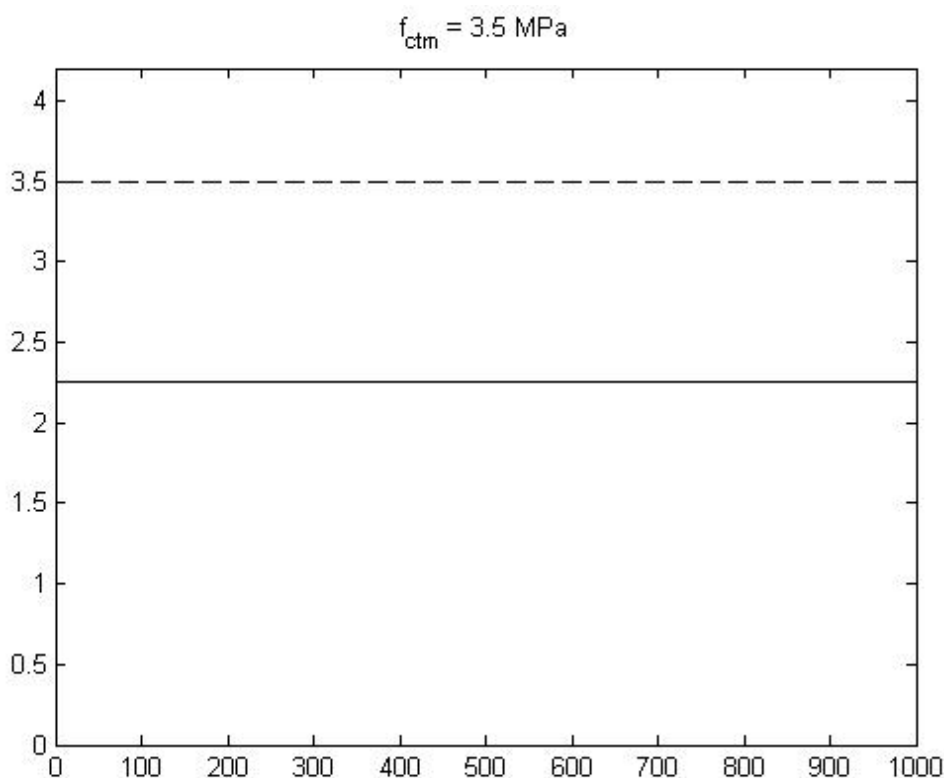


Figure 5.12 Distribution of concrete tensile stress along the member after 100 days from Matlab program

Table 5.4 and Figure 5.12 respectively, as stated above, imply the correctness of the Matlab program. Thus the calculation model was considered to be verified.

5.3.4 Verification of the deformation condition

As stated in Section 5.2.4 the adopted calculation model is based solely on the fundamental deformation condition that the sum of all deformations should be zero. This condition can be verified by summarizing all nodal displacements of the global

displacement vector (Section 5.2.1). Figure 5.13 illustrates computational results using different stiffness parameters for both crack and uncracked members intended for such a verification.

	End support stiffness [N/m]	Slab stiffness [-]	Time [days]	cracked [-]	Length [m]	sum(u) [m]	sum(u) /L [-]
1	2,00E+09	1,0	500	Y	20	1,66E-04	8,32E-06
2	2,00E+09	1,0	200	N	20	1,89E-14	9,43E-16
3	3,00E+09	1,0	500	Y	20	4,29E-04	2,14E-05
4	3,00E+09	1,0	200	N	20	3,38E-15	1,69E-16
5	1,00E+09	1,0	500	Y	20	4,38E-04	2,19E-05
6	1,00E+09	1,0	200	N	20	6,00E-15	3,00E-16
7	2,00E+09	2,0	500	Y	20	5,78E-04	2,89E-05
8	2,00E+09	2,0	200	N	20	4,19E-04	2,09E-05
9	3,00E+09	2,0	500	Y	20	8,10E-05	4,05E-06
10	3,00E+09	2,0	200	N	20	2,86E-15	1,43E-16
11	1,00E+09	2,0	500	Y	20	9,78E-04	4,89E-05
12	1,00E+09	2,0	200	N	20	4,17E-15	2,09E-16
13	2,00E+09	0,5	500	Y	20	2,29E-04	1,15E-05
14	2,00E+09	0,5	200	N	20	2,14E-15	1,07E-16
15	3,00E+09	0,5	500	Y	20	3,47E-04	1,73E-05
16	3,00E+09	0,5	200	N	20	4,59E-15	2,30E-16
17	1,00E+09	0,5	1000	N	20	4,80E-13	2,40E-14

Statistical parameters		
Min	2,14E-15	1,07E-16
Average	2,16E-04	1,08E-05
Median	8,10E-05	4,05E-06
Max	9,78E-04	4,89E-05

Figure 5.13 Summation of simulation results for verification of the deformation condition

As seen in Figure 5.13 the average value of the sum of all deformations are 0,000216 meters, which in relation to the element length corresponds to a difference of 0,00108 %. The equivalent median value is 0,0000810 meters and, in relation to the element length, corresponds to a difference of 0,000405 %. These differences are considered to be sufficiently small and dependent upon the numerical approximation related to the finite element method. Thus, the fundamental deformation condition of Section 5.2.4 is considered to be verified.

6 Parametric study

6.1 Introduction

In order to investigate the effects of various parameters on the cracking process of restrained concrete walls subjected to shrinkage, a parametric study, using the calculation model of Section 5, was carried out. Results from the study are presented in this chapter and a compilation of all performed simulations can be found in Appendix E.

A basic condition of the parametric study was determined by the design of a standard wall, see Section 6.2. The respective influences of different parameters on the reinforcement amount required for crack control were then investigated, with the respective parameters being wall thickness, relative humidity of the surrounding environment, concrete strength class, stiffness (restraint) of the interface to the connecting concrete slab, stiffness (restraint) of connecting end restraints, i.e. walls, and total wall length.

Each parameter was investigated by varying the reinforcement amount for a number of different values of that parameter. For instance, each of the six considered wall thicknesses was simulated using roughly 15-20 different reinforcement amounts. To increase the statistical accuracy each reinforcement amount for each parameter was simulated five times. Thus, running each of the simulations listed in Appendix E five times required around 2 300 simulations.

Based on the data obtained relations between reinforcement amount and mean crack width were obtained, one for each variation of each parameter, and subsequently diagrams illustrating the relation between needed reinforcement amount and an investigated parameter depending on the requested mean crack width. These diagrams are based on trend lines obtained for each relation between reinforcement amount and mean crack width.

The simulations in the parametric study were conducted by dividing the considered wall into 2 000 elements. Using too few elements would mostly affect the calculations of concrete stress and transmission length by round off-errors. The impact on crack width and steel stress is limited due to the special crack element used. If, on the other hand, too many elements were to be used, the calculation time becomes unreasonably long. With this in mind 2 000 elements was considered as a reasonable amount. Furthermore, the response during a period of 50 years was simulated, which corresponds to the normal design service life for “Building structures and other common structures” according to Eurocode, CEN (2002).

In diagrams of the subsequent sections crack widths are referred to using both mean crack widths and characteristic crack widths. Most often crack widths refer to mean crack widths. In diagrams where comparisons with design codes are made, crack widths are expressed as characteristic crack widths, since, e.g. in Eurocode 2, CEN (2004), the limiting values are characteristic. According to Engström (2011a) the relation between mean and characteristic cracks can, for restraint loading, be approximated as stated below. This equation was utilised in order to transform mean crack widths calculated into characteristic crack widths for comparison with design codes.

$$w_m = \frac{w_k}{1,3} \quad (6.1)$$

where w_m is the mean crack width
 w_k is the characteristic crack width

6.2 Standard wall segment in the parametric study

A standard wall was designed to provide a reference case throughout the entire parametric study. The parameters of the standard wall are summarised in Table 6.1. All references to reference values in the subsequent sections relate to these values.

Table 6.1 Parameters for the standard wall and reference values

Parameter	Value
Thickness [m]	0,3
Height [m]	3
Length [m]	20
Reinforcement area, vertical [m ²]	0,0151
Reinforcement diameter, vertical [m]	0,012
Reinforcement area, horizontal [m ²]	0,00522
Reinforcement diameter, horizontal [m]	0,012
Stiffness left connecting wall [N/m]	2*10 ⁹
Stiffness right connecting wall [N/m]	2*10 ⁹
Stiffness multiple for wall/slab interface [-]	1
Concrete strength class [-]	C30/37
Cement type [-]	N (normal)
Surface roughness factor [-]	Rough
Lowest compressive stress resulting from a normal force on the wall/slab interface [kPa]	700
Creep consideration [-]	Weighted average of several creep functions
Age when drying starts [days]	10
Age at first load application [days]	0
RH of surroundings [%]	60
Perimeter exposed to drying [m]	2*height

The values of the different parameters of the standard wall were chosen in an attempt to resemble realistic conditions of a typical extended concrete wall. Geometric conditions were chosen, too some extent, in accordance with the inspected walls of object A, see Section 4.3, and object B, see Section 4.4.

Values of the stiffness parameters of the end supports (connecting walls) were chosen based on the calculations found in Appendix D.1. The value for the end stiffness is aimed to reflect the stiffness of a perpendicular connecting wall. A value for the parameter 'lowest compressive stress resulting from a normal force on the interface' was chosen based on the calculations found in Appendix D.2. The lowest compressive stress, meaning self-weight only, is based on that load from some floors above the wall is transferred through the wall. The wall/slab interface stiffness multiple was chosen to one, which corresponds to a single slab connecting at the bottom edge of the wall.

The reference value of the horizontal reinforcement amount corresponds to the minimum requirement for crack distribution given in Eurocode 2, CEN (2004), if no specific limitation on crack widths exists. For the vertical reinforcement in the wall an area was estimated based on drawings from object A, see Section 4.3, and object B, see Section 4.4.

As stated in Section 5.2.2.5 creep can be considered using two alternate approaches. The second approach, which utilises several creep functions to calculate a weighted average, was chosen as the reference parameter, since it represents a more realistic approach.

Concrete strength class C30/37 is a commonly used strength class in concrete structures for buildings, as well as cement type N (Normal). In the description of the surface roughness factor in fib Model Code 2010, fib (2013) it is stated that it depends on the preparations before casting of the wall. For the standard wall a rough or smooth surface could be used and rough was chosen. Finally a relative humidity of 60% over a longer time span and double sided drying was considered to be reasonable.

6.3 Common case

As mentioned in Section 6.1 the effect of each investigated parameter was simulated by varying the reinforcement amount for each variation of an investigated parameter. Since all parameters have a reference value in the standard wall, a common case for all parameters to be varied exists and was obtained by varying the reinforcement amount for the standard wall.

The reference value of the horizontal reinforcement area was 0,00522 m², see Table 6.1, which corresponds to the design requirement given in Eurocode 2, CEN (2004), with no specific limitation regarding the crack width and using the yield strength of the reinforcing steel, see Section 3.6.1. While varying the reinforcement amount between 0,6 and 2,2 times the reference value in 16 steps, the remaining parameters were kept constant. Figure 6.1 illustrates the obtained relation between reinforcement amount and mean crack width for the standard wall assuming short term response, which is referred to as the common case in subsequent sections.

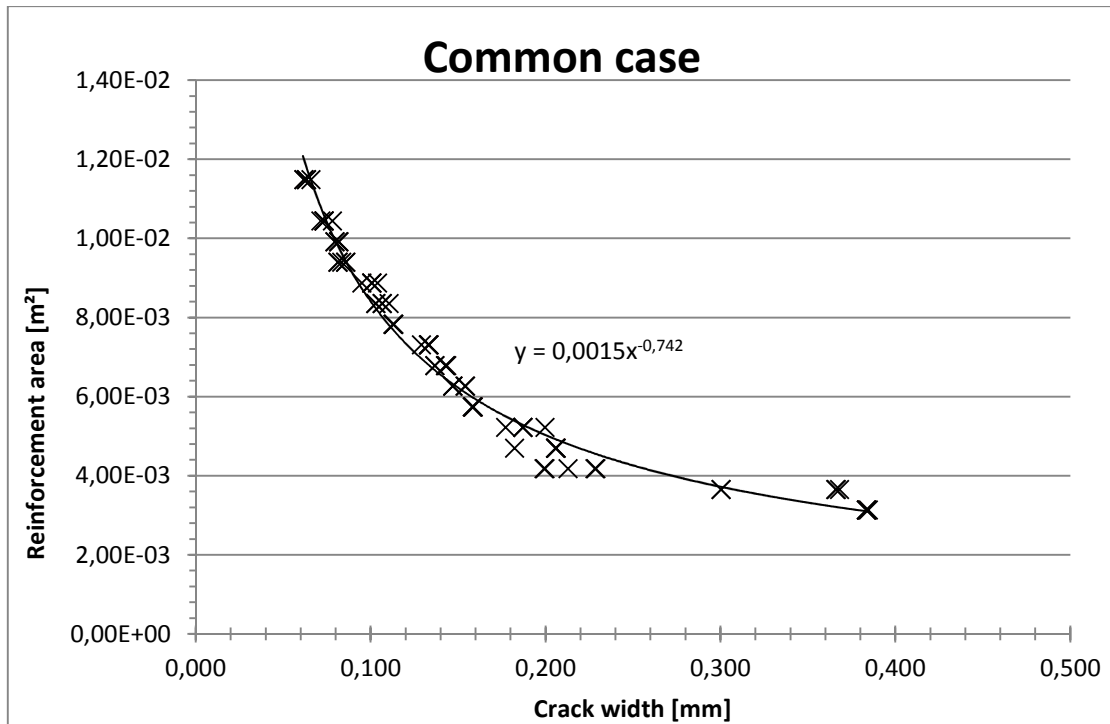


Figure 6.1 Plot of the relation between reinforcement area and mean crack width (short term response) for the common case with a trend line and its corresponding equation inserted

As demonstrated by Figure 6.1 low values of the mean crack width required greater amounts of reinforcement for crack control, while larger values of mean crack width required less amounts of reinforcement. This is supported theoretically, since an increased amount of reinforcement should reduce the steel stress and ensure that cracks are kept small and well-distributed, see Section 3.5. However, this is also dependent on e.g. the bar diameter which in this case was kept constant (which then corresponds to a decreased spacing). Based on the data from the simulations the trend line illustrated in the figure was, using Excel, obtained and found to correspond well with the following equation.

$$y = 0,0015 \cdot x^{-0,742} \quad (6.2)$$

where x is the mean crack width in mm
 y is the reinforcement amount in m^2 needed for a mean crack width x

6.4 Influence of restraint at wall/slab interface

6.4.1 Importance of restraint at wall/slab interface

The importance of restraint from a connecting slab with regard to crack control was initially investigated by varying the stiffness, and likewise restraint, of the wall/slab interface using the standard wall defined in Section 6.2. Since the stiffness (restraint) of the interface is dependent on a non-linear relation, see Section 3.1.5, and has different values in different nodes depending on the actual slip, see Section 5.2.2.2, it was not possible to control the stiffness (restraint) by a single numerical stiffness

value in N/m. Instead the variation was controlled by a so called stiffness multiple, which multiplies the numerical value of each node with a chosen factor.

As defined in Table 6.1 the reference value of the wall/slab interface stiffness multiple was one. The importance of the restraint was investigated by varying the stiffness multiple between 0.6-8, while all remaining parameters of the standard wall were kept constant at their respective reference values. Figure 6.2 illustrates the relation between the mean crack width (short term response) and the stiffness multiple, while Figure 6.3 illustrates the relation between the left end node displacement and the stiffness multiple.

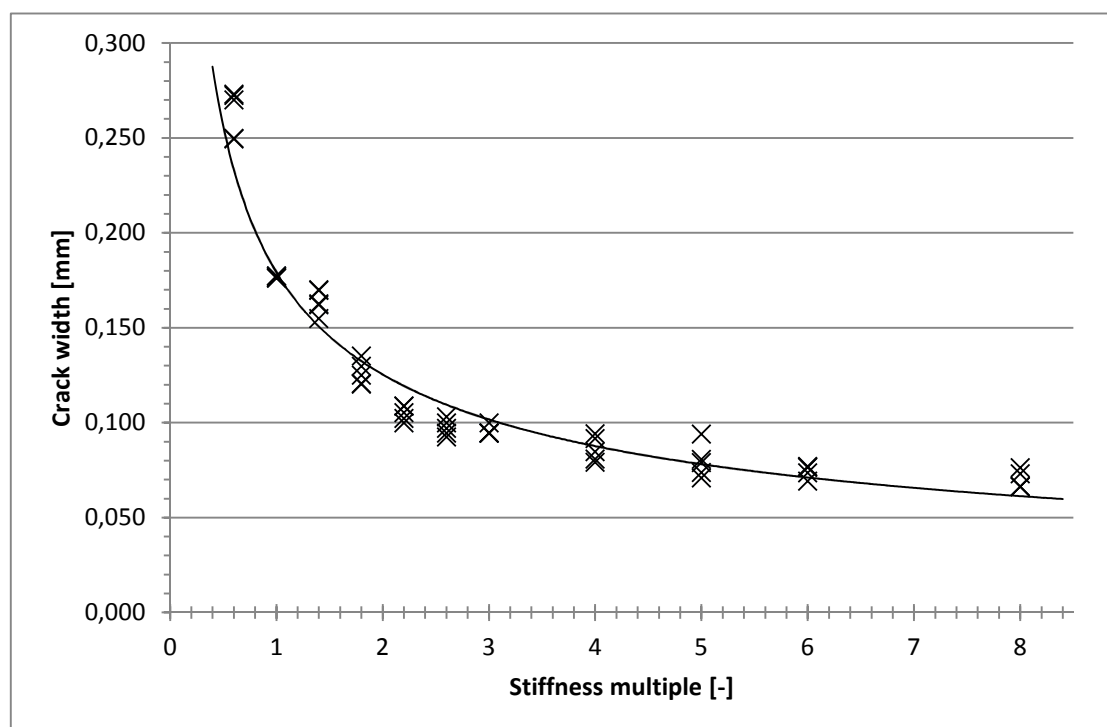


Figure 6.2 Relation between the wall/slab interface stiffness and the mean crack width (short term response)

Figure 6.2 clearly illustrates that, in case of the standard wall defined in Section 6.2, the mean crack width (short term response) decreases significantly while increasing the stiffness multiple and hence also the restraint. Since an increased amount of continuous edge restraint results in a greater tensile stress for the same magnitude of shrinkage, more cracks occur since the tensile strength is unaffected. The larger number of cracks decreased the mean crack width, since the number of cracks increased faster than the sum of all crack widths. Thus, an increased wall/slab interface stiffness multiple and, hence, increased restraint at the interface could result in an improved cracking situation with more, but smaller and more well-distributed, cracks.

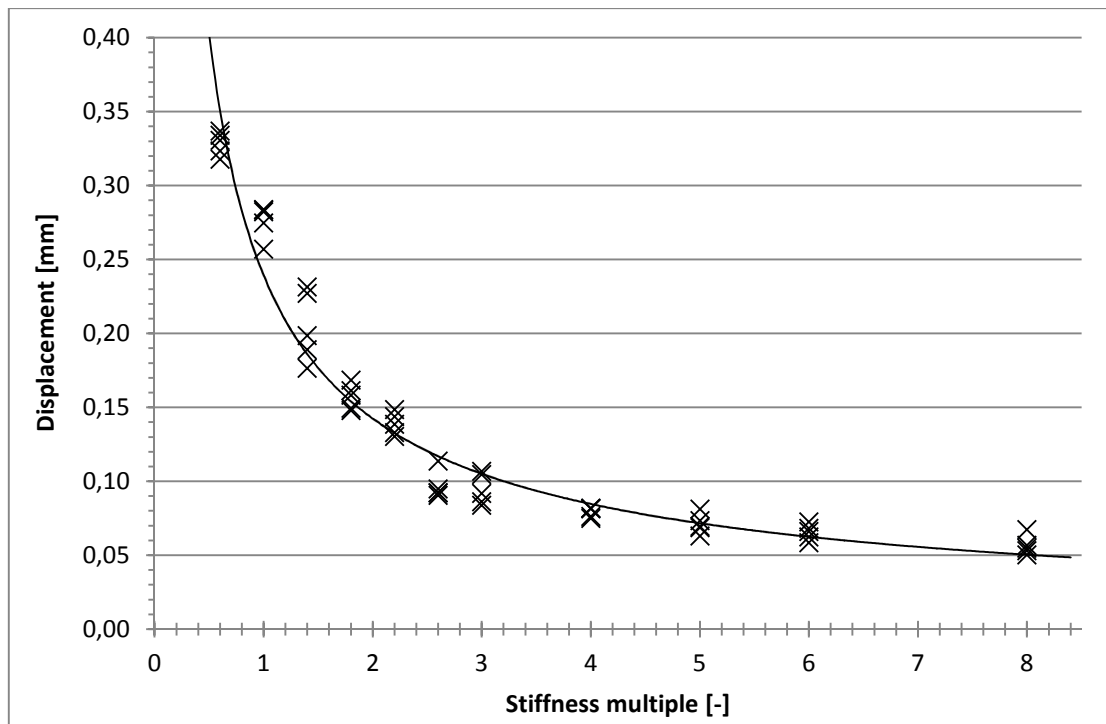


Figure 6.3 Left end node displacement plotted against the wall/slab interface stiffness

Figure 6.3 illustrates that for increasing values of the stiffness multiple the end displacement seems to approach a certain value. Meaning that after a certain point further increasing the stiffness of the wall/slab interface does not limit the end displacement, and such an increase is unnecessary. This pattern can also be observed in Figure 6.2 where the mean crack width seemed to approach a certain value for larger values of the stiffness multiple. Thus, increasing the stiffness multiple seems to only influence the mean crack width and end displacement below certain values.

As illustrated by Figure 6.2 and Figure 6.3 the amount of restraint provided at the wall/slab interface influences the cracking situation and end displacement of the standard wall. Hence, it is of interest to further investigate the impact on the reinforcement amount required for crack control.

6.4.2 Reinforcement area required for crack control

Figure 6.1, Figure 6.4, Figure 6.5 and Figure 6.6 respectively illustrates the relation obtained between reinforcement area and mean crack width (short term response) for wall/slab interface stiffness multiples of 1, 2, 4 and 0.6 respectively. These relations were obtained by varying the reinforcement amount in several steps for each of the stiffness multiples considered.

Figure 6.1 demonstrates the relation between reinforcement area and mean crack width obtained for the common case in Section 6.3, where the stiffness multiple was equal to one, which corresponds to the restraint of a single wall/slab interface. Equation 6.2 defines the trend line obtained based on the data of Figure 6.1.

By increasing the stiffness multiple too two a relation between reinforcement area and mean crack widths was obtained for a doubled amount of restraint at a wall/slab interface. The reinforcement amount was varied between 0,1 and 2,2 times the

reference value in 21 steps and the resulting relation is illustrated in Figure 6.4 and its trend line was expressed as

$$y = 0,0002 \cdot x^{-1,373} \quad (6.3)$$

where x is the mean crack width in mm
 y is the reinforcement amount in m^2 needed for a mean crack width x

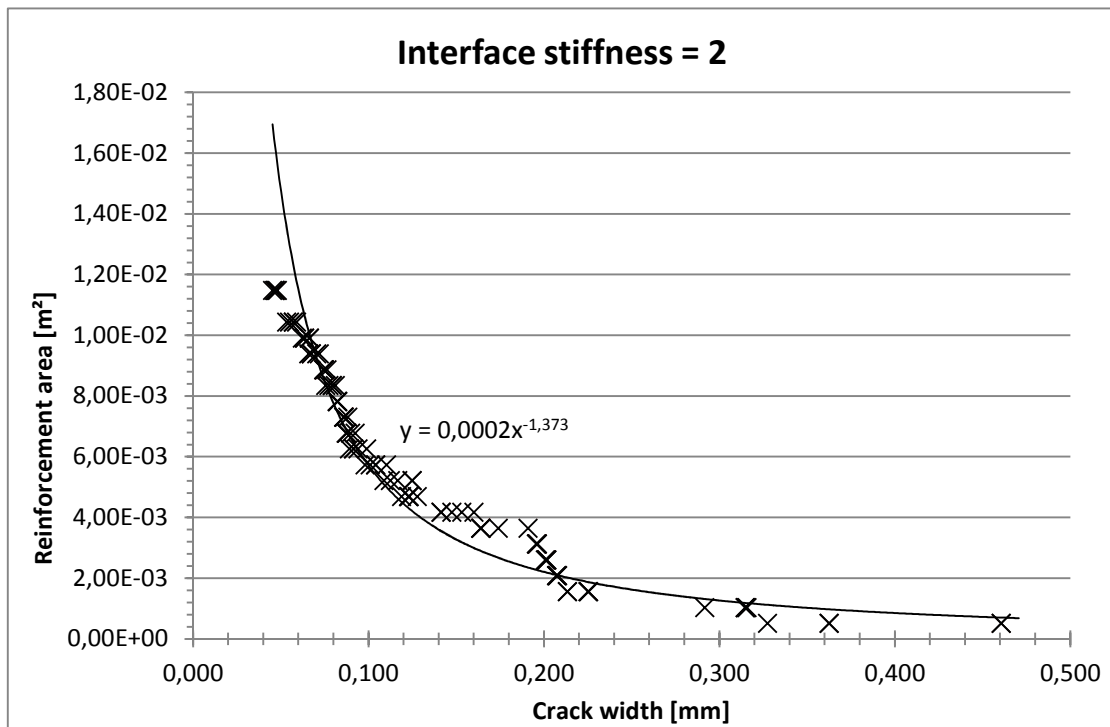


Figure 6.4 Plot of the mean crack width (short term response) versus the reinforcement area when the wall/slab interface stiffness multiple is 2

Figure 6.5 illustrates the relation obtained between reinforcement area and mean crack width for an interface stiffness multiple of four. Thus the restraint has quadrupled over that of the common case. In this case the reinforcement area varied in 20 steps between 0 and 1,6 times its reference value. A trend line was obtained and found to be defined by the following logarithmic expression.

$$y = -0,008 \cdot \ln(x) - 0,0132 \quad (6.4)$$

where x is the mean crack width in mm
 y is the reinforcement amount in m^2 needed for a mean crack width x

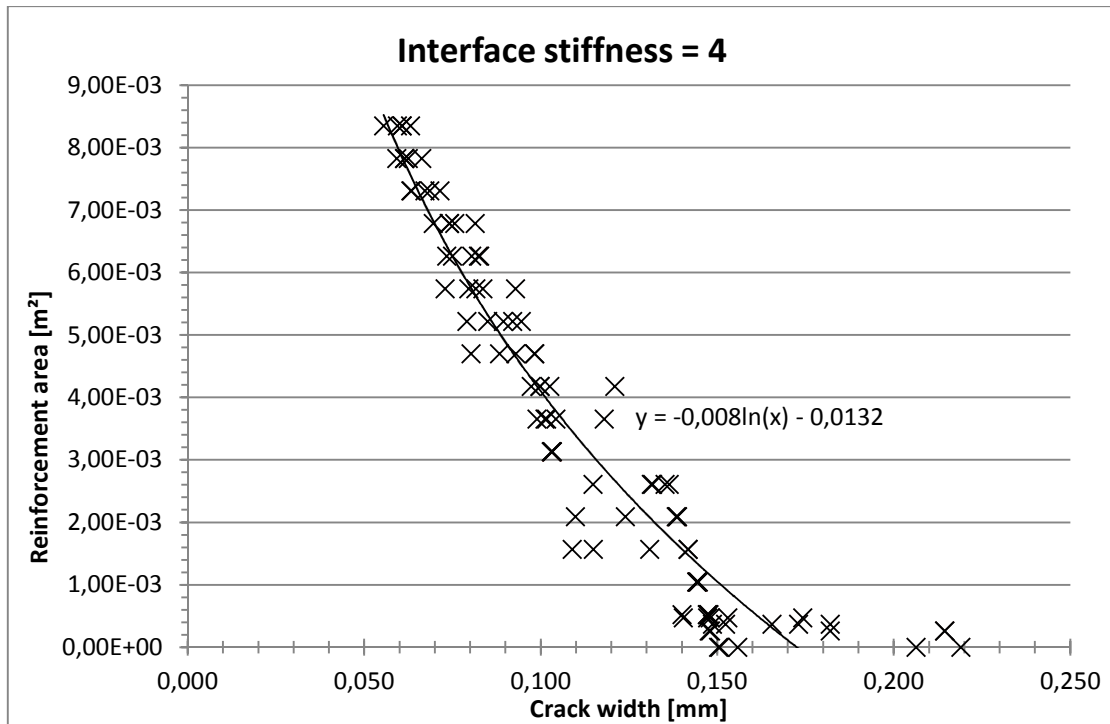


Figure 6.5 Plot of the mean crack width (short term response) versus the reinforcement area when the wall/slab interface stiffness multiple is 4

A decreased amount of restraint was also investigated by reducing the wall/slab interface stiffness multiple to a value of 0,6, corresponding to 60% of the restraint in the common case. The relation obtained between reinforcement area and mean crack width is demonstrated in Figure 6.6 and the resulting trend line is expressed below. Here the reinforcement area varied between 0,8 and 2,5 times its reference value in a total of 17 steps.

$$y = 0,0023 \cdot x^{-0,628} \quad (6.5)$$

where x is the mean crack width in mm
 y is the reinforcement amount in m^2 needed for a mean crack width x

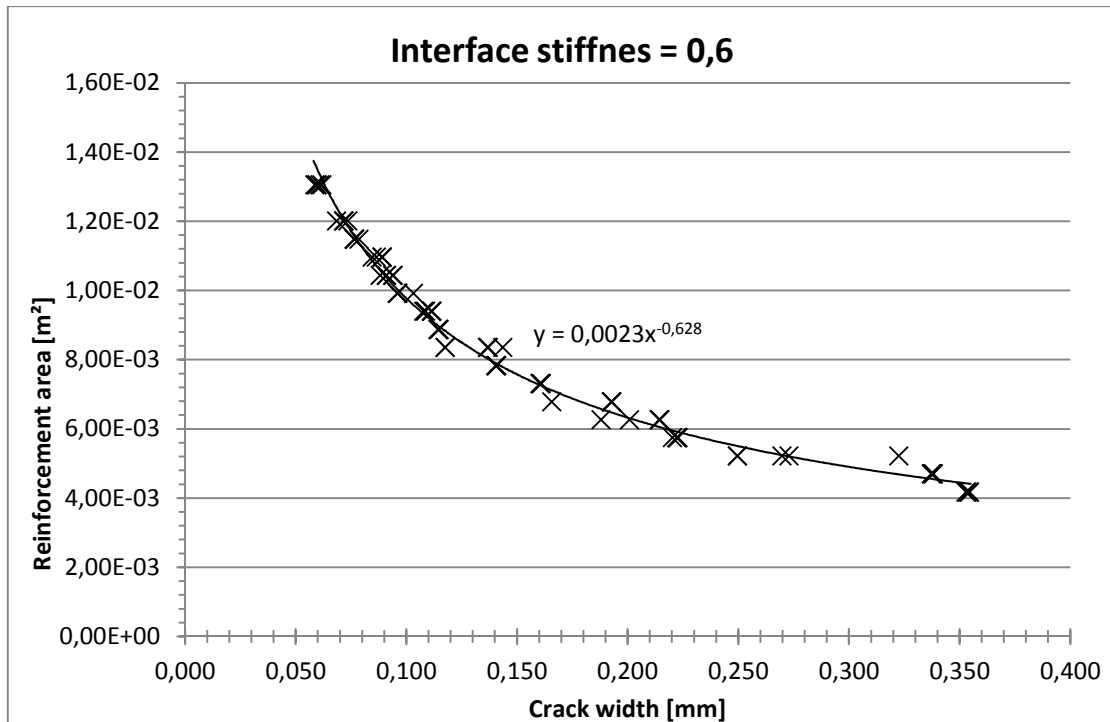


Figure 6.6 Plot of the mean crack width (short term response) versus the reinforcement area when the wall/slab interface stiffness multiple is 0,6

6.4.3 Design code comparison

Based on the respective trend lines of Figure 6.1, Figure 6.4, Figure 6.5 and Figure 6.6 relations between the needed reinforcement area and the interface stiffness multiple were achieved for different characteristic crack widths. These relations were obtained by, for each considered value of the stiffness multiple and using its respective trend line equation, finding the reinforcement amount corresponding to characteristic crack widths of 0,1, 0,2, 0,3 and 0,4 mm respectively. Since the trend line equations are based on the mean crack width, the characteristic crack widths are divided by 1,3, in order to correspond to its mean crack width, before being inserted into the trend line equations. Figure 6.7 illustrates these relations along with minimum reinforcement requirements from design codes.

Note that all crack widths, characteristic or mean, are those of short term response. As stated in Section 3.5.5, crack widths increase when accounting for the long term response, roughly 1,2 times. This should be kept in mind when comparing calculated crack widths with design code values in which long term effects are included.

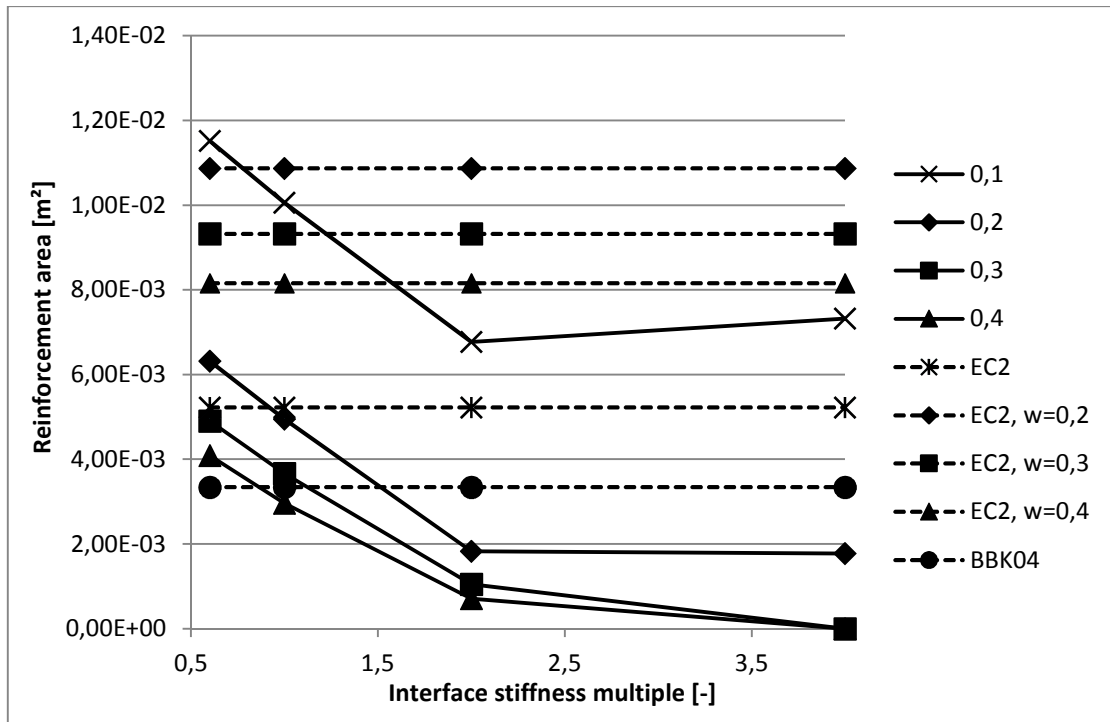


Figure 6.7 Interface stiffness multiple plotted versus the reinforcement area. Lines illustrate characteristic crack widths from the parametric study, Eurocode 2 and BBK 04

Based on Figure 6.7 that summarises the results in Figure 6.4, Figure 6.5 and Figure 6.6 and their respective trend lines, some remarks regarding the amount of reinforcement needed for crack control under a varying interface restraint were noted. A general remark regarding the slab interface restraint with regard to crack control is that for increased amount of restraint, the needed reinforcement area for a certain crack width decreased.

The increased needed reinforcement area for a characteristic crack width of 0,1 mm while increasing the stiffness multiple from two to four, found in Figure 6.7, might have numerical causes and is likely to be of minor importance with regard to crack control in real structures, mostly because such high restraint is not likely to exist in real structures.

As implied by Figure 6.7 characteristic cracks widths larger than 0,3 mm could be achieved without reinforcement for high amounts of slab restraint. This effect could be explained by the fact that the model is one-dimensional and does not consider variations in restraint over the height of the member. Thus, in the model this high amount of restraint exists throughout the height of the wall, which unlikely is the case for a real structure, see e.g. Figure 3.21. This implies that for large stiffnesses (restraints) of the wall/slab connection, reinforcement might be less important with regard to crack control than for lower restraints. However, since the reference value of the stiffness multiple and consequently also restraint was quadrupled to achieve that effect, the restraint needed must be considered as high and might not be feasible to achieve in real structures.

A comparison between Figure 6.1, Figure 6.4, Figure 6.5 and Figure 6.6 further demonstrate that the rate, of which the reinforcement area decreased with increased mean crack width, increased for higher amount of restraints. Thus, for higher interface

restraints additional reinforcement has a greater influence and reduces the mean crack width faster than for lower interface restraints.

Regarding the requirements given in design codes, Figure 6.7 indicates that the reinforcement areas actually needed to limit the characteristic crack width to 0,2, 0,3 and 0,4 mm respectively are significantly lower than the minimum amounts specified by Eurocode 2. For instance, the reinforcement area required by Eurocode 2 for a characteristic crack width of 0,4 mm is, in case of the standard wall, enough to keep crack widths less than 0,2 mm regardless of the magnitude of restraint at the interface to the connecting slab.

Furthermore, for values of the interface stiffness multiple that likely correspond to realistic cases, roughly between 0,5 and 1,5, characteristic crack widths are kept around 0,2 mm using the minimum reinforcement area required for crack control without limiting the crack widths to a certain value according to Eurocode 2.

6.5 Influence of end support stiffness

6.5.1 Importance of considering end support stiffness

The modelled wall segment was considered to be attached to connecting walls and hence end support stiffnesses existed. An estimate of the importance and influence of these stiffnesses was initially conducted by varying the end stiffness of the supports for the standard wall in Section 6.2 and evaluating the outcome by means of end node displacements and mean crack widths.

Actual values of the end support stiffnesses were estimated to be within the range of 10^8 to 10^{13} N/m, see Appendix D.1. As stated in Section 6.2 the reference value of the standard wall was chosen as $2 \cdot 10^9$ N/m, which roughly corresponds to a wall connecting perpendicularly to the ends of the considered wall. During the investigations 22 different end support stiffnesses ranging between $4 \cdot 10^8$ and $2 \cdot 10^{12}$ N/m were accounted for. Figure 6.8 illustrates how the left end node displacement varied with the connecting wall stiffness. Note that the figure was plotted using a logarithmic scale for stiffness on the x-axis. It should also be noted that all connecting wall stiffnesses were modelled symmetrically.

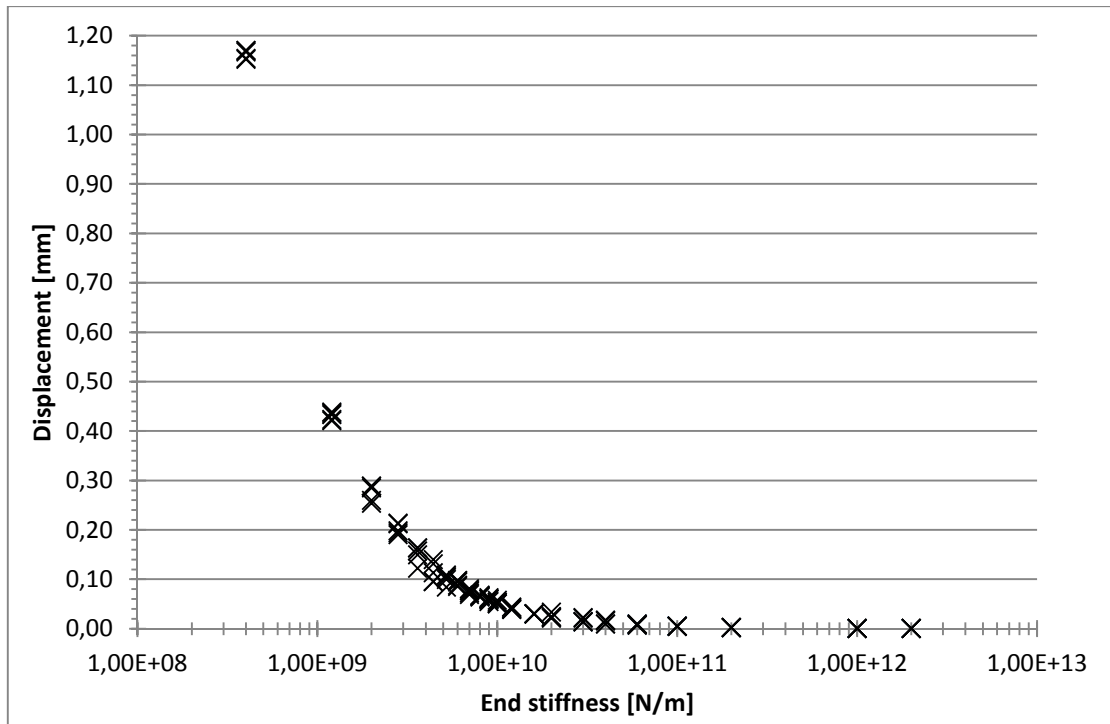


Figure 6.8 Plot of the end stiffness versus the displacement in the left support. It should be noted that the x-axis is plotted with a logarithmic scale

Figure 6.8 clearly demonstrates that for an increased end stiffness, the end node displacement approaches zero. Since no displacement in a support node corresponds to a fully fixed connection, the considered standard wall could be regarded as fixed for an end-stiffness exceeding, roughly, 10^{11} N/m. The obtained relation between end support stiffness and mean crack width is illustrated in Figure 6.9. It is evident that the mean crack width decreases for an increasing end stiffness.

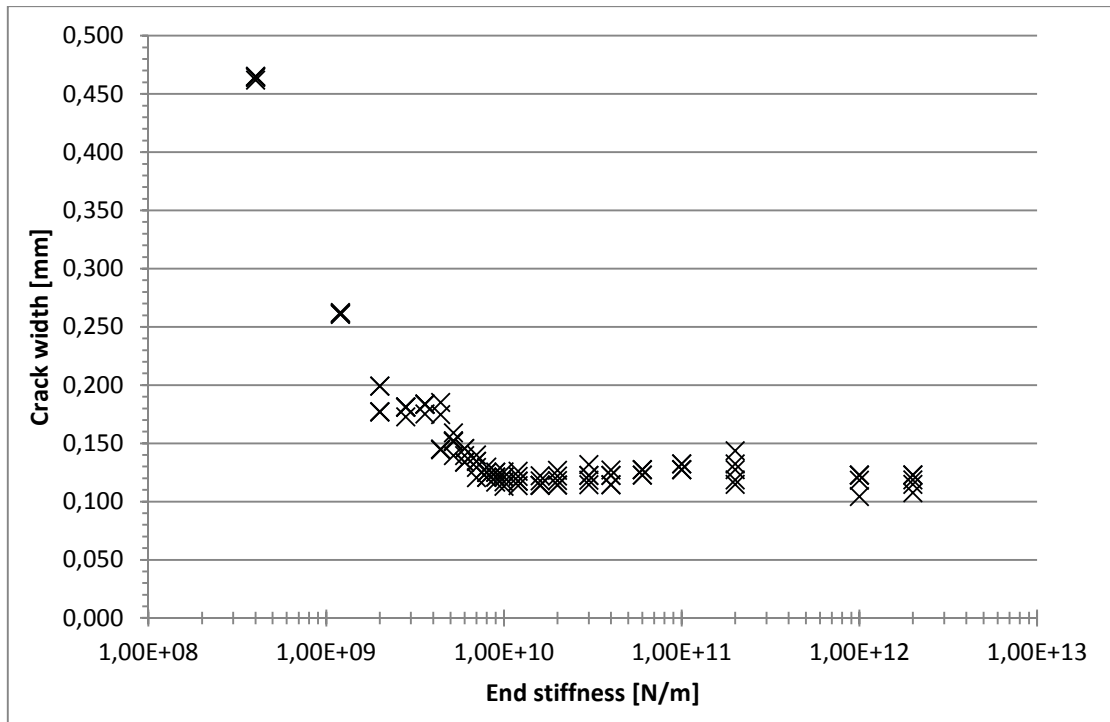


Figure 6.9 End stiffness plotted against the mean crack width (short term response). It should be noted that the x-axis is plotted with a logarithmic scale

The trend in Figure 6.9 for the end stiffness is similar to the trend in Figure 6.2 for the interface stiffness. For an increased stiffness the mean crack width decreased, since more cracks appeared, which were smaller and more well-distributed. Figure 6.9 further illustrates that the stiffness of the end support could influence the cracking situation despite not being a continuous edge restraint.

6.5.2 Reinforcement area needed for crack control

In order to further investigate the impact from the end support stiffness and relate it to the reinforcement amount needed for crack control, five different end support stiffnesses were modelled by varying the reinforcement amount. The considered end support stiffnesses are related to the reference value of Table 6.1 and are 0,6, 1, 3, 5 and 20 times the reference value of $2 \cdot 10^9$ N/m, as summarised in Table 6.2 below.

Table 6.2 Variation of end stiffness

Multiples [-]	End support stiffness [N/m]
0,6	$1,2 \cdot 10^9$
1	$2 \cdot 10^9$
3	$6 \cdot 10^9$
5	$10 \cdot 10^9$
20	$40 \cdot 10^9$

The standard wall has an end support stiffness of $2 \cdot 10^9$ N/m. Thus the common case in Section 6.3 represents the case where the end support stiffness is multiplied by one. Figure 6.1 illustrates the relation between reinforcement area and mean crack width obtained for the common case and Equation (6.2) expresses the corresponding trend line.

For an end stiffness multiple of 0,6, corresponding to a stiffness of $1,2 \cdot 10^9$ N/m, a relation between reinforcement area and mean crack width was obtained according to Figure 6.10. This relation was obtained by varying the reinforcement amount between 0,6 and 2,8 times its reference value in a total of 19 steps. A corresponding trend line was obtained and is expressed as

$$y = 0,0019 \cdot x^{-0,695} \quad (6.6)$$

where x is the mean crack width in mm
 y is the reinforcement amount in m^2 needed for a mean crack width x

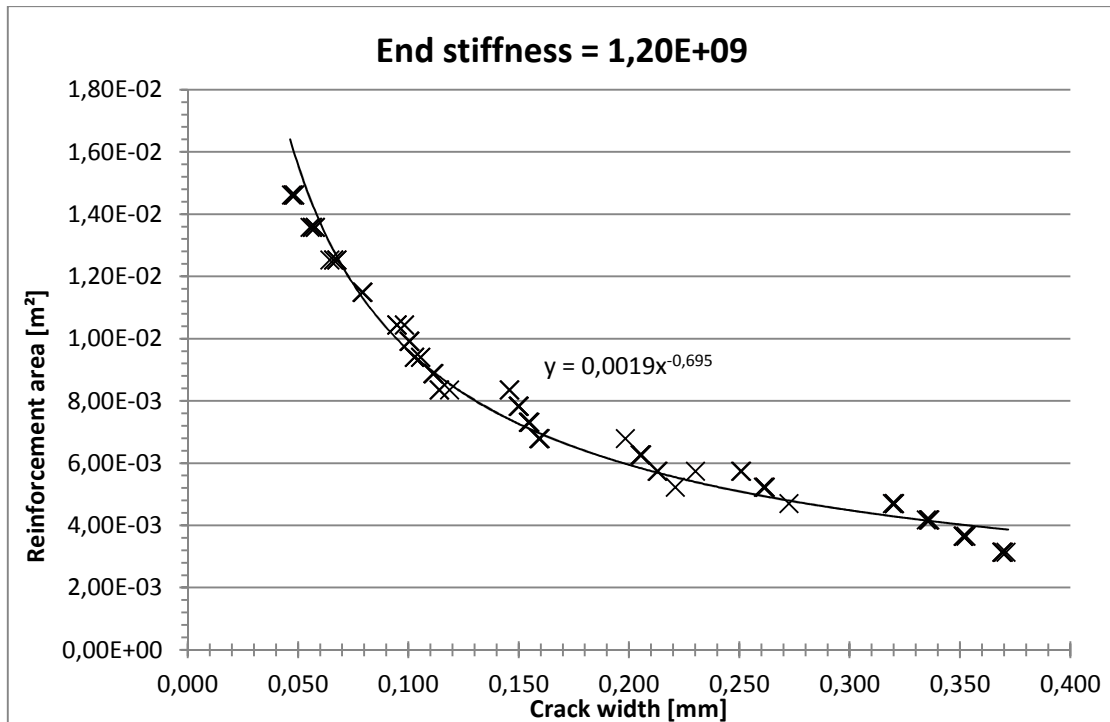


Figure 6.10 Mean crack width (short term response) plotted against the reinforcement area with the end stiffness of $1,2 \cdot 10^9$ and trend line with equation

By tripling the end support stiffness of the standard wall, i.e. by using a stiffness multiple of 3 and hence a stiffness of $6 \cdot 10^9$ N/m, the relation between reinforcement area and mean crack width demonstrated by Figure 6.11 was obtained by altering the reinforcement area in 20 steps between 0,6 and 2,6 times the reference value. Based on the computed data a corresponding trend line was established as expressed below

$$y = 0,001 \cdot x^{-0,823} \tag{6.7}$$

where x is the mean crack width in mm
 y is the reinforcement amount in m^2 needed for a mean crack width x

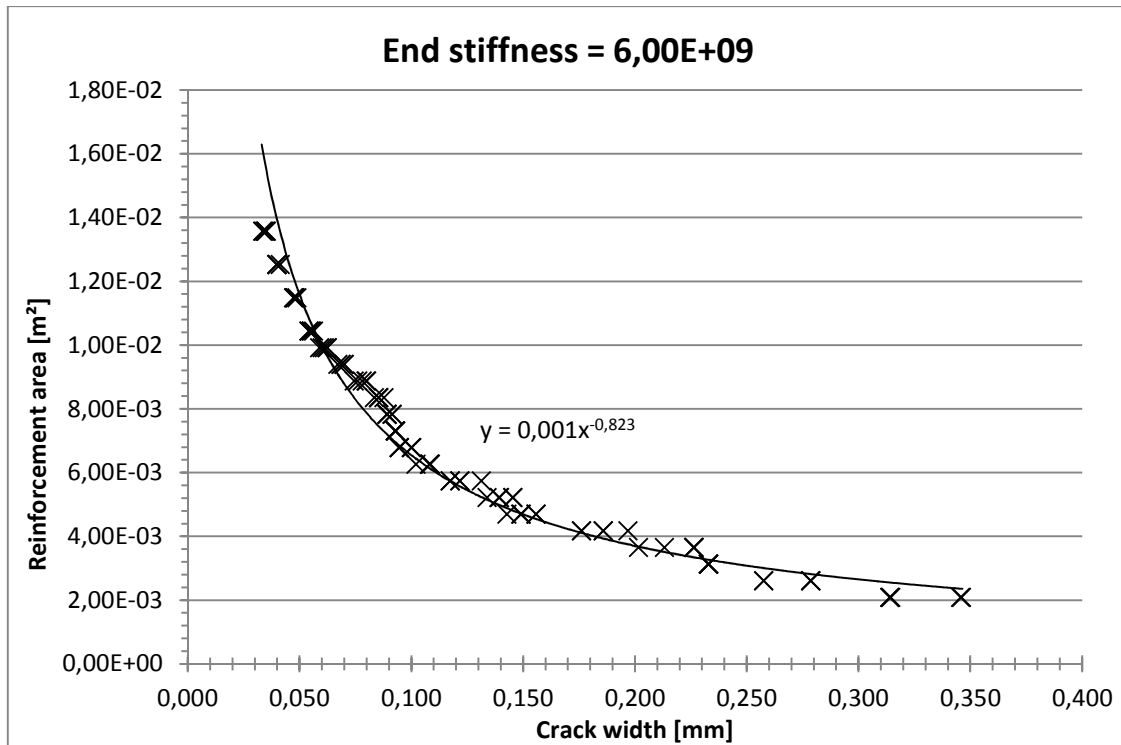


Figure 6.11 Mean crack width (short term response) plotted against the reinforcement area with the end stiffness of $6,0 \cdot 10^9$ and trend line with equation

By further increasing the end support stiffness by a stiffness multiple of 5 and hence utilising an end support stiffness of $10 \cdot 10^9$ N/m, the relation for a fivefold end support stiffness was obtained. Figure 6.12 illustrates this relation between reinforcement area and mean crack width which was obtained by varying the reinforcement amount between 0,6 and 2,6 times its reference value in 20 steps. The associated trend line is defined below.

$$y = 0,001 \cdot x^{-0,809} \quad (6.8)$$

where x is the mean crack width in mm
 y is the reinforcement amount in m^2 needed for a mean crack width x

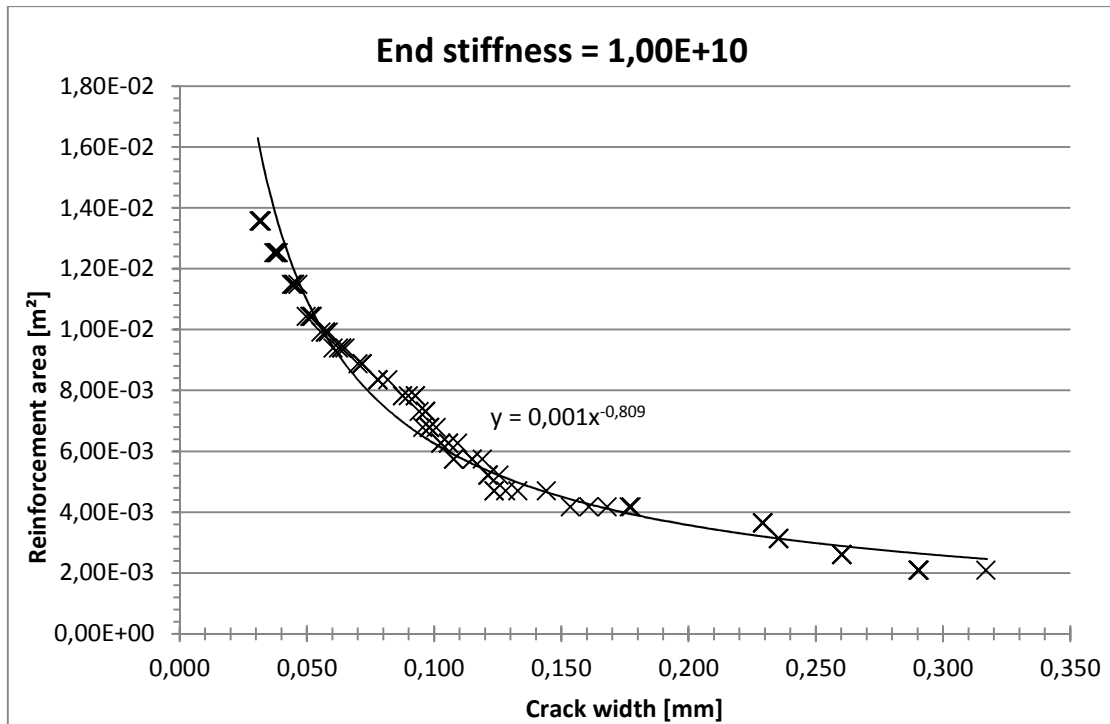


Figure 6.12 Mean crack width (short term response) plotted against the reinforcement area with the end stiffness of $1,0 \cdot 10^{10}$ and trend line with equation

A fifth and final end support stiffness was considered by the use of a stiffness multiple of 20, meaning that the end support stiffness was $40 \cdot 10^9$ N/m. In that case a relation between reinforcement area and mean crack width was computed and is plotted in Figure 6.13, while the equation of its associated trend line is expressed as

$$y = 0,0008 \cdot x^{-0,867} \quad (6.9)$$

where x is the mean crack width in mm
 y is the reinforcement amount in m^2 needed for a mean crack width x

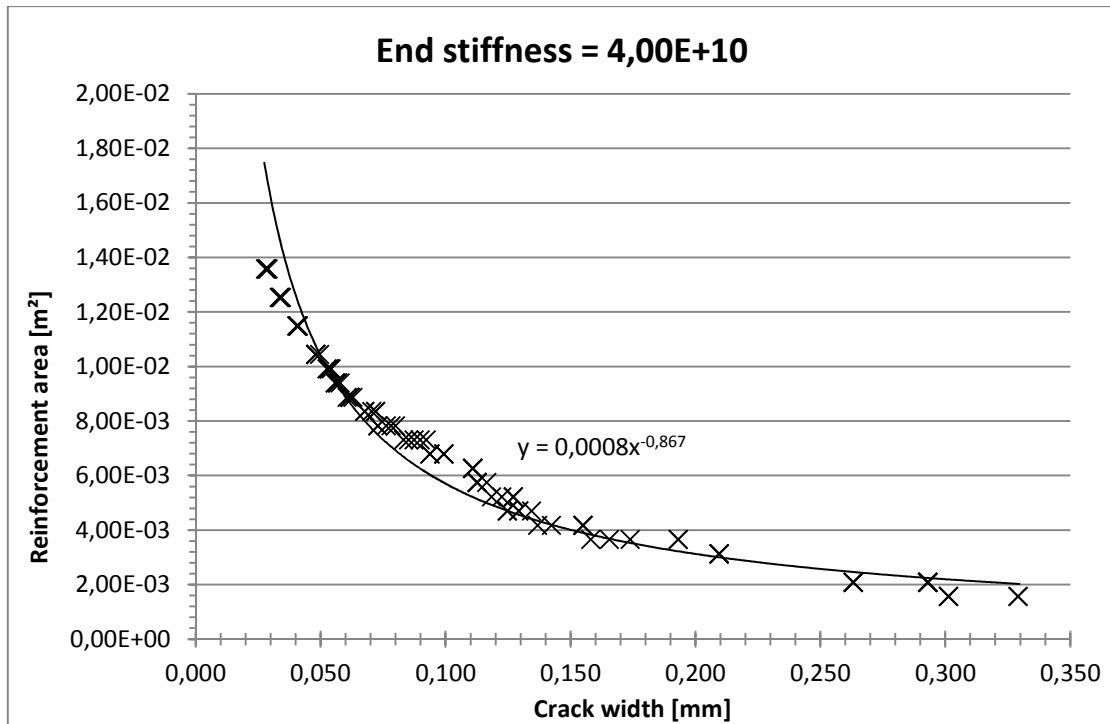


Figure 6.13 Mean crack width (short term response) plotted against the reinforcement area with the end stiffness of $4,0 \cdot 10^{10}$ and trend line with equation

6.5.3 Design code comparison

Utilising the respective trend lines corresponding to the five different end support stiffnesses of Figure 6.1, Figure 6.10, Figure 6.11, Figure 6.12 and Figure 6.13 relations between the reinforcement area needed for crack control and the end support stiffness for limiting characteristic crack width values of 0,1, 0,2, 0,3 and 0,4 mm were obtained. These relations are illustrated in Figure 6.14.

Note that all crack widths, characteristic or mean, are those of short term response. As stated in Section 3.5.5, crack widths increase when accounting for the long term response, roughly 1,2 times. This should be kept in mind when comparing calculated crack widths with design code values in which long term effects are included.

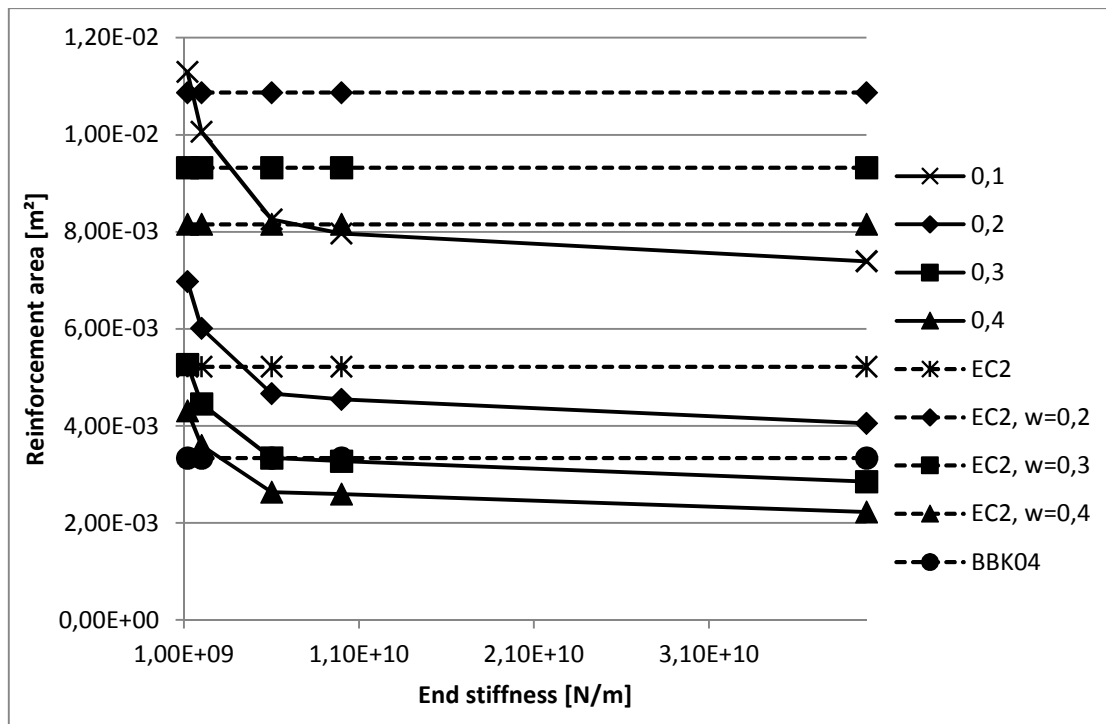


Figure 6.14 End support stiffness plotted versus the reinforcement area. Lines illustrate the characteristic crack widths (short term response) from the parametric study, Eurocode 2 and BBK 04

Figure 6.14 indicates a dependency between the needed amount of reinforcement and the magnitude of the end support stiffness. For lower values of the stiffness multiple, i.e. between 0,6-3, which corresponds to end stiffnesses in the range of $1,2 \cdot 10^9$ to $6 \cdot 10^9$ N/m, an increased stiffness reduces the needed reinforcement amount considerably. However, for values exceeding a stiffness multiple of 3, corresponding to an end support stiffness of $6 \cdot 10^9$ N/m, the rate of decrease is significantly smaller.

Thus, the influence on the needed reinforcement amount from the end support stiffness is considerable for low support stiffness but of minor importance for larger end support stiffness, where other effects could be more significant.

Figure 6.14 further demonstrates that the minimum reinforcement area for the studied case required by Eurocode 2, which is governed by the yield strength of the steel and not by a certain crack width, is able to keep characteristic crack widths around 0,2 mm. Furthermore, the requirement given for a characteristic crack width of 0,2 mm in Eurocode 2, is large enough to mostly keep characteristic crack widths below 0,1 mm and significantly greater than the reinforcement area needed for a 0,2 mm characteristic crack width in the figure.

6.6 Influence of wall thickness

6.6.1 Reinforcement area needed for crack control

In this section it is presented how the wall thickness influenced the reinforcement amount needed for crack control. The study was performed by varying the reinforcement amount for wall thicknesses of 200, 250, 300, 350, 400 and 450 mm respectively. Note however that, since the adopted calculation model is one-

dimensional along the length axis, it was not possible to consider the influence of effective concrete area, see Section 3.5.3, in the calculation procedure, which is discussed further in Section 7.5.

As stated in Table 6.1 the standard wall described in Section 6.2 has a thickness of 300 mm. Hence, the common case in Section 6.3 represents that case and Figure 6.1 illustrates the relation between reinforcement area and mean crack width, while Equation (6.2) defines the corresponding trend line equation for the case of a 300 mm thick wall.

In case of a 200 mm thick wall Figure 6.15 demonstrates the relation obtained between reinforcement area and mean crack width by altering the reinforcement area in 13 steps between 0,3 and 1,2 times the reference value. The equation below defines the corresponding trend line.

$$y = 0,0006 \cdot x^{-0,773} \quad (6.10)$$

where x is the mean crack width in mm
 y is the reinforcement amount in m² needed for a mean crack width x

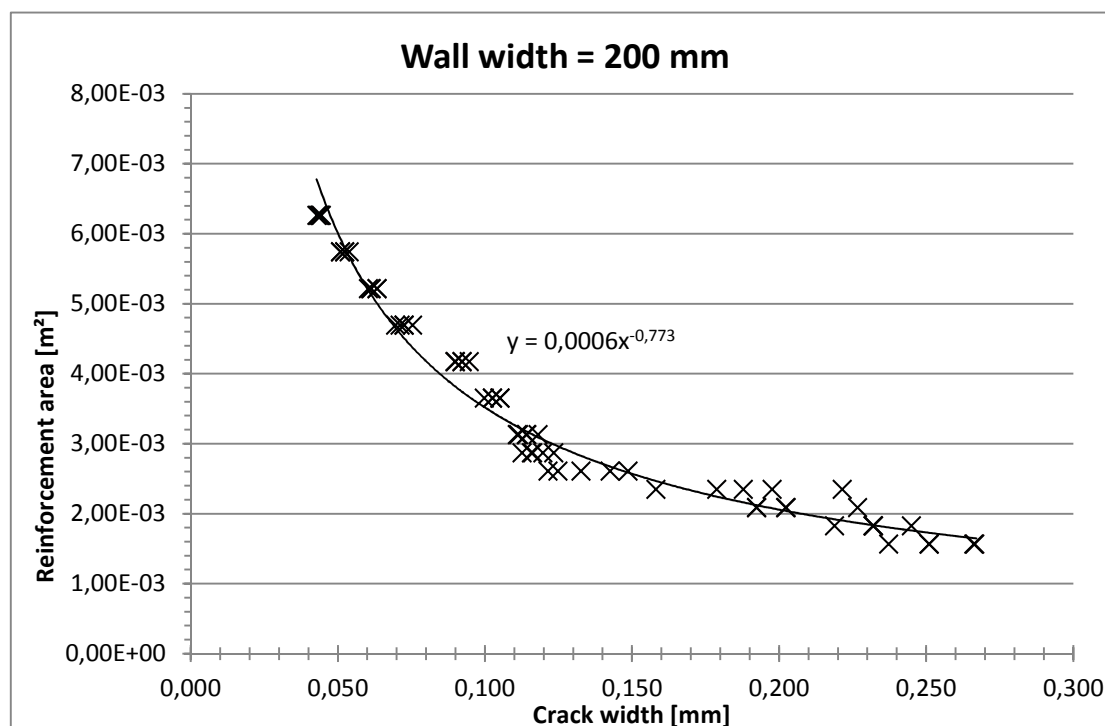


Figure 6.15 Plot of the mean crack width (short term response) versus the reinforcement area for a 200 mm thick wall

A relation between reinforcement area and mean crack width for a wall thickness of 250 mm was obtained by varying the reinforcement area between 0,4 and 1,6 times the reference value in 13 steps. The resulting relation is demonstrated by Figure 6.16 and its corresponding trend line defined as

$$y = 0,0008 \cdot x^{-0,81} \quad (6.11)$$

where x is the mean crack width in mm
 y is the reinforcement amount in m^2 needed for a mean crack width x

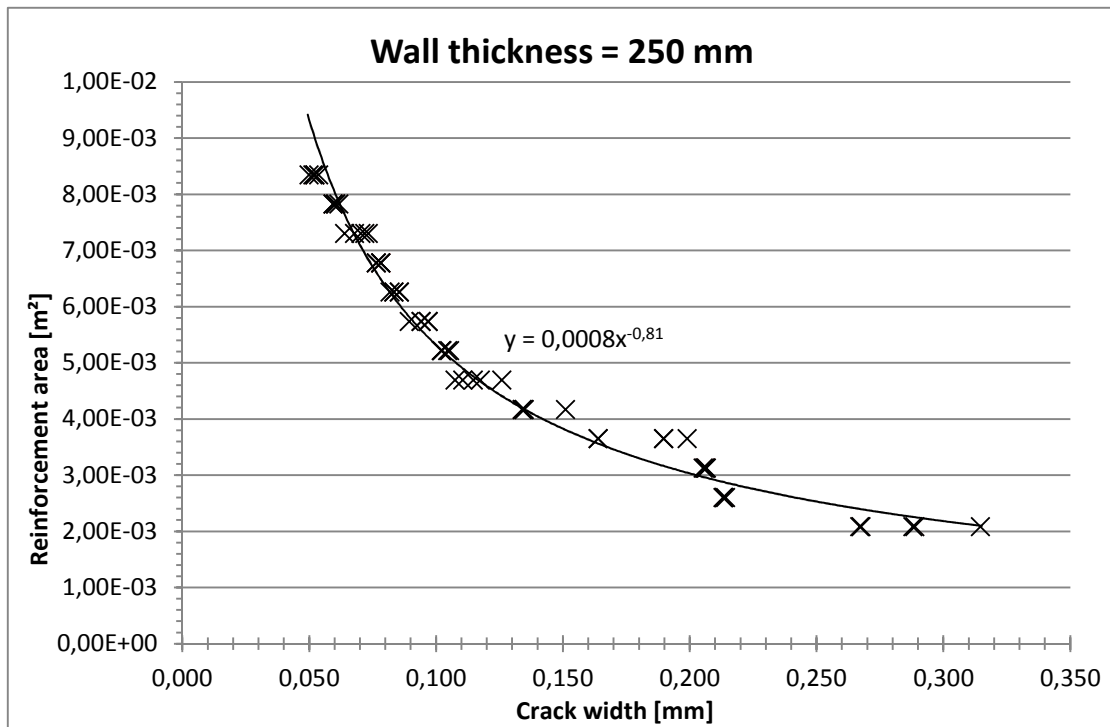


Figure 6.16 Plot of the mean crack width (short term response) versus the reinforcement area for a 250 mm thick wall

Figure 6.17 illustrates the relation between reinforcement area and mean crack width obtained while varying the reinforcement area in 16 steps between 0,7 and 2,8 times the reference value, while the equation stated below defines its corresponding trend line.

$$y = 0,002 \cdot x^{-0,78} \tag{6.12}$$

where x is the mean crack width in mm
 y is the reinforcement amount in m^2 needed for a mean crack width x

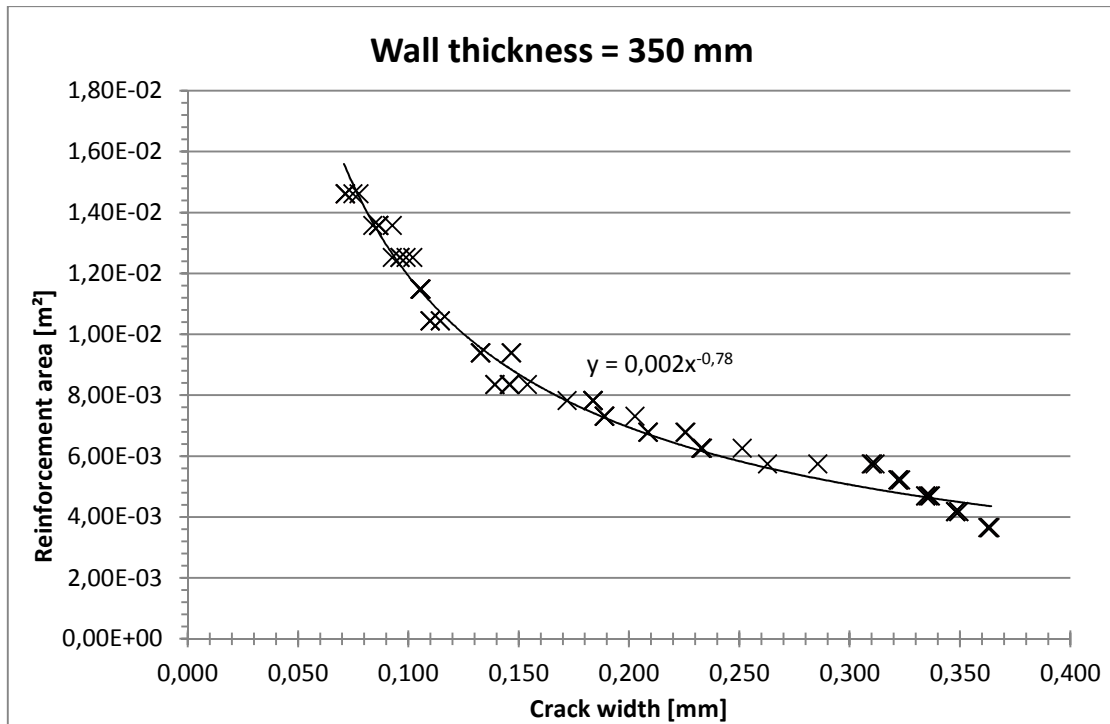


Figure 6.17 Plot of the mean crack width (short term response) versus the reinforcement area for a 350 mm thick wall

By varying the reinforcement area between 0,8 and 2,8 times its reference value in 19 steps a relation between reinforcement area and mean crack width was obtained for the wall thickness of 400 mm. This relation and its associated trend line is respectively presented in Figure 6.18 and expressed below.

$$y = 0,0003 \cdot x^{-1,308} \tag{6.13}$$

where x is the mean crack width in mm
 y is the reinforcement amount in m² needed for a mean crack width x

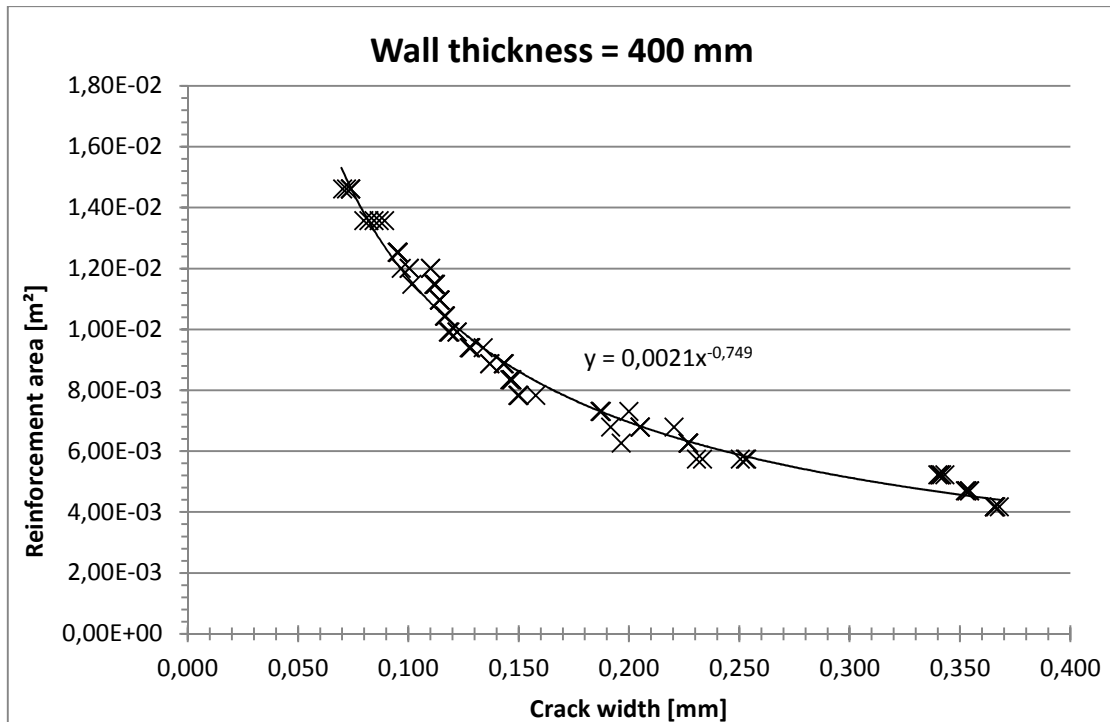


Figure 6.18 Plot of the mean crack width (short term response) versus the reinforcement area for a 400 mm thick wall

For the last considered wall thickness of 450 mm the relation between reinforcement area and mean crack width is illustrated in Figure 6.19, while its corresponding trend line is expressed below. The relation was obtained by altering the reinforcement area between 0,9 and 3 times its reference value in 19 steps.

$$y = 0,0021 \cdot x^{-0,771} \tag{6.14}$$

where x is the mean crack width in mm
 y is the reinforcement amount in m² needed for a mean crack width x

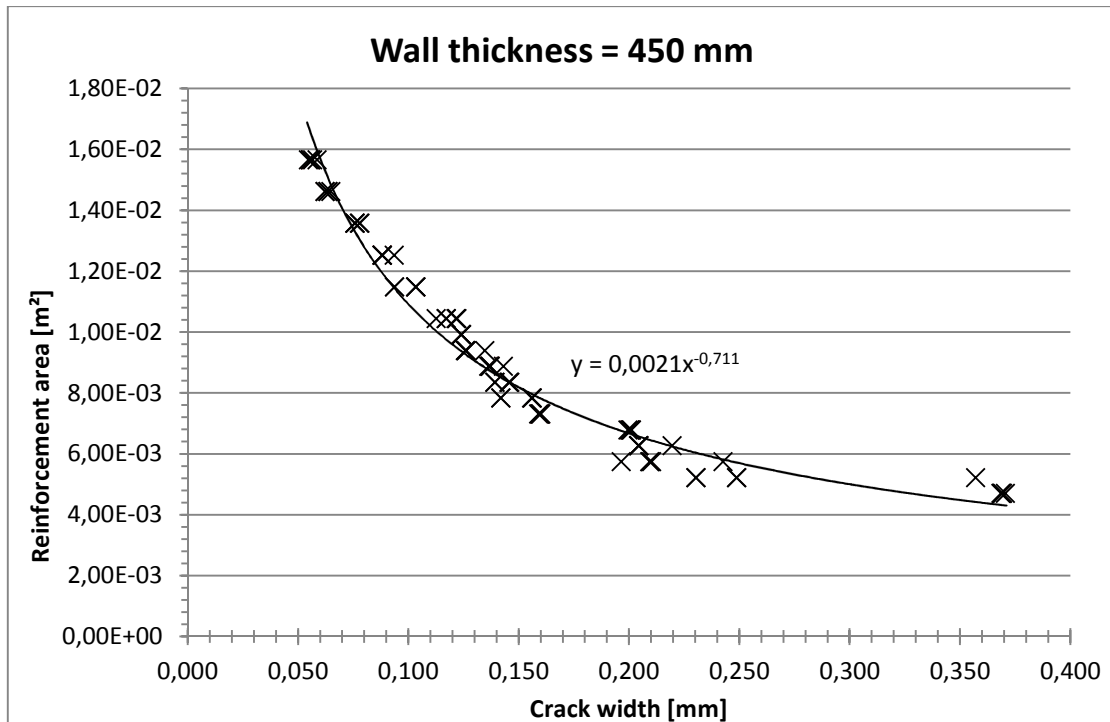


Figure 6.19 Plot of the mean crack width (short term response) versus the reinforcement area for a 450 mm thick wall

6.6.2 Design code comparison

Utilising the respective trend lines corresponding to the wall thicknesses of 200, 250, 300, 350, 400 and 450 mm, respectively illustrated by Figure 6.1, Figure 6.15, Figure 6.16, Figure 6.17, Figure 6.18 and Figure 6.19, relations between the reinforcement area needed for crack control and wall thickness for characteristic crack widths were obtained, relations which are illustrated by Figure 6.20 combined with design code requirements of minimum reinforcement areas for crack control.

Note that all crack widths, characteristic or mean, are those of short term response. As stated in Section 3.5.5, crack widths increase when accounting for the long term response, roughly 1,2 times. This should be kept in mind when comparing calculated crack widths with design code values in which long term effects are included.

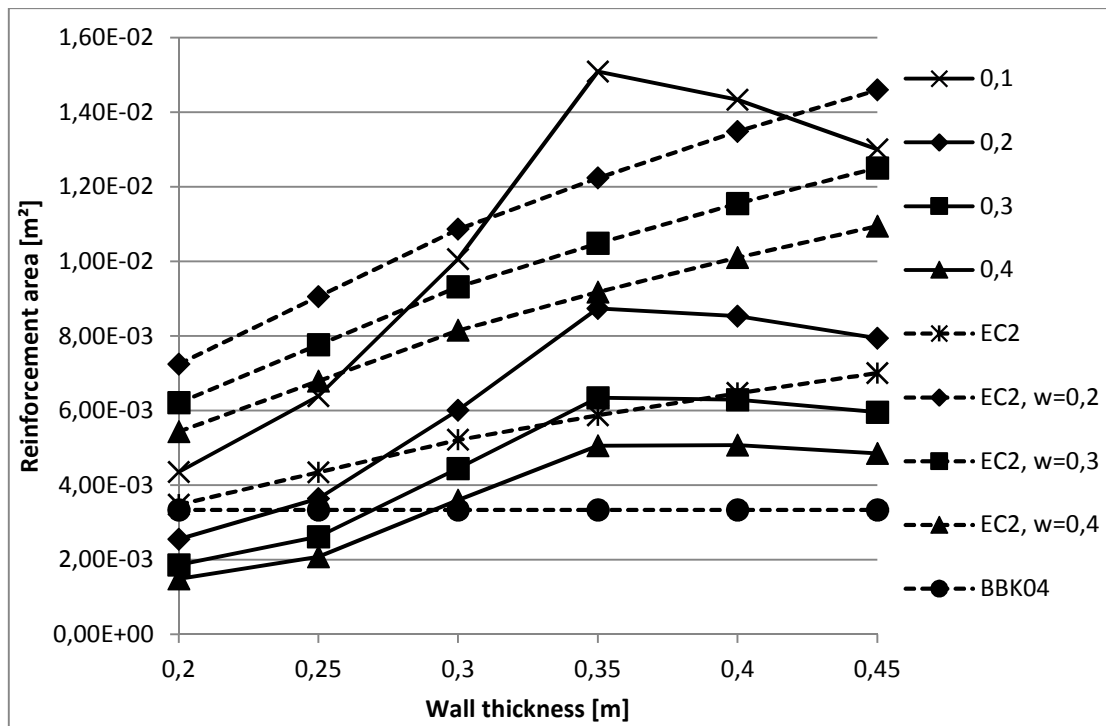


Figure 6.20 Plot of wall thickness versus reinforcement area. Lines illustrate characteristic crack widths (short term response) from the parametric study, Eurocode 2 and BBK 04

A general remark concerning Figure 6.20 is that the reinforcement areas actually needed for a characteristic crack width of 0,1, 0,2, 0,3 and 0,4 mm initially increased for an increasing wall thickness and subsequently stabilised and even decreased for thicknesses exceeding 350 mm. The decrease could be due to several reasons, since the thickness affects, among others, stiffness parameters, shrinkage strain and creep coefficients.

By comparing the reinforcement areas actually needed for characteristic crack widths with corresponding requirements in Eurocode 2 it is revealed that, for each of the characteristic crack widths 0,2, 0,3 and 0,4 mm, Eurocode 2 demands considerably more reinforcement than what seems to be needed for the studied case.

6.7 Influence of relative humidity

6.7.1 Importance of considering relative humidity

Moisture in the surrounding environment greatly influences the shrinkage of a concrete member, see Section 3.3 Hence, it was of interest to investigate this influence with respect to the cracking response of a concrete wall. The influence was initially investigated by varying the relative humidity of the surroundings between 30 and 80% for the standard wall defined in Section 6.2. In Figure 6.21 the resulting mean crack width is plotted against its corresponding relative humidity.

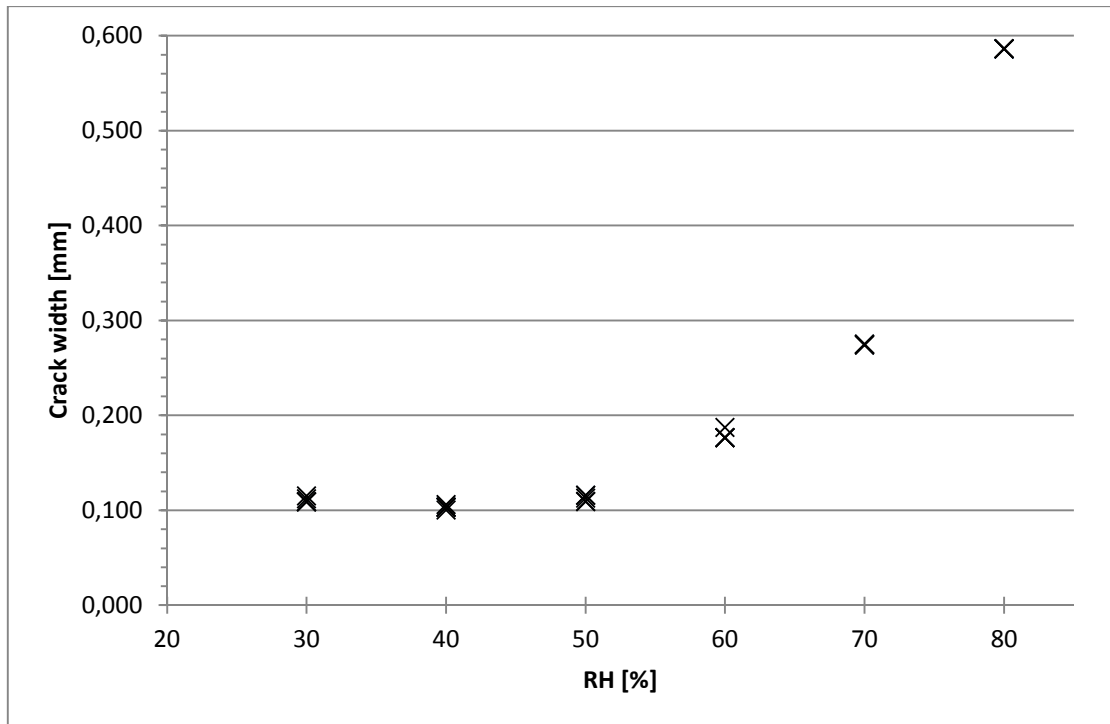


Figure 6.21 Mean crack width (short term response) plotted against the relative humidity of the surroundings

As seen in Figure 6.21 the mean crack widths for the standard wall are more or less stable for a relative humidity in the range of 30-50%, while they subsequently increase rapidly until a relative humidity of 80%. For a lower relative humidity where remaining parameters (e.g. restraints) are unchanged, the shrinkage strain develops faster than for a higher relative humidity. Consequently, also the imposed stress-dependent strain generating tensile stresses, see Section 5.2.2.8, develops faster. This result in several smaller and more well-distributed cracks as opposed to the higher ranges of relative humidity. Thus, for high relative humidities, not as many cracks occur and the mean crack width increases significantly.

6.7.2 Reinforcement area required for control

To further investigate the influence of relative humidity and specifically its influence on the needed reinforcement areas, a relative humidity of 40, 50, 60 and 70% respectively was further considered by varying the provided reinforcement area for each situation.

Since a relative humidity of 60% was chosen as the reference value of the standard wall, the common case in Section 6.3 provides the relation between reinforcement area and mean crack width for the case of a 60% relative humidity. This relation is displayed in Figure 6.1 and described by its trend line expressed in Equation 6.2.

In the case of a 40% relative humidity of the surroundings Figure 6.22 contains the resulting relation between reinforcement area and mean crack width. The relation was obtained by varying the reinforcement area in 16 steps between 0,55 and 1,9 times its baseline value and its describing trend line is expressed as

$$y = 0,0012 \cdot x^{-0,628} \quad (6.15)$$

where x is the mean crack width in mm
 y is the reinforcement amount in m^2 needed for a mean crack width x

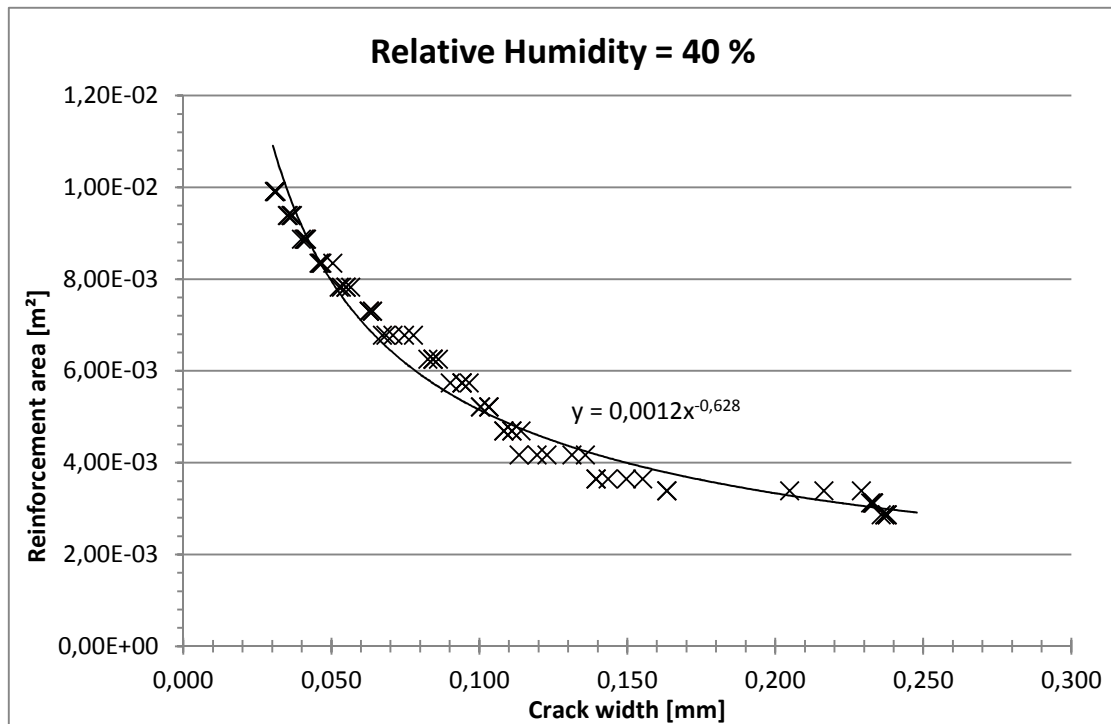


Figure 6.22 Mean crack width (short term response) plotted against the reinforcement area for a relative humidity of 40 %

In Figure 6.23 the relation between reinforcement area and mean crack width for a surrounding environment of 50% relative humidity is illustrated. It was obtained by altering the reinforcement area between 0,55 and 1,9 times its reference value in a total of 16 steps. The equation for the resulting trend line is specified below.

$$y = 0,0011 \cdot x^{-0,715} \tag{6.16}$$

where x is the mean crack width in mm
 y is the reinforcement amount in m^2 needed for a mean crack width x

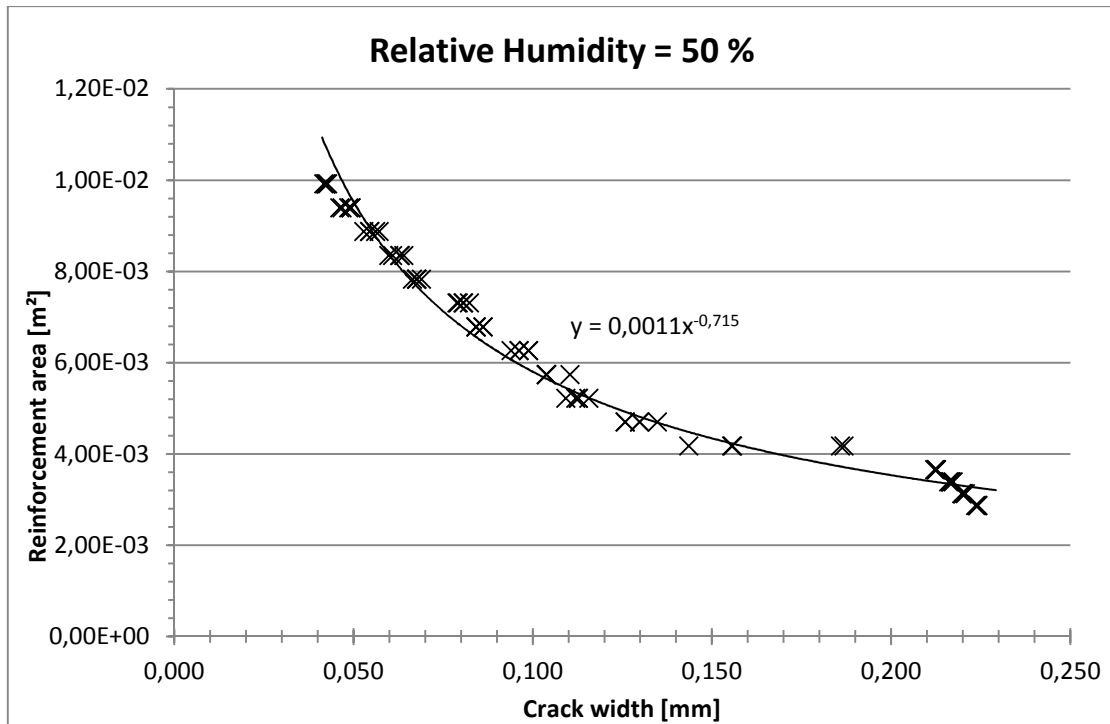


Figure 6.23 Mean crack width (short term response) plotted against the reinforcement area for a relative humidity of 50 %

A relation for the fourth considered relative humidity, 70%, can be found in Figure 6.24. In this case the reinforcement amount varied within a range of 0,5 and 3 times the reference value utilising 21 steps. Its resulting trend line equation is defined below.

$$y = 0,0021 \cdot x^{-0,806} \quad (6.17)$$

where x is the mean crack width in mm
 y is the reinforcement amount in m² needed for a mean crack width x

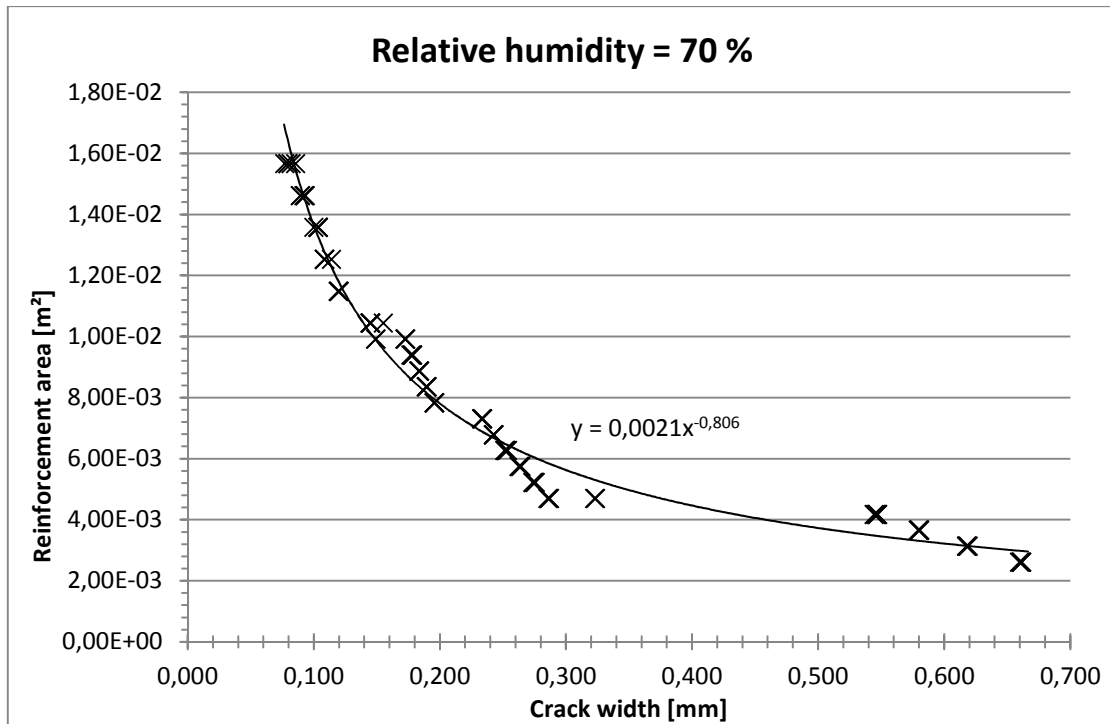


Figure 6.24 Mean crack width (short term response) plotted against the reinforcement area for a relative humidity of 70 %

6.7.3 Design code comparison

Based on the respective trend lines of Figure 6.1, Figure 6.22, Figure 6.23 and Figure 6.24 relations between needed reinforcement area and the moisture level of the surroundings, expressed by means of relative humidity, were acquired for different characteristic crack widths. These relations were obtained by, for each considered value of the relative humidity and using its respective trend line equation, finding the reinforcement amount corresponding to characteristic crack widths of 0,1, 0,2, 0,3 and 0,4 mm respectively. Figure 6.25 illustrates these relations along with design code requirements.

Note that all crack widths, characteristic or mean, are those of short term response. As stated in Section 3.5.5, crack widths increase when accounting for the long term response, roughly 1,2 times. This should be kept in mind when comparing calculated crack widths with design code values in which long term effects are included.

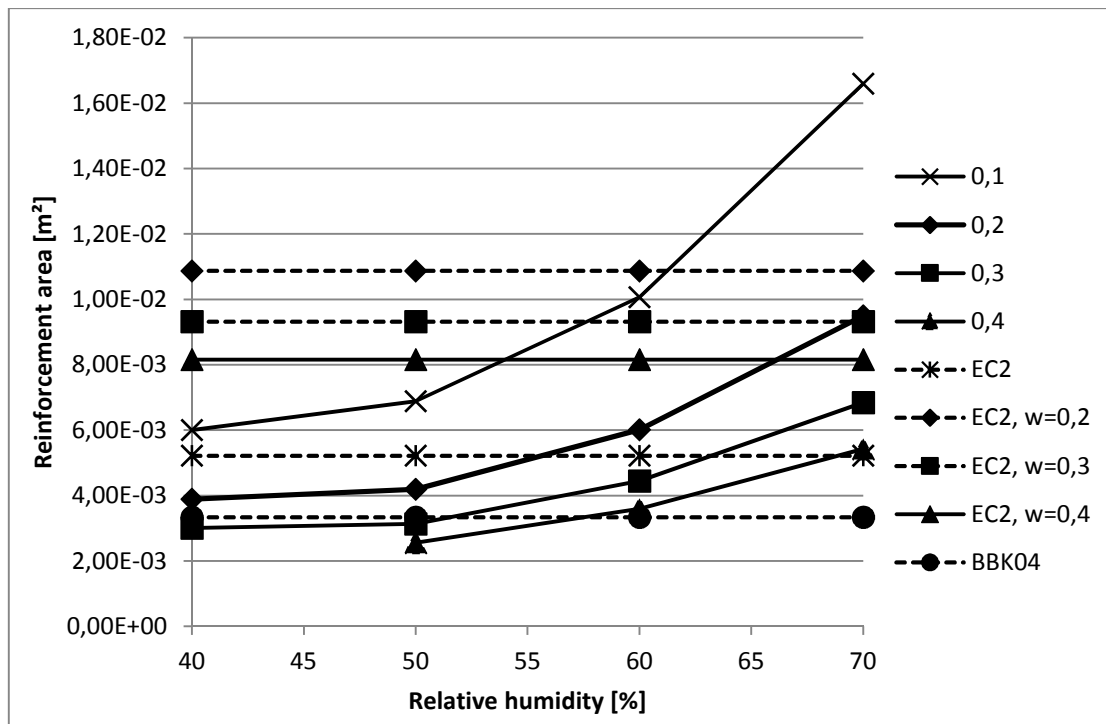


Figure 6.25 Plot of relative humidity against reinforcement area. Lines illustrates characteristic crack widths (short term response) from the parametric study, Eurocode 2 and BBK 04

Based on Figure 6.25, supported by the results shown in Figure 6.1, Figure 6.22, Figure 6.23 and Figure 6.24 and their respective trend lines, some remarks regarding the amount of reinforcement needed for crack control under a varying relative humidity were noted.

The pattern observed while varying the relative humidity for the standard wall, Figure 6.21, was confirmed by the relations in Figure 6.25. That is that a moist environment (high relative humidity) requires a larger amount of crack controlling reinforcement in order to limit crack widths as opposed to a dry environment (low relative humidity). Thus, a dry environment where the shrinkage strain is larger seems to need lower amounts of reinforcement in order to limit crack widths if remaining parameters (including the continuous restraint from at the wall/slab interface) are unchanged.

Note that the relative humidities are assumed to be constant values over the considered time period of 50 years. Although the relative humidity likely experience considerable alterations over time, the chosen values of 40, 50, 60 and 70% could represent different environments as mean values of time.

Figure 6.25 illustrates that for low relative humidities reinforcement amounts required for crack control according to Eurocode 2 are considerably overestimated. However, for relative humidities approaching the 70% mark, the difference between areas required by Eurocode 2 and according to the calculation results decreases. Likely, for even higher relative humidities, the reinforcement amount in Eurocode 2 could actually be underestimated. Although, such high relative humidities are not likely to realistically represent actual normal climates.

6.8 Influence of concrete strength class

6.8.1 Reinforcement area required for crack control

Physical properties of concrete vary considerably depending on the type of concrete used. The influence of these varying properties for different concrete types, represented by concrete strength classes, was investigated by varying the provided reinforcement amount for four different strength classes in relation to the obtained mean crack widths. The considered concrete strength classes were C20/25, C30/37, C40/50 and C50/60, which have mean tensile strengths of 2,2, 2,9, 3,5 and 4,1 MPa.

The standard wall of Section 6.2 has the concrete strength class C30/37. Thus the reference case in Section 6.3 represents that concrete strength class. Hence Figure 6.1 and Equation 6.2 illustrate the relation between reinforcement area and mean crack width and express its corresponding trend line respectively.

A relation between reinforcement area and mean crack width for the concrete strength class C20/25 was obtained by varying the reinforcement area between 0,065 and 0,6 times the reference value in 13 steps. The resulting relation is plotted in Figure 6.26 and its trend line is expressed as

$$y = -0,0245 \cdot x + 0.0039 \quad (6.18)$$

where x is the mean crack width in mm
 y is the reinforcement amount in m^2 needed for a mean crack width x

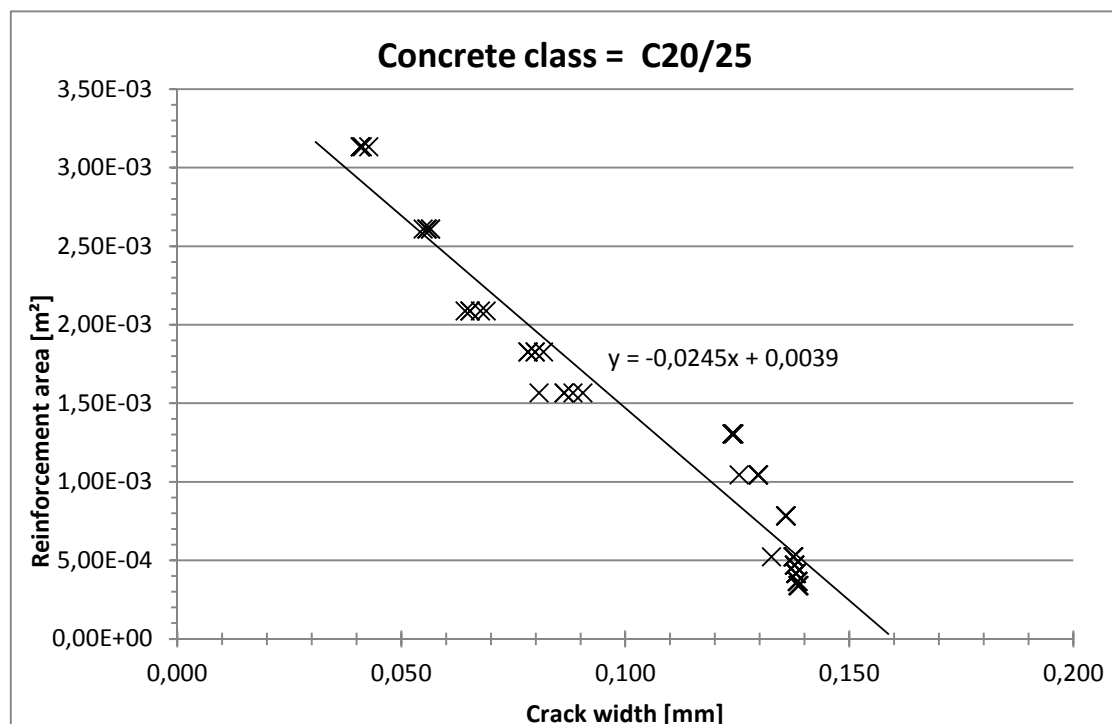


Figure 6.26 Results showing the mean crack width (short term response) versus the reinforcement area for concrete strength class C20/25

Utilising the concrete strength class C40/50 the relation between reinforcement area and mean crack width, plotted in Figure 6.27, and its associated trend line, expressed

below were obtained by varying the reinforcement amount between 0,9 and 3,2 times the reference value in 17 steps.

$$y = 0,0011 \cdot x^{-0,795} \quad (6.19)$$

where x is the mean crack width in mm
 y is the reinforcement amount in m^2 needed for a mean crack width x

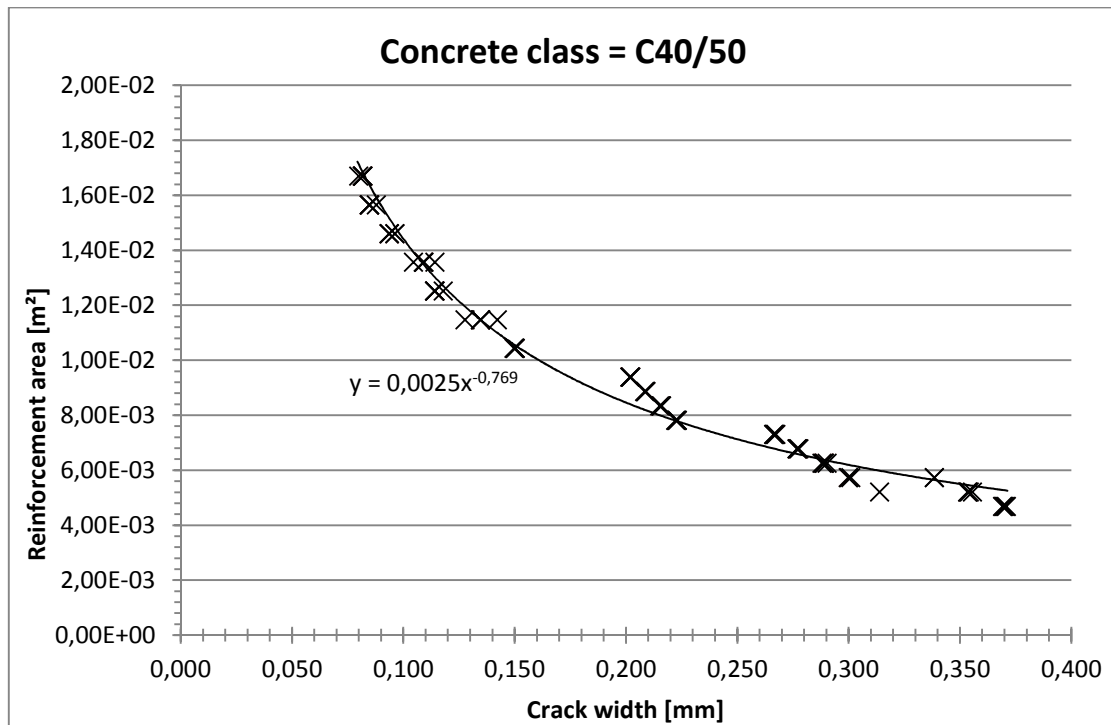


Figure 6.27 Results showing the mean crack width (short term response) versus the reinforcement area for concrete strength class C40/50

In the case of concrete strength class C50/60 a relation between reinforcement area and mean crack width, illustrated by Figure 6.28, was acquired by varying the reinforcement area in 22 steps between 1,2 and 6 times the reference value. A corresponding trend line is expressed as

$$y = 0,0011 \cdot x^{-0,795} \quad (6.20)$$

where x is the mean crack width in mm
 y is the reinforcement amount in m^2 needed for a mean crack width x

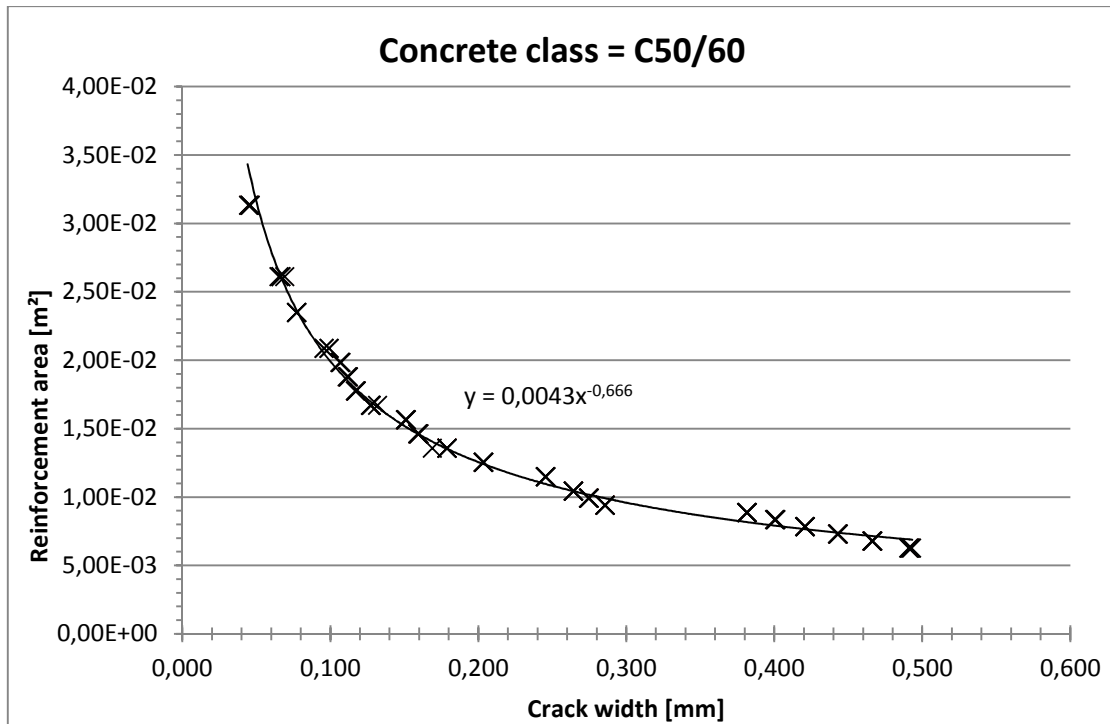


Figure 6.28 Results showing the mean crack width (short term response) versus the reinforcement area for concrete strength class C50/60

6.8.2 Design code comparison

Based on the respective trend lines in Figure 6.1, Figure 6.26, Figure 6.27 and Figure 6.28 relations between needed reinforcement area and characteristic concrete compressive strength were acquired for different characteristic crack widths. These relations were obtained by, for each considered strength class and using its respective trend line equation, finding the reinforcement amount corresponding to the characteristic crack widths of 0,1, 0,2, 0,3 and 0,4 mm respectively. Figure 6.29 illustrates these relations.

Note that all crack widths, characteristic or mean, are those of short term response. As stated in Section 3.5.5, crack widths increase when accounting for the long term response, roughly 1,2 times. This should be kept in mind when comparing calculated crack widths with design code values in which long term effects are included.

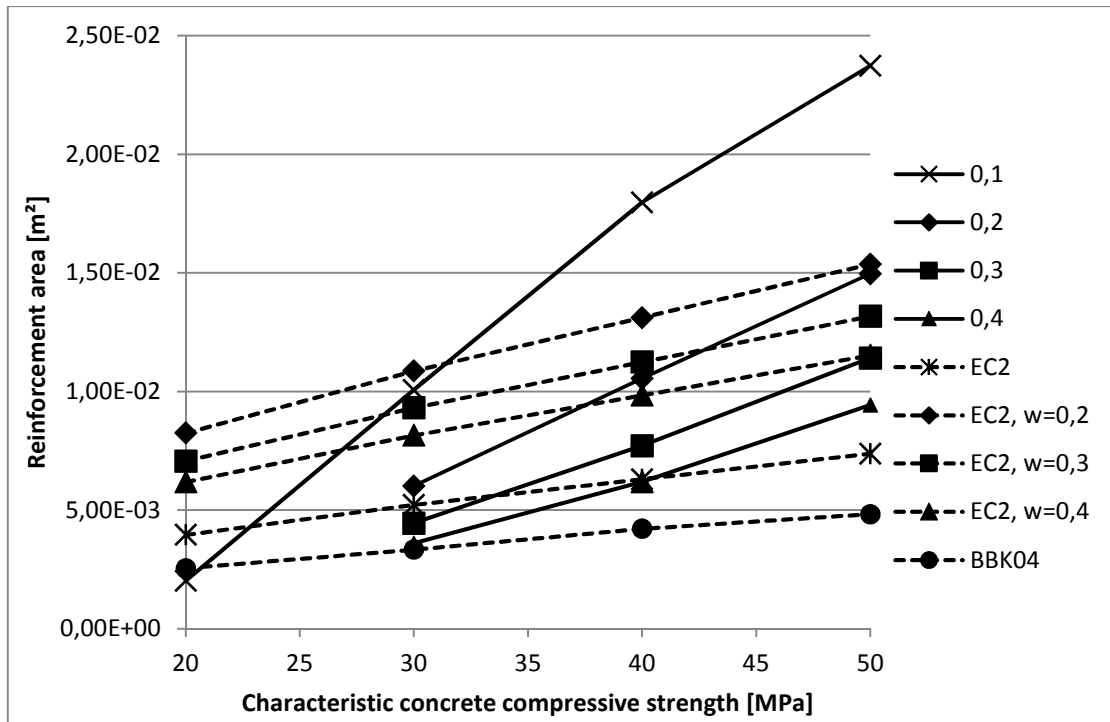


Figure 6.29 Characteristic concrete compressive strength plotted against reinforcement area. Lines illustrate characteristic crack widths (short term response) from the parametric study, Eurocode 2 and BBK 04

Figure 6.29 clearly illustrates that an increased concrete strength class, expressed by means of the characteristic concrete compressive strength, considerably increased the reinforcement amount needed to limit crack widths. For instance, if a characteristic crack width of 0,2 mm is considered, the needed reinforcement area increases 2,5 times, if C50/60 is used instead of C30/37. However, this difference is also dependent upon other parameters of the standard wall and the magnitude of it could differ, if some of those parameters are changed.

Nevertheless, stronger concrete requires more crack controlling reinforcement due to its increased tensile strength. During long time the influence of reduced shrinkage strain is minor compared to the influence of a corresponding increase of tensile strength. Consequently the imposed stress-dependent strain generating tensile stress is similar, but the tensile strength of the concrete increases. Thus, when remaining parameters are unchanged, a lower characteristic crack width is achieved for a lower concrete strength class and vice versa.

Regarding the design code requirements on minimum reinforcement Eurocode 2 seems to overestimate the needed reinforcement area for normal strength concrete, such as e.g. C30/37. Although, by following the trend that the actual needed amount of reinforcement approaches the Eurocode 2 requirement for an increasing concrete strength class, the Eurocode 2 requirement could perhaps underestimate the needed reinforcement areas for restrained concrete walls of high strength concrete exposed to shrinkage.

6.9 Influence of bar diameter

6.9.1 Reinforcement area required for crack control

Several parameters accounted for in the calculation model are dependent on the bar diameter of the provided crack controlling reinforcement. For instance, the expressions for mean crack width and transmission length in Section 5.2.2.9 and the stiffness contribution from reinforcement in Section 5.2.2.3 are all dependent on the bar diameter. The influence on the reinforcement amount needed for crack control was studied by varying the reinforcement amount for bar diameters of 8, 10, 12 and 16 mm respectively, while remaining parameters remained at their respective reference values stated in Table 6.1.

For the standard wall of Section 6.2 horizontal reinforcement was provided by means of 12 mm bars. Thus the common case presented in Section 6.3 already contains the relation, expressed by Figure 6.1 and Equation 6.2, between reinforcement area and mean crack width using 12 mm bars.

When reinforcement is provided by means of 8 mm bars, Figure 6.30 demonstrates the relation between reinforcement area and mean crack width obtained while altering the reinforcement area between 0,65 and 2,1 times the reference value in 16 steps. A resulting trend line was obtained and is expressed as stated below.

$$y = 0,0011 \cdot x^{-0,795} \quad (6.21)$$

where x is the mean crack width in mm
 y is the reinforcement amount in m^2 needed for a mean crack width x

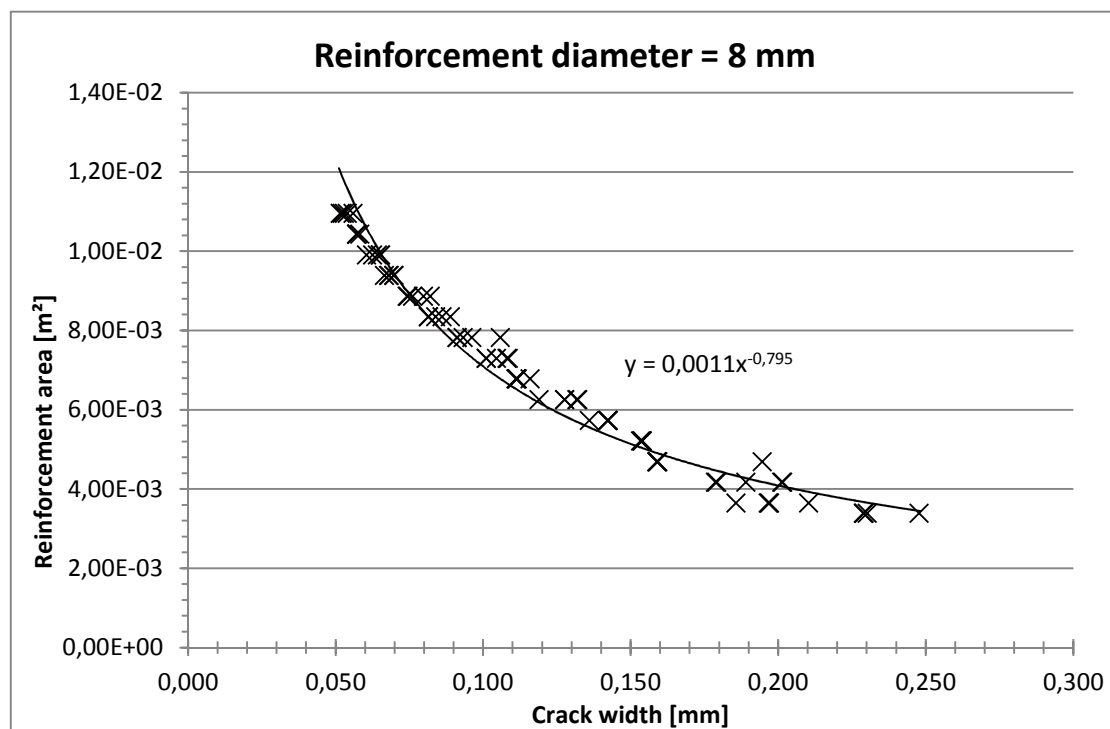


Figure 6.30 Mean crack width (short term response) plotted against reinforcement area with a bar diameter of 8 mm

For a bar diameter of 10 mm the obtained relation between reinforcement area and mean crack width is plotted in Figure 6.31 and was achieved by varying the reinforcement area in 15 steps between 0,6 and 2,2 times the reference value. Using the obtained relation a trend line was found and is expressed as

$$y = 0,0013 \cdot x^{-0,764} \quad (6.22)$$

where x is the mean crack width in mm
 y is the reinforcement amount in m^2 needed for a mean crack width x

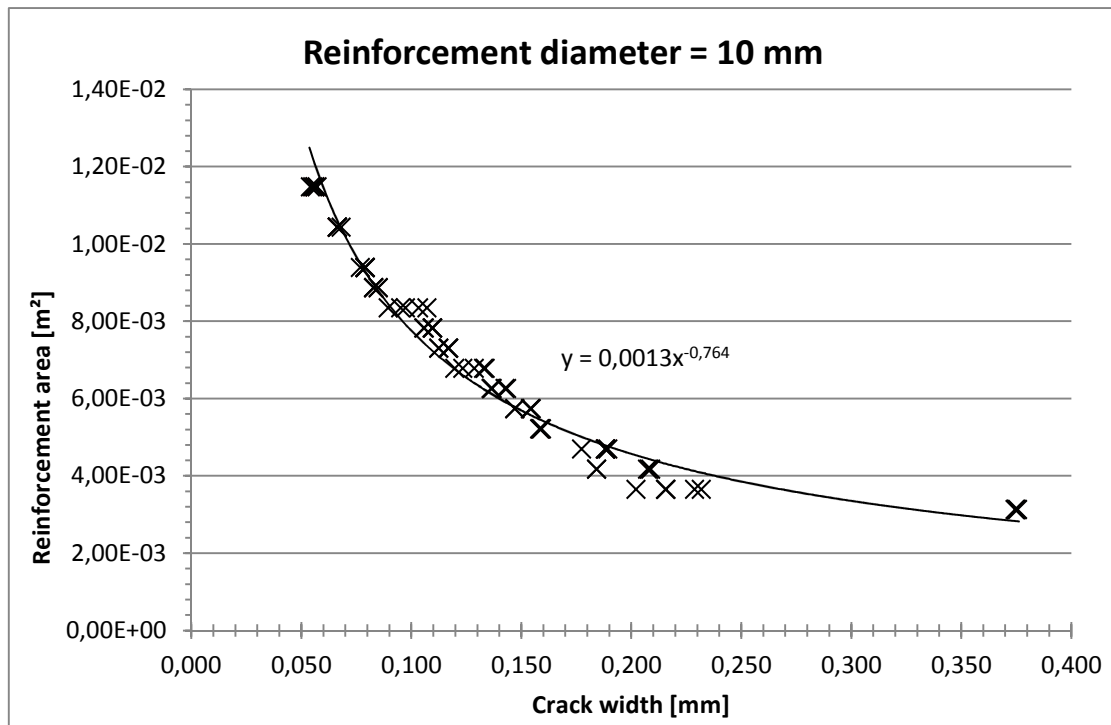


Figure 6.31 Mean crack width (short term response) plotted against reinforcement area with a bar diameter of 10 mm

The fourth considered bar diameter, 16 mm, resulted in a relation between reinforcement area and mean crack width that was obtained by altering the reinforcement area between 0,8 and 2,2 times the reference value in 16 steps and is illustrated in Figure 6.32. Its corresponding trend line equation can be expressed

$$y = 0,0018 \cdot x^{-0,721} \quad (6.23)$$

where x is the mean crack width in mm
 y is the reinforcement amount in m^2 needed for a mean crack width x

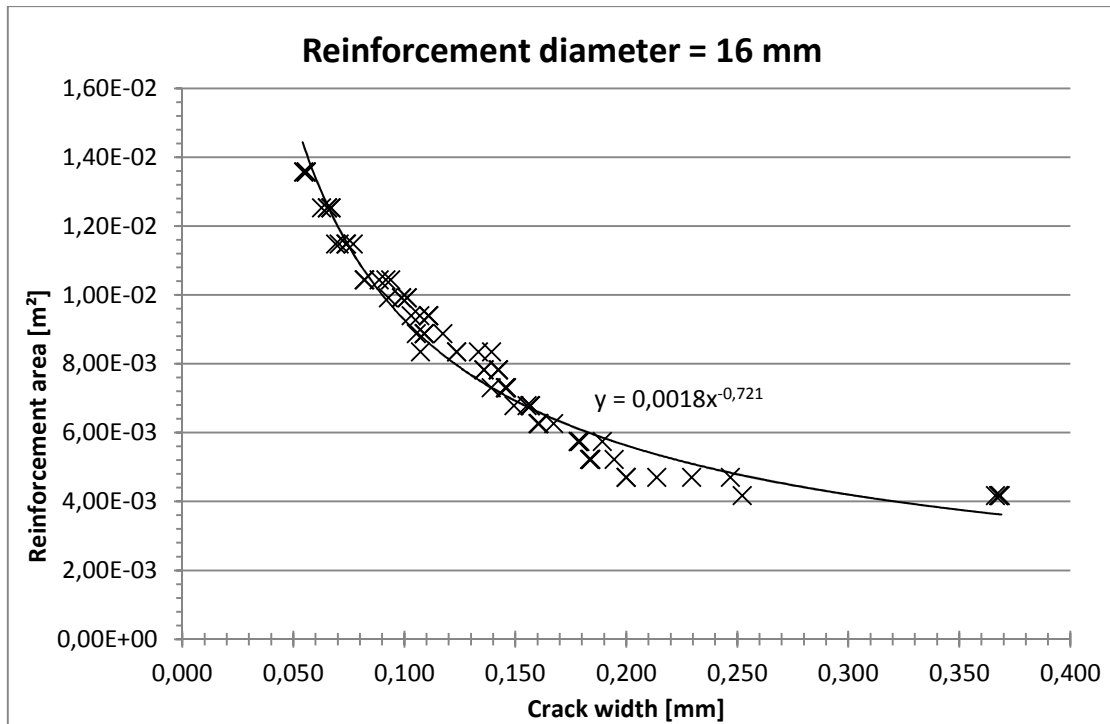


Figure 6.32 Mean crack width (short term response) plotted against reinforcement area with a bar diameter of 16 mm

6.9.2 Design code comparison

Based on the respective trend lines in Figure 6.1, Figure 6.30, Figure 6.31 and Figure 6.32, relations between needed reinforcement area and the bar diameter were acquired for different characteristic crack widths. These relations were obtained by, for each considered bar diameter and using its respective trend line equation, finding the reinforcement amount corresponding to the characteristic crack widths of 0,1, 0,2, 0,3 and 0,4 mm respectively. Figure 6.33 illustrates these relations.

Note that all crack widths, characteristic or mean, are those of short term response. As stated in Section 3.5.5, crack widths increase when accounting for the long term response, roughly 1,2 times. This should be kept in mind when comparing calculated crack widths with design code values in which long term effects are included.

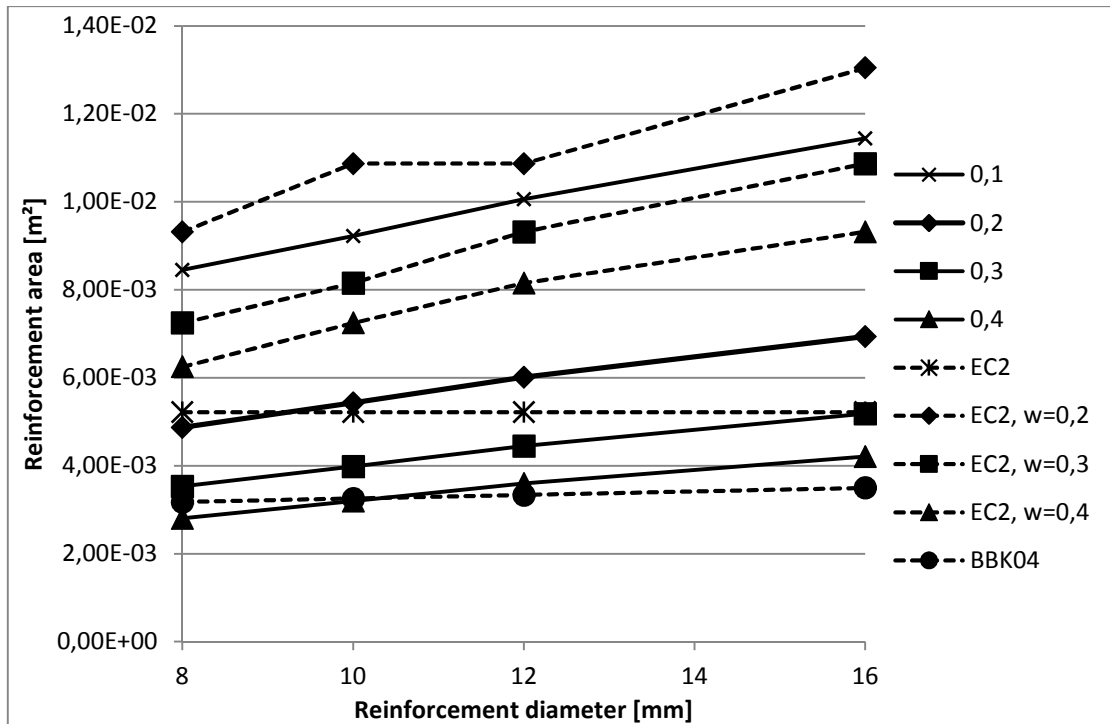


Figure 6.33 Plot of reinforcement bar diameter versus reinforcement area. Lines illustrate characteristic crack widths (short term response) from the parametric study, Eurocode 2 and BBK 04

Figure 6.33 demonstrates that, regardless of the value of characteristic crack width, an increased bar diameter results in an increased reinforcement area. In order to limit crack widths to a certain value, Eurocode 2, CEN (2004), defines a limiting steel stress depending on the bar diameter, see Section 3.6.1. Table 3.4 lists these steel stresses and evidently indicates that larger steel stresses are allowed for smaller bar diameters. This implies that, due to the higher allowable steel stress, a smaller bar can be utilised more efficiently in control of cracking and thus a lower total reinforcement area can be sufficient.

As for the Eurocode 2 requirements regarding minimum reinforcement areas for characteristic crack widths of 0,2, 0,3 and 0,4 mm, they are considerably larger than what, in case of the standard wall, is needed regardless of bar diameter, at least between 8-16 mm.

6.10 Influence of wall length

6.10.1 Importance of considering wall length

The results presented in Section 6.5 indicate that the end support stiffness from connecting walls could have a large impact on the overall cracking response. Since the total wall length affects the effect of restraint from these ends within the wall, the total wall length might also have a large impact on the cracking response.

The influence of wall length was initially investigated by varying the total wall length of the standard wall, see Section 6.2, in 10 steps between 8 and 42 meters. Figure 6.34 illustrates the obtained relation between mean crack width and wall length.

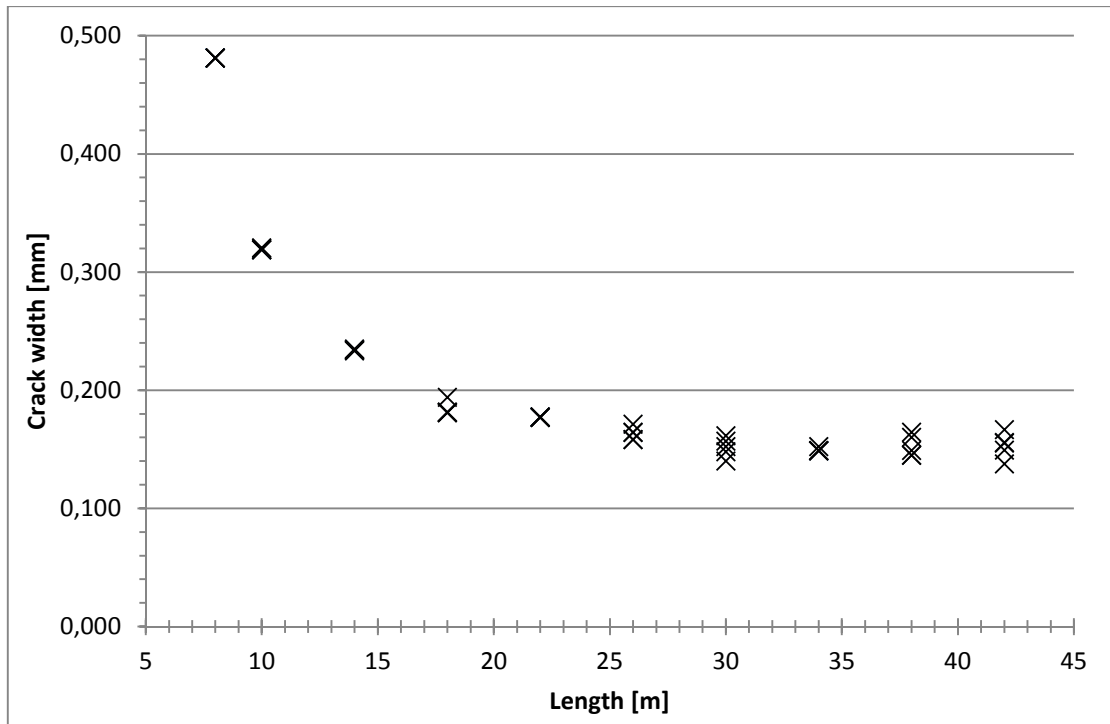


Figure 6.34 Wall length plotted against the mean crack width (short term response) for the standard wall

Figure 6.34 clearly demonstrates that the mean crack width decreased, while the total wall length increased, although, eventually the mean crack width more or less stabilised. As further demonstrated by the figure, short walls were found to have very large mean crack widths, likely caused by the large influence of the connecting walls in a short wall segment. While the length increased, this effect decreased and for longer walls the restraint along to interface to the connecting slab was the main factor influencing the mean crack width. Sections 6.4 and 6.5 treat the influence of the wall/slab interface stiffness and the end support stiffness respectively.

6.10.2 Reinforcement area needed for crack control

The influence of wall length was further investigated by varying the reinforcement amount for wall lengths of 10, 20 and 30 meters respectively. For each of these wall lengths relations between reinforcement area and mean crack width were obtained together with relations between reinforcement area and wall length for different crack widths.

Since the standard wall has a length of 20 meters, see Table 6.1, the common case in Section 6.3 provides the relation between reinforcement area and mean crack width for that case. Thus Figure 6.1 illustrates the relation and Equation (6.2) expresses its corresponding trend line.

An equivalent relation between reinforcement area and mean crack width for a wall length of 10 meters was obtained by varying the reinforcement amount in 20 steps between 0,6 and 3,2 times the reference value. The resulting relation is plotted in Figure 6.35 and its associated trend line is expressed as

$$y = 0,003 \cdot x^{-0,598} \quad (6.24)$$

where x is the mean crack width in mm
 y is the reinforcement amount in m^2 needed for a mean crack width x

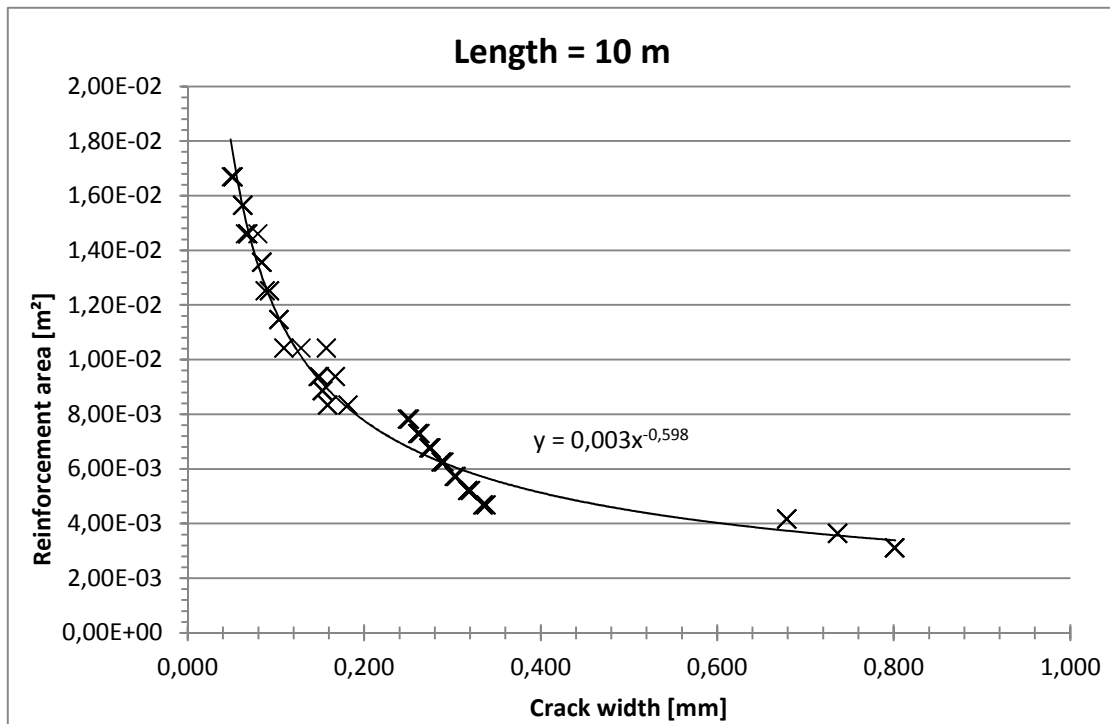


Figure 6.35 Plot of the mean crack width (short term response) versus the reinforcement area for a 10 meter long wall

For a wall length of 30 meters Figure 6.36 illustrates the relation between reinforcement area and mean crack width obtained by varying the reinforcement amount between 0,45 and 1,9 times its reference value in 16 steps. A corresponding trend line was found and is defined below

$$y = 0,001 \cdot x^{-0,866} \quad (6.25)$$

where x is the mean crack width in mm
 y is the reinforcement amount in m^2 needed for a mean crack width x

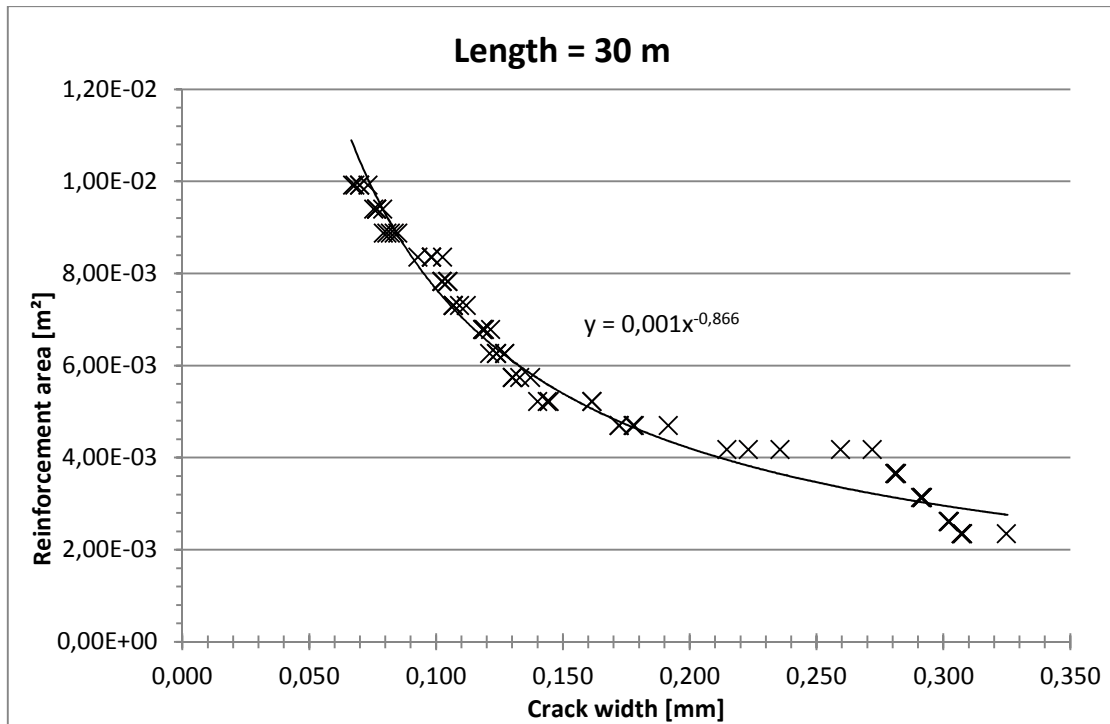


Figure 6.36 Plot of the mean crack width (short term response) versus the reinforcement area for a 30 meter long wall

6.10.3 Design code comparison

Using the trend lines related to Figure 6.1, Figure 6.35 and Figure 6.36 relations between reinforcement area and wall length for different characteristic crack widths were obtained. These relations are plotted in Figure 6.37.

Note that all crack widths, characteristic or mean, are those of short term response. As stated in Section 3.5.5, crack widths increase when accounting for the long term response, roughly 1,2 times. This should be kept in mind when comparing calculated crack widths with design code values in which long term effects are included.

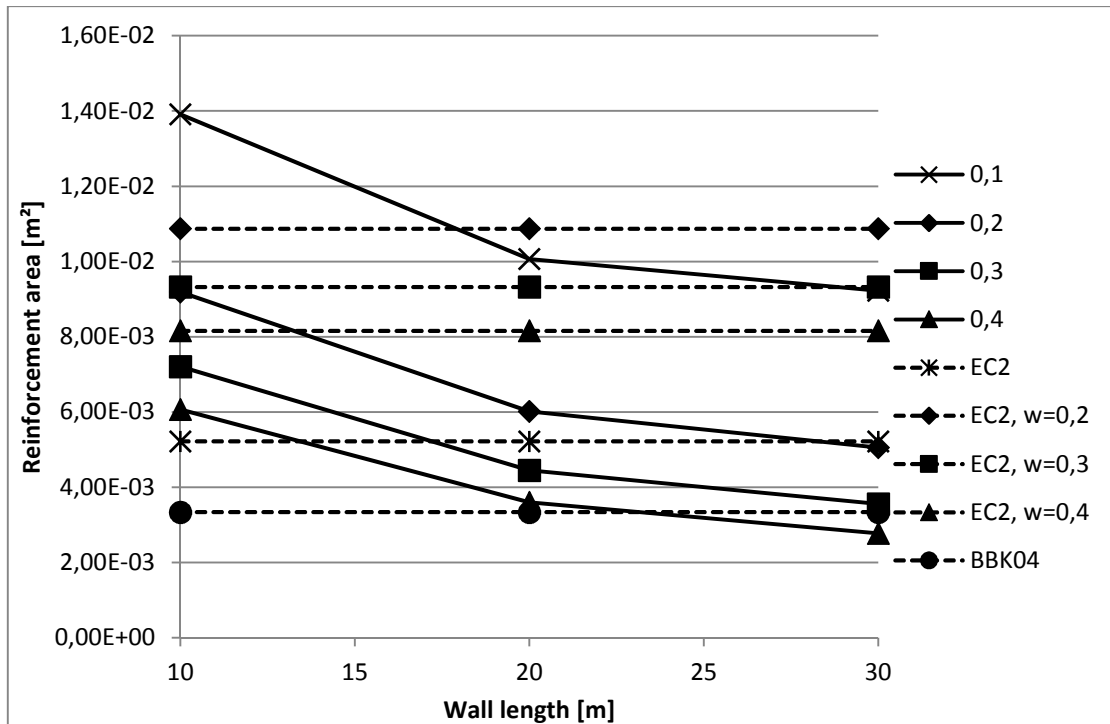


Figure 6.37 Results from variations of the wall length versus reinforcement area. Lines illustrate characteristic crack widths (short term response) from the parametric study, Eurocode 2 and BBK 04

By studying Figure 6.37 it was clear that the reinforcement area needed to limit crack widths to a certain value decreased for an increased wall length, which corresponds well with the indications observed in Figure 6.9 and Figure 6.14. End restraints, in the form of connecting walls, influenced the cracking response more in shorter walls than in longer walls, since the effect of end restraints along the length of a wall is less than in shorter walls. The reason for this is that a continuous restraint exists along the connecting slab, if no such restraint exists the effect would be different.

Regarding the reinforcement areas which, according to the calculations, are needed for limiting crack widths to the characteristic values of 0,2, 0,3 and 0,4 mm respectively, Eurocode 2 overestimates the area needed for each limit.

7 Evaluation

7.1 Introduction

In this chapter the observations from the visited objects of Chapter 4 and the modelling results from the parametric study presented in Chapter 5.3.4 are presented together with conclusions.

7.2 Fibre reinforced concrete

These conclusions are based on the general material properties and the cracking process of fibre reinforced concrete treated in Sections 3.1.6 and 3.5.4 respectively. As stated in Section 3.1.6 fibres can greatly influence the behaviour of concrete and, depending on the type of fibre added, the main influence is on either the pre- or post-cracking behaviour.

Löfgren (2005) states that the addition of microfibres could influence the pre-cracking behaviour and slightly increase the tensile strength as well as delay the growth of micro-cracks. However, the actual increase, which is schematically illustrated by Figure 3.33, is not large enough to significantly influence the ratio between concrete's compressive and tensile strengths, mentioned in Section 3.1.1, and roughly corresponds to an increase of the concrete strength class. This increase in tensile strength could actually affect the reinforcement area needed for crack control negatively since, as illustrated in Figure 6.29, an increase in concrete strength class increases the needed reinforcement amount.

According to Purnell (2010) fibre reinforced concrete excels in controlling restraint related cracking caused by e.g. shrinkage due to the distributed nature of its reinforcement. However, as pointed out by Antona and Johansson (2011), ordinary reinforcement bars are likely needed as a complement to the fibre reinforcement. So in terms of concrete cellar walls, fibre reinforcement by means of long fibres probably offers an approach which could limit crack widths and reduce the amount of conventional reinforcement needed. However, it does not feasibly eliminate cracks or the need for conventional reinforcement bars.

7.3 Visited objects

During the inspections of the visited objects, presented in Sections 4.3 and 4.4 respectively, cracks were found to mostly exist in the middle part of the inspected walls not propagating to or originating from either the upper or lower connecting floor slabs.

Both objects were provided with extra reinforcement bars in the bottom part of their respective walls, see Figure 4.4, Figure 4.11 and Figure 4.18, likely due to an assumption by the designers that the significantly larger amount of restraint present near the connecting floor slab requires larger amounts of crack controlling reinforcement. Figure 3.20 evidently illustrates that the restraint is large close to the slab. However, Figure 3.21 equally evidently illustrates that the amount of restraint for a wall with high length to height ratio remains large throughout the entire height. If the top slab also generates a restraint, the restraint throughout the wall will likely be even higher. Thus, the extra reinforcement provided in the visited objects might not be

necessary, since the continuous restraint at the wall/slab interface that greatly influence the crack distribution is large throughout most of the height and most cracks were observed in the middle parts of the walls.

Furthermore, both objects were designed using the no longer valid Swedish handbook BBK 04, Boverket (2004), which required less amounts of reinforcement than Eurocode 2, CEN (2004), and, according to Björnberg and Johansson (2013), could underestimate the needed amount of reinforcement. As stated in Sections 4.3.3.2, 4.3.4.2 and 4.4.3.2 the characteristic crack widths of the examined walls were 0,17 mm, 0,28 mm and 0,20 mm respectively, which are decent values with regard to crack control. The three measured walls were chosen because of the presence of several cracks and most of the other walls examined by visually inspection had less cracks. However, none of the investigated walls were older than six years, implying that the crack formation has not yet been fully developed. On this basis the provided horizontal reinforcement in the walls of the visited objects is generally sufficient.

7.4 Parametric study

Since restrained shrinkage strains introduce tensile stresses in reinforced concrete, larger restraints for the same magnitude of shrinkage might easily be thought of as negative with regard to crack widths. However, the results from Section 6.4 indicate that increasing the continuous edge restraint along the wall/slab interface decreases the mean crack width and improves the cracking response. Furthermore, the results from Section 6.5 indicate that increasing the end support restraint from connecting walls could also decrease the mean crack width and improve the cracking response. Although, the results from Section 6.5 are dependent on the fact that there is still a significant continuous edge restraint at the wall/slab interface. If such a continuous restraint is small or absent, the results could differ significantly. The mean crack width is likely to increase and the cracking response impair. Thus, an increase in restraint could, under the right circumstances, improve the cracking response by decreasing the mean crack width. However, there are too many combinations, regarding both type and magnitude, of different restraints to state that increasing restraints generally improves the cracking response and decreases the mean crack width.

Besides increased restraints also increased shrinkage strains are easily believed to have a negative effect on the overall cracking response of a restrained concrete member, because of their increase of the imposed stress-dependent strain. Although, the influence of relative humidity on the crack widths, treated in Section 6.7, indicates that so might not always be the case. Figure 6.25 illustrate that, decreasing the relative humidity and consequently increasing the imposed stress-dependent strain (since the shrinkage strain increases) decreased the characteristic crack width and improved the cracking response. The number of cracks increases faster than the total sum of crack widths and hence decreased the characteristic crack width. This should be possible to observe for other effects that increases the imposed stress-dependent strain in a restrained concrete member as well, such as a significant temperature decrease in the ambient environment.

There are two possible approaches to handle cracking of a restrained concrete member exposed to shrinkage. The first approach is to avoid cracking by minimizing the shrinkage strain and/or the restraints. This minimizes tensile stresses generated by the

imposed stress-dependent strain. The second approach is to accept cracking and ensure sufficient crack control. A conclusion drawn from what is stated above is that a good crack control can be achieved with lower amounts of crack controlling reinforcement if a significant continuous edge restraint is present.

In order to obtain a sound final cracking response a continuous restraint could have a positive effect on the cracking response and significantly lower the reinforcement amount needed for crack control. But even if such a restraint is present, there are still several other parameters that also influence the cracking response, see e.g. Section 6.6 for the influence of wall thickness, Section 6.8 for the influence of concrete strength class, Section 6.9 for the influence of reinforcement bar diameter and Section 6.10 for the influence of wall length.

7.5 Minimum reinforcement amount

Figure 6.1 clearly illustrates the importance of the provided reinforcement amount with regard to crack control. It also illustrates that the relation between reinforcement area and mean crack width is non-linear, meaning that both under- and overestimations of the reinforcement area could have a significant influence on the cracking response of a restrained concrete wall. Using the results from Chapter 5.3.4 the following can be stated regarding the amount of reinforcement needed for crack control of restrained concrete walls exposed to shrinkage.

Figure 6.7, Figure 6.14, Figure 6.20, Figure 6.25, Figure 6.29, Figure 6.33 and Figure 6.37 respectively illustrates that Eurocode 2, CEN (2004), in general seemed to largely overestimate the reinforcement area needed to limit characteristic crack widths (short term response) to certain values for the studied wall. Furthermore, the figures illustrate that the minimum reinforcement area required in Eurocode 2 generally resulted in a crack distribution, which fairly well limited the characteristic crack widths (short term response) to widths in the region of 0,3 mm.

Regarding the required minimum reinforcement area, which should, as stated above, control cracking without a specific limitation of the crack width, it seems to limit crack widths more than necessary and thus overestimates the needed reinforcement area.

Consequently, Eurocode 2 seems to overestimate the reinforcement area needed for crack control regardless of if a specific characteristic crack width limitation exists or not. It should however be noted that, as demonstrated in Sections 6.4 through 6.10, there are numerous parameters which influences and controls the cracking situation of a restrained concrete member. Thus, depending on these parameters the results could differ considerably and further investigations and a more comprehensive parametric study possibly combined with testing are required before finally stating that Eurocode 2 overestimates the amount of minimum reinforcement needed for crack control in restraint situations.

This indicated overestimation further strengthens the statements from Sections 1.1 and 2.2 as well as from Alfredsson and Spåls (2008), Björnberg and Johansson (2013) and Dahlgren and Svensson (2013) that the Eurocode 2 equation is not fully applicable in restraint situations. Additional support can be found theoretically by the fact that the equation utilises the complete cross-sectional area of concrete, see Section 3.6.1. This does not correspond well with the actual behaviour of thicker reinforced concrete

members, see Section 3.5.3, where an effective concrete area is more realistic. Thus the equation likely overestimates the needed amount of reinforcement for thick members. Table 7.1 below illustrates the difference between the concrete area possible to account for while using complete cross-sectional area, effective concrete area according to Eurocode 2 and effective concrete area according to BBK 04 respectively. Furthermore, the Eurocode 2 method does not consider the cracking of the member and the flexibility of restraining components.

Table 7.1 Example of cross-sectional concrete area and corresponding effective concrete areas from Eurocode 2 and BBK 04

Thickness [mm]	Concrete area [m ²]	Effective concrete area, Eurocode 2 [m ²]	Effective concrete area, BBK 04 [m ²]
100	0,3	0,3	0,3
150	0,45	0,45	0,45
200	0,6	0,6	0,492
250	0,75	0,615	0,492
300	0,9	0,615	0,492
350	1,05	0,615	0,492
400	1,2	0,615	0,492
450	1,35	0,615	0,492
500	1,5	0,615	0,492
Prerequisites: $h=3000$ mm, $c=35$ mm, $\phi=12$ mm			

Despite any uncertainties about the magnitude of the overestimation, it remains undoubted that the expression was not derived for restraint situations, European Concrete Platform ASBL (2008). In order to adequately consider restraints and obtain well motivated and proper amount of reinforcement for crack control, the development of an expression considering restraints is favorable and encouraged. The sheer magnitude of parameters influencing restraint cracking of concrete alone motivates the consideration of them in an equation used to consider such cracking.

7.6 Suggested alterations of Eurocode 2 equation for minimum reinforcement

Several suggestions to alter the approach to determine minimum reinforcement amounts for crack control given in Eurocode 2, CEN (2004), have been presented. Two of these are treated in Section 3.6.3. Both these suggestions, from the German

national annex, see Section 3.6.3.1, and Björnberg and Johansson, see Section 3.6.3.2, present changes to the existing equation.

As stated in Section 2.2 this equation is derived using a beam section subjected to both moment and axial force where equilibrium between steel and concrete stresses determines the minimum amount of reinforcement. Hence, the Eurocode 2 equation might not be fully applicable in restraint situations, a conclusion supported by e.g. Chapter 5.3.4 and indicated by Alfredsson and Spåls (2008), Björnberg and Johansson (2013) and Dahlgren and Svensson (2013).

Thus, the alterations presented by the German national annex and Björnberg and Johansson modify the existing equation of questionable applicability, see Section 2.2, which is likely to overestimate the actual needs of minimum reinforcement, see e.g. Section 7.5. Hence, in order to obtain a fully applicable expression for the needed amount of reinforcement, a quite new expression is preferable and coveted instead of a slight modification of the existing equation, which is derived inconsiderate of the flexibility of restraints and the cracking response.

8 Final remarks

8.1 Conclusions

Based on all previous chapters the following conclusions can be drawn.

Fibre reinforcement likely represents a suitable complementary option to ordinary reinforcement bars in controlling restraint related cracking caused by intrinsic deformations. Furthermore, it could potentially allow for a reduction of the reinforcement area of ordinary bars, perhaps especially in situations where considerable and/or unpredictable localised deformations are expected. The reason for these effects is the distributed nature of the fibres and thus the reinforcement.

Most cracks found at the visited objects were localised to the middle part, likely due to high amounts of restraint throughout the entire height. The observations indicate that the extra reinforcement often placed in bottom of concrete cellar walls might be unnecessary.

The visited objects were both designed using BBK 04, which required reinforcement amounts considerably smaller than Eurocode 2. Although, the measured cracks in walls of the visited objects showed relatively small crack widths and good crack distribution.

Increased restraints along the wall/slab interface and at the short ends of the wall decreased the mean crack width and the needed reinforcement amounts, provided that there always is a significant stiffness between the wall and slab. Since increased amount of restraint increased the number of cracks faster than the total sum of crack widths, this positive effect could be observed.

A lowered relative humidity and consequently an increased imposed stress-dependent strain (since the shrinkage strain increases while the continuous restraint is constant), could have a positive influence on the cracking response. Since the number of cracks increases faster than the sum of all crack widths the mean crack width decreased.

Eurocode 2 overestimates the amount of minimum reinforcement needed to limit crack widths to certain characteristic values when considering restraints and shrinkage. Also, the minimum reinforcement area required by Eurocode 2, which does not limit crack widths to certain values, seems to be unnecessary large. However, these statements are not supported by enough data to make a final statement and are too some extent dependent on the parameters of the standard wall segment studied. But these statements provide a strong indication that Eurocode 2 overestimates the minimum amount of reinforcement needed for crack control.

Since the Eurocode 2 equation for minimum reinforcement with regard to crack control is derived inconsiderate of restraints, its applicability in restraint situations is questionable. A design method considering restraints is preferable to the current design method. This questionability is further supported by the seemingly large overestimations.

The proposed changes to the Eurocode 2 equation both does not account for but only adapt an existing equation of questionable applicability with regard to restraint situations. In order to properly consider various restraints, the derivation of a new equation considerate of restraints is preferable and encouraged.

8.2 Further investigations

Four possible approaches of further investigations related to the calculation model, the parametric study, the development of an improved design method and the water tightness of concrete are presented in the following.

Build further on the calculation model of this thesis by, for instance:

- Considering movements of the slab, caused by e.g. shrinkage, in relation to the ground and connecting elements.
- Including the height of the wall as an additional dimension in order to account for variations in that direction and vertical crack propagation.
- Including the width of the wall as an additional dimension in order to account for variations in that direction and, by doing so, investigating the aspects of effective concrete area.

Using either the model of this thesis, an updated version of it or another model increase the parametric study by:

- Including more parameters and/or larger ranges of these parameters
- Obtaining relations for the amount of crack controlling reinforcement needed in numerous different situations and, based on the obtained relations and data, if possible further strengthen the belief that Eurocode 2 overestimates the reinforcement amounts needed for crack control.

Develop an improved design method for the amount of minimum reinforcement needed for crack control.

Investigate necessary requirements for concrete subjected to an arbitrary ground water pressure to be considered as water tight.

9 References

- Alfredsson, H. Spåls, J. (2008): *Cracking Behaviour of Concrete Subjected to Restraint Forces*. Master's thesis. Chalmers University of Technology, Göteborg, Sweden.
- Antona, B. Johansson, R. (2011): *Cracking Control of Concrete Structure Subjected to Restraint Forces*. Master's thesis. Chalmers University of Technology, Göteborg, Sweden.
- Bjerking, S. (1989): *Grunder*. Statens råd för byggnadsforskning, Stockholm, Sweden.
- Björk, C. Kallstenius, P. Reppen, L. (2003): *Så byggdes husen 1880-2000*. Formas förlag, Stockholm, Sweden.
- Björnberg, M. Johansson, V. (2013): *Numeriska simuleringar av betongkonstruktioner med minimiarmering för sprickbredds begränsning*. Master's thesis. KTH Royal Institute of Technology, Stockholm, Sweden.
- Boverket (2004): *Boverkets handbok om betongkonstruktioner, BBK 04*. Boverket, Karlskrona, Sweden.
- CEB (1993): *CEB-FIP Model Code 1990*. Thomas Telford Services Ltd., London, Great Britain.
- fib (2013): *fib Model Code for Concrete Structure 2010*. Wilhelm Ernst & Sohn, Verlag für Architektur und technische Wissenschaften GmbH & Co. KG, Berlin, Germany.
- CEN (2002): *Eurocode: Basis of structural design*. European Committee for Standardization, Brussels, Belgium.
- CEN (2004): *Eurocode 2: Design of concrete structures - Part 1-1: General rules and rules for buildings*. European Committee for Standardization, Brussels, Belgium.
- Dahlblom, O. Olsson K.-G. (2010): *Strukturmekanik*. Studentlitteratur, Lund, Sweden.
- Dahlgren, A. Svensson, L. (2013): *Guidelines and Rules for Detailing of Reinforcement in Concrete Structures*. Master's thesis. Chalmers University of Technology, Göteborg, Sweden.
- Domone, P. (2010): *Construction Materials, Part 3 Concrete*. Spoon Press, Abingdon, Great Britain.
- Engström, B. (2011a): *Restraint cracking of reinforced concrete structures*. Chalmers University of Technology, Göteborg, Sweden.
- Engström, B. (2011b): *Design and analysis of continuous beams and columns*. Chalmers University of Technology, Göteborg, Sweden.
- Engström, B. (2011c): *Design and analysis of slabs and flat slabs*. Chalmers University of Technology, Göteborg, Sweden.
- Engström, B. (2011d): *Bärande konstruktioner, Del 1*. Chalmers University of Technology, Göteborg, Sweden.

- Engström, B. (2011e): *Bärande konstruktioner, Del 2*. Chalmers University of Technology, Göteborg, Sweden.
- European Concrete Platform ASBL (2008): *COMMENTARY EUROCODE 2*. European Concrete Platform ASBL, Brussels, Belgium.
- Löfgren, I. (2005): *Fibre-reinforced Concrete for Industrial Construction*. Ph.D. Thesis. Chalmers University of Technology, Göteborg, Sweden.
- Normenausschuss Bauwesen (NABau) im DIN (2012): *Nationaler Anhang – National festgelegte Parameter – Eurocode 2: Bemessung und Konstruktion von Stahlbeton- und Spannbetontragwerken – Teil 1-1: Allgemeine Bemessungsregeln und Regeln für den Hochbau*. Normenausschuss Bauwesen (NABau) im DIN, Hannover, Germany.
- Ottosen, N. Petersson, H (1992): *Introduction to the finite element method*. Pearson Education Limited, Essex, England.
- Plos, M. (2000): *Finite element analyses of reinforced concrete structures*. Chalmers University of Technology, Göteborg, Sweden.
- Purnell, P. (2010): *Construction Materials, Part 7 Section 2*. Spoon Press, Abingdon, Great Britain.
- Svensk byggtjänst (1994): *Betonghandbok – Material*. AB Svensk Byggtjänst och Cementa AB, Stockholm, Sweden.
- Tepfers, R. (1973): *A Theory of bond applied to overlapped tensile reinforcement splices for deformed bars*. Ph.D. Thesis. Chalmers University of Technology, Göteborg, Sweden.